

U. S. NAVAL AIR ENGINEERING CENTER

PHILADELPHIA, PENNSYLVANIA

AD 733988

NAEC-ENG-7699

24 Nov 1971

MARK 7 ARRESTING GEAR PURCHASE CABLE
DEVELOPMENT PROGRAM,
JULY 1969 THROUGH DECEMBER 1970

NATIONAL TECHNICAL
INFORMATION SERVICE



DDC
RECEIVED
DEC 20 1971
C

PLATE NO. 11749

125

DOCUMENT CONTROL DATA - R & D

(Security classification of title, body of abstract and indexing annotation must be entered when the overall report is classified)

1. ORIGINATING ACTIVITY (Corporate author) Naval Air Engineering Center Engineering Department (SI) Philadelphia, Pa. 19112		2a. REPORT SECURITY CLASSIFICATION Unclassified	
		2b. GROUP	
3. REPORT TITLE Mark 7 Arresting Gear Purchase Cable Development Program, July 1969 through December 1970			
4. DESCRIPTIVE NOTES (Type of report and inclusive dates)			
5. AUTHOR(S) (First name, middle initial, last name) Robert Black			
6. REPORT DATE		7a. TOTAL NO. OF PAGES 124	7b. NO. OF REFS Twelve (12)
8a. CONTRACT OR GRANT NO.		9a. ORIGINATOR'S REPORT NUMBER(S) NAEC-ENG-7699	
8b. PROJECT NO.			
c. AIRTASK Nos. A05-537-020/200/5/000-000-03 A34537/200B/1F32461402		9b. OTHER REPORT NO(S) (Any other numbers that may be assigned this report)	
10. DISTRIBUTION STATEMENT Approved for public release; distribution unlimited			
11. SUPPLEMENTARY NOTES		12. SPONSORING MILITARY ACTIVITY Naval Air Systems Command Washington, D. C. 20360	
13. ABSTRACT This report summarizes wire rope testing conducted at the Naval Air Engineering Center on the various test machines during the indicated period. The effects of synthetic and fiber cores upon wire rope fatigue and interstrand notching are examined, as well as their relation to wire rope creep and its interrelation with fatigue. The influence of the number of wires in a round strand rope is investigated, and an analysis is performed to determine the effect of the loss of metallic area from abrasion upon rope strength for these constructions. Fatigue data is given for ropes with variable wire strength and also for two non-rotating wire ropes. Load-strain and load-torque data is presented for a number of 6 X 25 FWLLRS fiber and synthetic core ropes.			

ACCESSION FOR	
STY	WHITE SECTION <input checked="" type="checkbox"/>
DOC	BUFF SECTION <input type="checkbox"/>
UNANNOUNCED	<input type="checkbox"/>
JUSTIFICATION	
BY	
DISTRIBUTION/AVAILABILITY CODES	
DIST.	AVAIL. CODE OR SPECIAL
A	

NOTICE

Reproduction of this document in any form by other than naval activities is not authorized except by special approval of the Secretary of the Navy or the Chief of Naval Operations as appropriate.

The following Espionage notice can be disregarded unless this document is plainly marked CONFIDENTIAL or SECRET.

This document contains information affecting the national defense of the United States within the meaning of the Espionage Laws, Title 18, U.S.C., Sections 793 and 794. The transmission or the revelation of its contents in any manner to an unauthorized person is prohibited by law.

14. KEY WORDS	LINK A		LINK B		LINK C	
	ROLE	WT	ROLE	WT	ROLE	WT
Wire Rope						
Purchase Cable						
Non-rotating Cables						
Round Strand Cables						
Sheave Bending Tests						
Failure Modes						
Fatigue						
Abrasion						
Creep						
Constitutive Relations						
Wire Rope Geometry						
Wire Rope Torque						

NAVAL AIR ENGINEERING CENTER
PHILADELPHIA, PENNSYLVANIA 19112

ENGINEERING DEPARTMENT (SI)
CODE IDENT NO. 80020

NAEC-ENG-7699

24 Nov 1971

MARK 7 ARRESTING GEAR PURCHASE CABLE
DEVELOPMENT PROGRAM,
JULY 1969 THROUGH DECEMBER 1970

Approved for Public Release: Distribution Unlimited

PREPARED BY

Robert Black
ROBERT BLACK

APPROVED BY

H. Dell
H. DELL

I. INTRODUCTION

A. The presently used purchase cable for the Mark 7 Mods 1, 2 and 3 arresting engines is 1-3/8 6 X 25 FWLLRS fiber core wire rope. This rope is limited, in service, to a maximum of 1500 total engagements with 24 inch PD fairlead sheaves or 2000 total engagements with 28 inch PD fairlead sheaves. There are also limitations for "heavy aircraft", varying from 150 to 225 engagements depending upon engine type and fairlead sheave size.

The replacement of a purchase cable means the loss of an arresting engine for a considerable period of time, with a corresponding reduction in overall shipboard recovery efficiency. Therefore, it is desired to obtain a new or improved purchase cable capable of withstanding an increased total energy, both in terms of an improvement in the total number of arrestments and in the percentage of high energy engagements. The ideal purchase cable will also perform more consistently, possess a high fatigue reserve strength and give evidence of impending failure in its outer layer wires, where such failures can be noted, rather than in its inner layers where damage cannot be visually observed, thereby preventing sudden and catastrophic failure.

B. To accomplish these objectives, it is necessary to explore the mechanism of wire rope failure and to establish a set of parameters characteristic of a high fatigue life wire rope peculiar to arresting gear use. Investigations have been previously undertaken and are continuing into the areas of rope construction, rope core, rope size and wire strength, plus an evaluation of the effects of sheave size, groove surface and geometry. It is expected that the final superior purchase cable system will embody a coupling of the improvements in all of these areas.

II. SUMMARY OF PROCEDURES AND RESULTS

A. Wire rope sheave bending fatigue data presented in this report is grouped into two distinct fatigue regions, a "F" range associated with moderate to high loads and roughly corresponding to 15% to 45% of the rope's breaking strength, and a "H" range for the very high loads above 45% of the breaking strength of the cable. These bounds are very general and the percentages will vary with respect to rope construction, rope core material, sheave size and the number of stress reversals. On the basis of the results of this investigation with 24 inch PD sheaves, the following conclusions can be made:

1. The substitution of dacron core or nylon core for the standard fiber core will produce a significant increase in the fatigue life of 6 X 25 FW LL RS wire rope in both the "F" fatigue region and the "H" region. The use of polypropylene core offers no particular advantage in the "F" region, but does yield an increased rope life in the "H" region.
2. Rope internal damage is independent of core material as tests of 1-3/8 6 X 25 FW LL RS ropes with fiber, polypropylene, dacron and nylon cores exhibit equivalent magnitudes of inter-strand notching when normalized on a life basis. However, deformation was found to increase with cable load and the number of stress reversals.
3. The shape of the accumulative normalized elongation curves for fiber, dacron and nylon core wire rope as a function of life (cyclic creep) was observed to be qualitatively similar to a creep curve of ordinary time. A power relation between minimum cyclic creep rate and fatigue life exists for the "F" range and was found to be independent of cable load, rope size and number of stress reversals per cycle.
4. Dacron core rope evinces considerably more elongation per cycle than fiber or nylon core ropes. This will be a serious problem and will probably preclude the use of dacron core ropes in shipboard arresting engine service.
5. Fatigue tests of 6 X 21, 6 X 25 and 6 X 29 FW LL RS fiber core ropes show an exponential increase in fatigue life relative to the number of wires in the strand, and a slight increase in the cable load transition point between the "F" and "H" range as the number of wires increases. Analysis shows that loss of metallic area for a constant depth of abrasion is negligible for wire sizes of .080 to .106 inches.
6. The high stresses induced by inter-strand contact during sheave bending of 18 X 7 and 12 X 6/6 X 30 LL non-rotating wire ropes preclude a high fatigue life for these ropes relative to the standard purchase cable. Initial failures of the latter rope were concentrated in the inner strands, while the early signs of impending failure for the 18 X 7 rope were observed to be in the outer strands.

B. A number of 6 X 25 FW LL RS wire ropes were tested with both ends fixed to determine the load-elongation characteristics for these ropes. The following observations were drawn from these tests:

1. Synthetic core (dacron and nylon) ropes demonstrate greater degrees of "constructional stretch" than fiber core ropes, but all these ropes displayed moduli in the range of 12-14 X 10⁶ psi.

2. Rope proportional limits were found to increase with respect to wire strength.

3. Rope strain hardening exponents rise relative to increasing wire ductility.

4. It is well documented that rope lay angle diminishes with respect to tensile load. Test data for the nylon core rope also shows a proportionate decrease in the strand lay angle.

III. TABLE OF CONTENTS

		PAGE
I	INTRODUCTION	i
II	SUMMARY OF PROCEDURES AND RESULTS	ii
III	TABLE OF CONTENTS	iv
IV	LIST OF TABLES AND FIGURES	v
V	LIST OF ABBREVIATIONS	xiv
VI	DISCUSSION OF WIRE ROPE TESTS	1
	A. Wire Rope Fatigue Tests	1
	1. General Introduction and Definitions	1
	2. The Effects of Core Material upon Wire Rope Fatigue	4
	3. The Effects of Core Material upon Wire Rope Cyclic Creep	5
	4. Influence of Core Material upon Wire Rope Interstrand Notching	8
	5. The Influence of Number of Wires on Round Strand Wire Rope Performance	10
	6. The Effect of Wire Size on Round Strand Wire Rope Abrasion Resistance	12
	7. Fatigue Tests of Variable Strength Round Strand Wire Ropes	13
	8. Fatigue Tests of Non-rotating Wire Ropes	14
	B. Wire Rope Properties	15
	1. Fiber Core Ropes	15
	2. Synthetic Core Ropes	20
VII	REFERENCES	23
	Appendix A: Wire Rope Geometry	

IV. LIST OF TABLES AND FIGURES

A. LIST OF TABLES

TABLE NO.	TITLE	PAGE
1	Transition Load as a Function of Core Material for 1-3/8 6X25 FW LL RS Wire Rope Construction with 24 Inch PD Sheaves	4
2	Physical Properties of 1-7/16 6X21, 6X25 and 6X29 FW LL RS Fiber Core Wire Ropes	10
3	Wire Strengths and Torsions for 1-7/16 6 X 21, 6 X 25 and 6 X 29 FW LL RS Fiber Core Wire Ropes	11
4	"F" to "H" Region Transition Loads for 1-7/16 6 X 21, 6 X 25 and 6 X 29 FW LL RS Fiber Core Wire Ropes	11
5	Single Wire Properties for Variable Strength 1-3/8 6 X 25 FW LL RS Fiber Core Wire Ropes	13
6	Fatigue Data for Non-rotating Wire Rope with 24 inch PD Sheaves and Four Stress Reversals per Cycle	14
7	Wire Rope Response Coefficients for Initial Inelastic Phase for 6 X 25 FW LL RS Fiber Core Wire Ropes	17
8	Wire Rope Phase 2 Properties for 6 X 25 FW LL RS Fiber Core Wire Ropes	18
9	Wire Rope Phase 3 Constitutive Relations for 6 X 25 FW LL RS Fiber Core Wire Ropes	19
10	Wire Rope Response Coefficients for Initial Inelastic Phase for 6 X 25 FW LL RS Synthetic vs Fiber Core Wire Ropes	20
11	Wire Rope Phase 2 Properties for 6 X 25 FW LL RS Synthetic vs Fiber Core Wire Ropes	20
12	Wire Rope Phase 3 Constitutive Relations for 6 X 25 FW LL RS Synthetic and Fiber Core Wire Ropes	21
13	Fatigue Data for 1-3/8 6 X 25 FW LL RS Polypropylene Core Wire Rope (P/N 414465-5) with 24 Inch PD Sheaves	24

TABLE NO.	TITLE	PAGE
14	Fatigue Data for 1-3/8 6 X 25 FW LL RS Dacron Core Wire Rope (P/N 414465-35) with 24 Inch PD Sheaves	25
15	Fatigue Data for 1-3/8 6 X 25 FW LL RS Nylon Core Wire Rope (P/N 414465-36) with 24 Inch PD Sheaves	26
16	Fatigue Data for 1-7/16 6 X 21 FW LL RS Fiber Core Wire Rope (P/N 414465-37) with 24 Inch PD Sheaves	27
17	Fatigue Data for 1-7/16 6 X 25 FW LL RS Fiber Core Wire Rope (P/N 414465-30) with 24 Inch PD Sheaves	28
18	Fatigue Data for 1-7/16 6 X 29 FW LL RS Fiber Core Wire Rope (P/N 414465-38) with 24 Inch PD Sheaves	29
19	Fatigue Data for 1-3/8 6 X 25 FW LL RS Fiber Core Wire Rope (P/N 414465-47) with 24 Inch PD Sheaves	30
20	Fatigue Data for 1-3/8 6 X 25 FW LL RS Fiber Core Wire Rope (P/N 414465-39) with 24 Inch PD Sheaves	31
21	Outer Layer Wire Notching Data for 1-3/8 6 X 25 FW LL RS Construction with Dacron, Nylon, Polypropylene and Fiber Cores Tested under Four Stress Reversals per Cycle	32
22	Outer Layer Wire Notching Data for 1-3/8 6 X 25 FW LL RS Construction with Dacron, Nylon, Polypropylene and Fiber Cores Tested under Ten Stress Reversals per Cycle	33
23	Summary of Steady State Creep Data for "F" Region Fatigue for 6 X 25 FW LL RS Wire Rope with Dacron, Nylon and Fiber Cores	34

B. LIST OF FIGURES

FIGURE NO.	TITLE	PAGE
1	Definition of Failure Regions and Failure Modes for 1-3/8 6 X 25 FW LL RS Fiber Core Wire Rope under Four Stress Reversals per Cycle and 24 Inch PD Sheaves	3
2	Typical Creep Behavior	5
3	Outer Layer Wire Notch Depth vs Purchase Cable Life from TC11 Deadload Spectrum Program	9
4	Wire Geometry for Calculation of Abrasive Area Loss	12
5	Typical Load-Strain Response for 6 X 25 FW LL RS Fiber Core or Synthetic Core Wire Rope	16
6	Wire Rope Proportional Limit vs Average Wire UTS for 6 X 25 FW LL RS Fiber Core Construction	18
7	Wire Rope Strain Hardening Exponent vs Average Wire Ductility for 6 X 25 FW LL RS Fiber Core Construction	19
8	Wire Rope Fatigue "F" to "H" Range Transition Load vs Rope Proportional Limit for 1-3/8 6 X 25 FW LL RS Construction	21
9	Fatigue Data for 1-3/8 6 X 25 FW LL RS Fiber Core Wire Rope under Four, Eight and Ten Stress Reversals per Cycle and 24 Inch PD Sheaves	35
10	Composite of Fatigue Data for 1-3/8 6 X 25 FW LL RS Fiber Core Wire Ropes (BE and WRI Manufacture) under Four Stress Reversals per Cycle and 24 Inch PD Sheaves	36
11	Composite of Fatigue Data for 1-3/8 6 X 25 FW LL RS Fiber Core Wire Ropes (BE and WRI Manufacture) under Ten Stress Reversals per Cycle and 24 Inch PD Sheaves	37
12	Fatigue Data for 1-3/8 6 X 25 FW LL RS Polypropylene Core Wire Rope Tested under Four, Eight and Ten Stress Reversals per Cycle and 24 Inch PD Sheaves	38
13	Fatigue Data for 1-3/8 6 X 25 FW LL RS Dacron Core Wire Rope Tested under Four, Eight and Ten Stress Reversals per Cycle and 24 Inch PD Sheaves	39

FIGURE NO.	TITLE	PAGE
14	Fatigue Data for 1-3/8 6 X 25 FW LL RS Nylon Core Wire Rope Tested under Four, Eight and Ten Stress Reversals per Cycle and 24 Inch PD Sheaves	40
15	Comparison of Polypropylene Core vs Fiber Core Wire Rope, 1-3/8 6 X 25 FW LL RS Construction, Tested under Four Stress Reversals per Cycle and 24 Inch PD Sheaves	41
16	Comparison of Polypropylene Core vs Fiber Core Wire Rope, 1-3/8 6 X 25 FW LL RS Construction, Tested under Ten Stress Reversals per Cycle and 24 Inch PD Sheaves	42
17	Comparison of Dacron Core vs Fiber Core Wire Rope, 1-3/8 6 X 25 FW LL RS Construction, Tested under Four Stress Reversals per Cycle and 24 Inch PD Sheaves	43
18	Comparison of Dacron Core vs Fiber Core Wire Rope, 1-3/8 6 X 25 FW LL RS Construction, Tested under Ten Stress Reversals per Cycle and 24 Inch PD Sheaves	44
19	Comparison of Nylon Core vs Fiber Core Wire Rope, 1-3/8 6 X 25 FW LL RS Construction, Tested under Four Stress Reversals per Cycle, and 24 Inch PD Sheaves	45
20	Comparison of Nylon Core vs Fiber Core Wire Rope, 1-3/8 6 X 25 FW LL RS Construction, Tested under Ten Stress Reversals per Cycle and 24 Inch PD Sheaves	46
21	"F" Region Comparison of Nylon and Dacron Core Wire Rope, 1-3/8 6 X 25 FW LL RS Construction, Tested under Four Stress Reversals per Cycle and 24 Inch PD Sheaves	47
22	Notch Depth Rate vs Cable Load for 1-3/8 6 X 25 FW LL RS Construction with Dacron, Nylon, Polypropylene and Fiber Core, "F" Region Fatigue, Tested Under Four Stress Reversals per Cycle and 24 Inch PD Sheaves	48
23	Notch Depth Rate vs Cable Load for 1-3/8 6 X 25 FW LL RS Construction with Dacron, Nylon, Polypropylene and Fiber Core, "F" Region Fatigue, Tested under Ten Stress Reversals per Cycle and 24 Inch PD Sheaves	49

FIGURE NO.	TITLE	PAGE
24	Total Cyclic Strain for 1-3/8 6 X 25 FW LL RS Fiber Core Wire Rope Tested under Four Stress Reversals per Cycle and 24 Inch PD Sheaves	50
25	Total Cyclic Strain for 1-3/8 6 X 25 FW LL RS Dacron Core Wire Rope Tested under Four Stress Reversals per Cycle and 24 Inch PD Sheaves	51
26	Total Cyclic Strain for 1-3/8 6 X 25 FW LL RS Nylon Core Wire Rope Tested under Four Stress Reversals per Cycle and 24 Inch PD Sheaves	52
27	Total Cyclic Strain for 1-3/8 6 X 25 FW LL RS Dacron Core Wire Rope Tested under Ten Stress Reversals per Cycle and 24 Inch PD Sheaves	53
28	Total Cyclic Strain for 1-3/8 6 X 25 FW LL RS Fiber Core Wire Rope Tested under Ten Stress Reversals per Cycle and 24 Inch PD Sheaves	54
29	Total Cyclic Strain for 1-7/16 6 X 25 FW LL RS Fiber Core Wire Rope Tested under Ten Stress Reversals per Cycle and 24 Inch PD Sheaves	55
30	Empirical Relation between Cyclic Creep Rate and Fatigue Life for 1-3/8 and 1-7/16 6 X 25 FW LL RS Fiber, Nylon and Dacron Wire Rope Tested on the Two and Five Sheave Cycle Testers with 24 Inch PD Sheaves	56
31	Cyclic Creep Rate vs Cycles to Failure for 1-3/8 and 1-7/16 6 X 25 FW LL RS Fiber, Nylon and Dacron Core Wire Rope Tested on the Two and Five Sheave Cycle Testers with 24 Inch PD Sheaves	57
32	Fatigue Data for 1-7/16 6 X 21 FW LL RS Fiber Core Wire Rope Tested under Four, Eight and Ten Stress Reversals per Cycle and 24 Inch PD Sheaves	58
33	Fatigue Data for 1-7/16 6 X 25 FW LL RS Fiber Core Wire Rope Tested under Four, Eight and Ten Stress Reversals per Cycle and 24 Inch PD Sheaves	59
34	Fatigue Data for 1-7/16 6 X 25 FW LL RS Fiber Core Wire Rope Tested under Four, Eight and Ten Stress Reversals per Cycle and 24 Inch PD Sheaves	60
35	Fatigue Data vs Stress Reversals for 1-7/16 6 X 21, 6 X 25 and 6 X 29 FW LL RS Fiber Core Wire Ropes under 75000 Pounds Cable Load and 24 Inch PD Sheaves	61

FIGURE NO.	TITLE	PAGE
36	Fatigue Data vs Number of Wires per Strand for 1-7/16 6 X 21, 6 X 25 and 6 X 29 FW LL RS Fiber Core Wire Ropes Tested under Four Stress Reversals per Cycle and 24 Inch PD Sheaves	62
37	Fatigue Data vs Number of Wires per Strand for 1-7/16 6 X 21, 6 X 25 and 6 X 29 FW LL RS Fiber Core Wire Ropes Tested under Eight Stress Reversals per Cycle and 24 Inch PD Sheaves	63
38	Fatigue Data vs Number of Wires per Strand for 1-7/16 6 X 21, 6 X 25 and 6 X 29 FW LL RS Fiber Core Wire Ropes Tested under Ten Stress Reversals per Cycle and 24 Inch PD Sheaves	64
39	Comparison of Fatigue Data for 1-7/16 6 X 21, 6 X 25 and 6 X 29 FW LL RS Fiber Core Wire Rope Constructions Tested under Four Stress Reversals per Cycle and 24 Inch PD Sheaves	65
40	Wire Area Reduction from Loss of Outer Layer Wire Cross-section due to Abrasion for 1-7/16 6 X 21, 6 X 25 and 6 X 29 FW LL RS Fiber Core Wire Rope Constructions	66
41	Strand Area Reduction from Loss of Outer Layer Wire Cross-section due to Abrasion for 1-7/16 6 X 21, 6 X 25 and 6 X 29 FW LL RS Fiber Core Wire Rope Constructions	67
42	Comparison of Fatigue Data for Increased Strength vs Standard Strength Wires for 1-3/8 6 X 25 FW LL RS Fiber Core Wire Rope Tested under Four Stress Reversals per Cycle and 24 Inch PD Sheaves	68
43	Comparison of Fatigue Data for Reduced Strength vs Standard Strength Wires for 1-3/8 6 X 25 FW LL RS Fiber Core Wire Rope Tested under Four Stress Reversals per Cycle and 24 Inch PD Sheaves	69
44	Comparison of Fatigue Data for Reduced Strength vs Standard Strength Wires for 1-3/8 6 X 25 FW LL RS Fiber Core Wire Rope Tested under Ten Stress Reversals per Cycle and 24 Inch PD Sheaves	70
45	Fatigue Comparison of Lang Lay Round Strand, Flattened Strand and Seale Ropes vs Non-rotating Ropes Tested under Four Stress Reversals per Cycle	71

FIGURE NO.	TITLE	PAGE
46	Cable Load vs Wire Rope Strain for 1-3/8 6 X 25 FW LL RS Fiber Core Wire Rope with Production (XIP) Wires	72
47	Cable Load vs Wire Rope Strain for 1-3/8 6 X 25 FW LL RS Fiber Core Wire Rope with Extra Strength Wires	73
48	Cable Load vs Wire Rope Strain for 1-3/8 6 X 25 FW LL RS Fiber Core Wire Rope with Reduced Strength Outer Layer Wires	74
49	Cable Load vs Wire Rope Strain for 1-7/16 6 X 25 FW LL RS Fiber Core Wire Rope with Production (XIP) Wires	75
50	Cable Load vs Wire Rope Strain for 1-7/16 6 X 25 FW LL RS Fiber Core Wire Rope Previously Loaded Beyond Yield Limit	76
51	Cable Load vs Wire Rope Strain for 1-1/2 6 X 25 FW LL RS Fiber Core Wire Rope with Production (XIP) Wires	77
52	Wire Rope Torque vs Cable Load for 1-3/8 6 X 25 FW LL RS Fiber Core Wire Rope with Extra Strength Wires	78
53	Wire Rope Torque vs Cable Load for 1-3/8 6 X 25 FW LL RS Fiber Core Wire Rope with Reduced Strength Outer Layer Wires	79
54	Wire Rope Torque vs Cable Load for 1-7/16 6 X 25 FW LL RS Fiber Core Wire Rope with Production (XIP) Wires	80
55	Cable Load vs Wire Rope Strain for 1-3/8 6 X 25 FW LL RS Dacron Core Wire Rope	81
56	Cable Load vs Wire Rope Strain for 1-3/8 6 X 25 Nylon Core Wire Rope	82
57	Wire Rope Torque vs Cable Load for 1-3/8 6 X 25 FW LL RS Dacron Core Wire Rope	83
58	Variation of Rope Diameter and Lay Length for 1-3/8 6 X 25 FW LL RS Fiber Core Wire Rope, First Cycle of Loading	84
59	Variation of Rope Diameter and Lay Length for 1-3/8 6 X 25 FW LL RS Fiber Core Wire Rope, Thirtieth Cycle of Loading	85

FIGURE NO.	TITLE	PAGE
60	Variation of Rope Diameter and Lay Length for 1-3/8 6 X 25 FW LL RS Dacron Core Wire Rope, First Cycle of Loading	86
61	Variation of Rope Diameter and Lay Length for 1-3/8 6 X 25 FW LL RS Dacron Core Wire Rope, Thirtieth Cycle of Loading	87
62	Variation of Rope Diameter and Lay Length for 1-3/8 6 X 25 FW LL RS Nylon Core Wire Rope, First Cycle of Loading	88
63	Variation of Rope Diameter and Lay Length for 1-3/8 6 X 25 FW LL RS Nylon Core Wire Rope, Thirtieth Cycle of Loading	89
64	Variation of Rope Radius and Lay Angle vs Cable Load for 1-3/8 6 X 25 FW LL RS Fiber Core Wire Rope, First Cycle of Loading	90
65	Variation of Rope Radius and Lay Angle vs Cable Load for 1-3/8 6 X 25 FW LL RS Fiber Core Wire Rope, Thirtieth Cycle of Loading	91
66	Variation of Rope Radius and Lay Angle vs Cable Load for 1-3/8 6 X 25 FW LL RS Dacron Core Wire Rope, First Cycle of Loading	92
67	Variation of Rope Radius and Lay Angle vs Cable Load for 1-3/8 6 X 25 FW LL RS Dacron Core Wire Rope, Thirtieth Cycle of Loading	93
68	Variation of Rope Radius and Lay Angle vs Cable Load for 1-3/8 6 X 25 FW LL RS Nylon Core Wire Rope, First Cycle of Loading	94
69	Variation of Rope Radius and Lay Angle vs Cable Load for 1-3/8 6 X 25 FW LL RS Nylon Core Wire Rope, Thirtieth Cycle of Loading	95
70	Rope and Strand Lay Angles, Variation with Respect to Cable Load for 1-3/8 6 X 25 FW LL RS Nylon Core Wire Rope, Thirtieth Cycle of Loading	96
71	Rope-Strand Cross-section for 6 X 21 FW LL RS Wire Rope	97
72	Rope-Strand Cross-section for 6 X 25 FW LL RS Wire Rope	98

FIGURE NO.

TITLE

PAGE

73	Rope-strand Cross-section for 6 X 29 FW LL RS Wire Rope	99
74	Rope-strand Cross-section for 18 X 7 Non-rotating Wire Rope	100
75	Rope-strand Cross-section for 12 X 6/6 X 30 Non- rotating Wire Rope	101

V. LIST OF ABBREVIATIONS**A. Wire Rope Terminology**

CTR	Center Wire (of strand)
FC	Fiber Core
FS	Flattened Strand
FW	Filler Wire
IL	Inner Layer
LL	Lang's Lay
OL	Outer Layer
RS	Round Strand

B. Manufacturers

ACCO	American Chain and Cable Company
BE	Bethlehem Steel Corporation
CFI	Colorado Fuel and Iron Company
PW	Paulsen-Weber Co.
WRI	Wire Rope Industries Ltd.

VI. DISCUSSION OF WIRE ROPE TESTS

A. Wire Rope Fatigue Tests

1. General Introduction and Definitions

a. Cycle testing of wire rope at NAVAIRENGCEN was accomplished on two Two-Sheave Testers and one Five-Sheave Tester. The former devices contain one sheave at each end and test two wire rope specimens at a time. Each rope specimen is translated around a sheave while under a constant static cable load. The Five-Sheave Tester contains three sheaves at one end and two sheaves at the other; again, two specimens are tested at a time under a constant loading. Functional descriptions of these testers are contained in reference (a).

b. Both of the Two-Sheave Testers are utilized to translate rope completely around a sheave. Since the stress pattern of an element of rope is changed from the effects of a straight rope tensile loading to tensile loading plus rope flexure and then changed to rope tensile loading alone, and then with reverse stroking, back around the sheave to its initial configuration, it is said that the rope has experienced four reversals of stress per cycle. Similarly, specimens at one end of the Five-Sheave Tester are displaced around two 90° sheave wraps for eight stress reversals per cycle. Due to physical limitations, specimens at the three-sheave end of the Five-Sheave Tester experience ten stress reversals per cycle, including reverse bending.

c. When fatigue data for the several wire ropes discussed in this report are presented as a function of load, the plot divides into two separate regions, characterized by distinctive modes of failure. The observations of Gibson, et. al. (reference (b)) of cycle machine tested ropes show Mode 1 failures resulting from fractures on a plane oriented approximately 45° from the longitudinal axis of the wire. The fracture surface is relatively smooth and shows little evidence of gross plastic yielding. This mode of failure predominates at the higher cable loads.

When the test load is reduced, the appearance of the majority of the failures changes. This new type of failure, designated Mode 2, occurs on a plane 90° from the longitudinal axis of the wire and is nucleated from crack initiation at a point where the combination of tensile stress and bending stress is a maximum.

d. Freudenthal (reference (c)) has attempted the classification of the strain level effect into three ranges based on the character of the microstructural changes within the grain boundaries:

The "H" or high amplitude region is characterized by severe crystal fragmentation and grain disorientation, accompanied by hardening induced by the cyclic strain.

The "F" or true fatigue region is characterized by areas of concentrated slip, such as structural defects, material impurities and flaws, and these develop into striations with little or no hardening.

The "S" or safe range exhibits widely distributed slippage along grain boundaries, but with neither hardening nor substantial microcrack formation.

e. A typical cable load - cycles to failure mean valued curve for 1-3/8 6 x 25 FW LL RS FC wire rope (standard fleet purchase cable) subjected to four stress reversals per cycle is sketched in Figure 1. Fatigue data is not available for cable loads less than 20,000 pounds, but the life data does show a definite increasing into a "S" region. The data does not sharply change from "F" to "H" fatigue as shown, but there is in reality an intermingling of failure modes at the transition load, where the longer life specimens predominantly fail in the Mode 2 manner while the majority of the reduced life specimens exhibit Mode 1 failures.

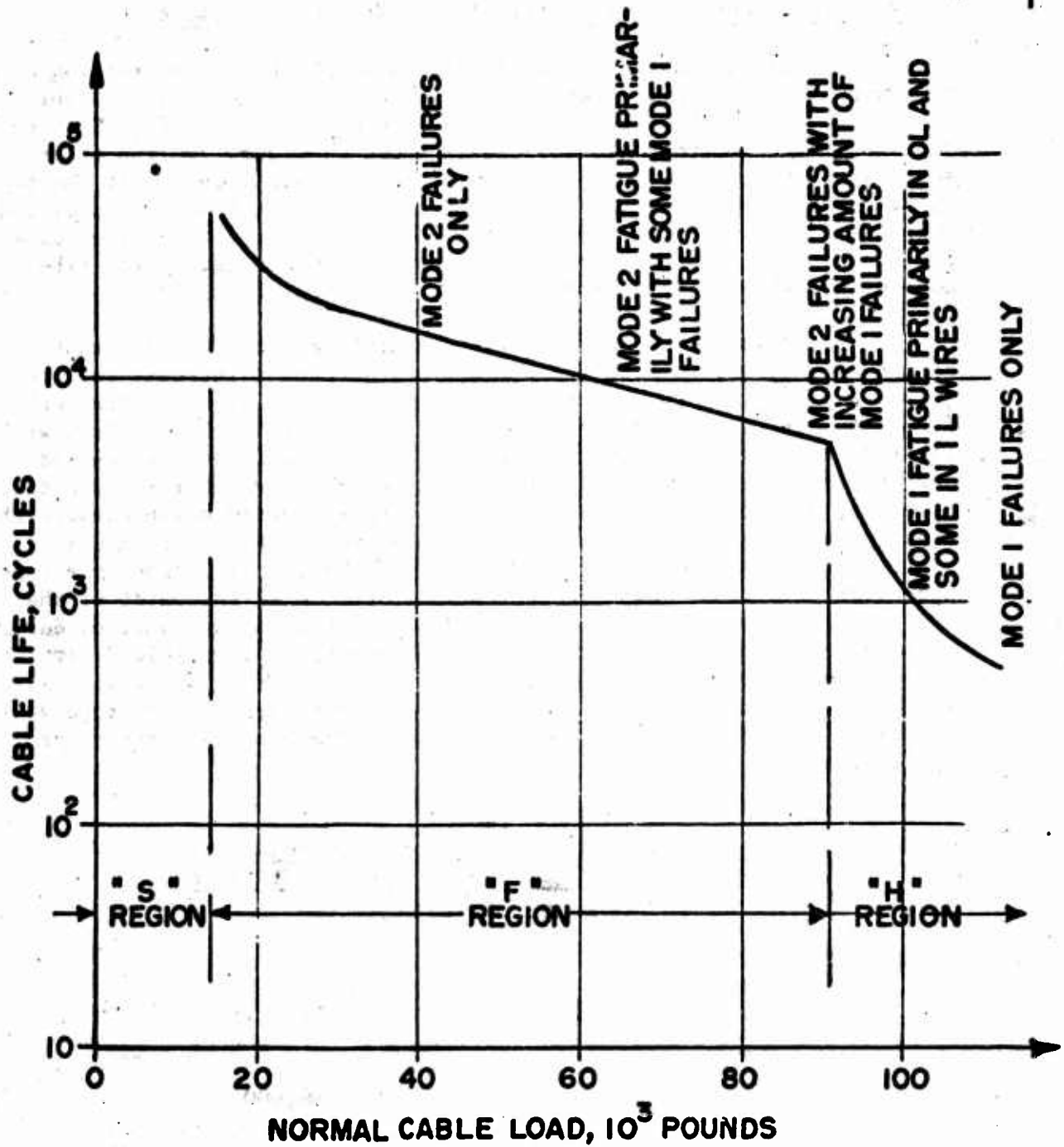


Figure 1
Definition of Failure Regions
and Failure Modes
1-3/8 6 x 25 FW LL RS FC Wire Rope
Four Stress Reversals per Cycle
24 Inch P.D. Sheaves

2. The Effects of Core Material Upon Wire Rope Fatigue

a. Fatigue data for the 1-3/8 6 x 25 FW LL RS construction with polypropylene core, nylon core and dacron core are presented in Tables 13 through 15 and Figures 12 through 14. Equivalent data for fiber core rope is listed in reference (d) and is shown in Figure 9. The fiber core wire rope fatigue data is of sufficient quantity to permit the calculation of a mean-square deviation of sample points from the estimated regression curve (Figures 10 and 11). Comparisons of the fatigue data for the several synthetic core wire ropes with the envelope for fiber core wire rope are given in Figures 15 through 20.

b. Testing at four stress reversals per cycle reveals that dacron and nylon core wire ropes offer a significant increase in life relative to fiber core rope throughout the "F" region, while the performance of polypropylene core wire rope is essentially coincident with fiber core rope in the "F" region. A closer comparison of nylon and dacron performance is given in Figure 21, which shows no real advantage to either rope in the "F" region. All three synthetic cores advance the transition load as shown in Table I, while the greatest increase is exhibited by dacron core wire rope, followed by polypropylene core rope and nylon core rope. Since wire rope performance in the onset of the "H" region may be conceived as a family of approximately parallel curves originating from the transition point when plotted against load, it follows that the rope possessing the highest transition point will also exhibit the best performance in this area. Thus, dacron core rope would be highly recommended if arresting engine purchase cable service were concentrated solely in this region.

Table I
Transition Load as a Function of Core Material
1-3/8 6 x 25 FW LL RS Wire Rope Construction
24 Inch P.E. Sheaves

<u>No. of Stress Reversals per Cycle</u>	<u>Core Material</u>	<u>Transition Load Pounds</u>
4	Fiber	89,000
	Nylon	95,000 (approx.)
	Polypropylene	105,000 (approx.)
	Dacron	110,000
10	Fiber	79,000
	Nylon	100,000
	Polypropylene	100,000
	Dacron	105,000 (approx.)

The value of load transition point for nylon core rope at four stress reversals appears to be low and testing at 100,000 pounds cable load could be repeated as a matter of academic interest.

c. Testing at ten stress reversals per cycle showed equivalence between fiber core and polypropylene core wire ropes, a significant advantage for nylon core rope over fiber core rope and yet a greater advantage for dacron core rope relative to fiber core rope in the "F" region. All three synthetic cores raised the transition load and all three exhibited increased fatigue lives with respect to fiber core rope in the "H" region.

3. The Effects of Core Material Upon Wire Rope Cyclic Creep

a. Time dependent inelastic deformation is known as creep. The creep of materials under static load was first observed by Andrade in 1910 (reference (e)). In the past ten years, certain aspects of the behavior of metals subjected to combined creep (mean constant loading) and fatigue (alternating loading) have attracted increasing attention. The effect which is of the most interest is the unexpectedly large plastic deformation which accumulates on a cyclic basis. This deformation is very similar to ordinary time and temperature dependent creep. The main difference is the significantly higher rate of creep deformation observed for the cyclic case in comparison to the static case.

Creep is traditionally divided into three stages, although not all are always present. The first stage is called transient or primary creep, the intermediate stage is called steady-state or secondary creep, while the last stage is called tertiary creep. Usually the increase in the creep rate in the tertiary stage is due to an increase in stress as the area is reduced either by thinning down or by internal fracture or the formation of voids.

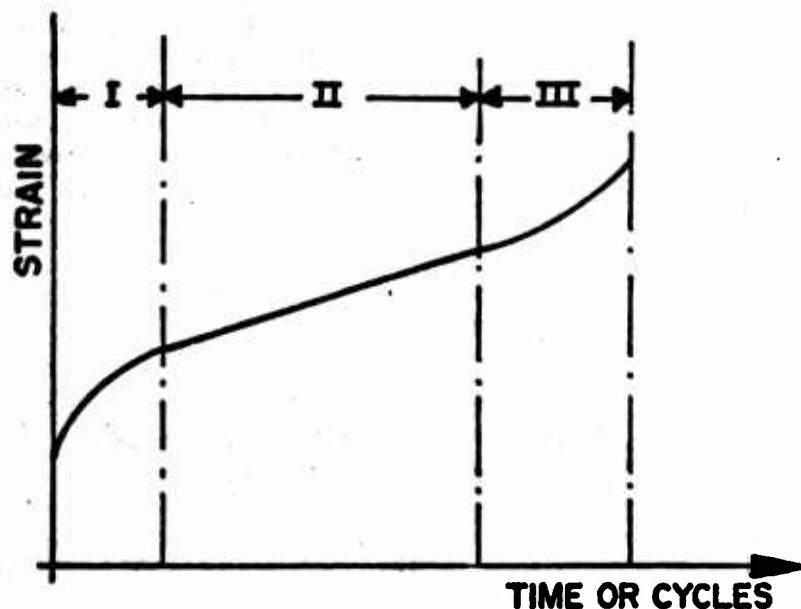


Figure 2
Typical Creep Behavior

b. Longitudinal extensional data was recorded during the sheave bending fatigue tests of the 1-3/8 6 x 25 FW LL RS wire rope specimens with fiber, dacron and nylon cores. The extensions were converted to engineering strain and are plotted against number of cycles in Figures 24 through 29. These cyclic creep curves are similar in shape to those observed for ordinary time and temperature dependent creep. Test specimens that failed in the "F" range of the fatigue curve manifested definite transient and steady-state creep regions and generally a pronounced tertiary region, while specimens that fail in the "H" range of the fatigue curve have limited or non-existent steady-state creep regions.

c. Studies of ordinary (static load) creep by Monkman and Grant (reference (f)) have found that an empirical relation exists between rupture life (time to rupture) and the minimum creep rate for a wide variety of materials. The relation was of the form

$$\log \frac{t_r}{t_0} + m \log(\dot{\epsilon}_{min}) = c$$

where

t_r = rupture life

$\dot{\epsilon}_{min}$ = minimum creep rate

and

m and c are constants.

The authors found that the value of m was generally less than, but very close, to unity.

Now the question of similarity between ordinary and cyclic creep arises again. The wire rope cyclic creep data displays a linear relation between extension and life throughout the steady-state creep region. Since this is the minimum creep rate, its value can be accurately determined by the method of least squares. These creep rates and the specimen fatigue lives were analyzed together, again using least squares, with fatigue life as a function of minimum creep rate. The results pictured in Figure 30 show excellent agreement with an equation of the same form as that proposed by Monkman and Grant. The relation for cyclic creep is

$$N_f \left(\frac{d\epsilon}{dN} \right)^a = b$$

where

N_f = fatigue life

$\frac{d\epsilon}{dN}$ = minimum cyclic creep rate

and

a and b are constants.

The data for fiber core and nylon core data are coincident, yielding the relation

$$N_f \left(\frac{d_s}{JN} \right)^{.9432} = .001910$$

while the governing equation for dacron core wire rope is

$$N_f \left(\frac{d_s}{JN} \right)^{.9226} = .01130$$

The two constants are thus found to be dependent upon material, and dacron core wire rope observed to exhibit greater inelastic flow during the steady-state region than fiber core or nylon core wire ropes. The exponents are slightly less than unity, but are found to be independent of cable load and rope size (that is rope stress), and the number of stress reversals per cycle.

d. Since the exponents in the above equations are found to be very close to unity, simplified expressions relating minimum creep rate and fatigue life are obtainable when the exponent is taken to be one. The resulting relations are now

$$N_f \left(\frac{d_s}{JN} \right) = .002293$$

for fiber core and nylon core wire rope and

$$N_f \left(\frac{d_s}{JN} \right) = .005169$$

for dacron core wire rope. These constants we obtained as average of the constants for individual data points (Table 23). Figure 31 shows that the mean value of the constants are in exceptional agreement with the data.

e. The requirements for shipboard arresting engine use of a wire rope as a purchase cable must include a long trouble-free period of sustained usage. Specifically, the wire rope must not elongate at a rate which will unduly interrupt operations for elimination of accumulated stretch. Laboratory tests have demonstrated the increased fatigue performance of dacron core wire rope relative to fiber core rope, and the only slightly diminished advantage of nylon core rope with respect to dacron core rope. However, these same tests have also shown the more than two-fold increase in extensionability for dacron core ropes over fiber core and nylon core ropes at a life corresponding to that required of a fleet purchase cable. Thus, the recommendation for a new purchase cable core material must be given to nylon on the basis of a greater recovery from large cyclic extensions (see reference (g)).

4. Influence of Core Material on Interstrand Notching

a. When a wire rope is loaded in axial tension, the strand pitch is slightly elongated while the rope diameter exhibits a significantly greater degree of contraction. Any initial gap between the strands that may exist is soon dissipated and the strands come into physical contact with each other. These tractions are essentially applied over an extremely limited area and thus produce a plastic flow of the outer layer wire material. This loss of cross-sectional area due to interstrand contact is called "interstrand notching".

When a wire rope is bent around a radius, the above process is more pronounced and the notching or decrease in cross-sectional area is more severe. As the strands realign themselves to conform to the new geometry, the traction areas of one strand are scrubbed by adjacent strands, thereby inducing a fretting action in conjunction with the contact stresses. The degree of notching, as measured by the reduction in cross-section, increases as the sheave radius is decreased. The effect upon the strength of the wire rope is mixed, as the wire strength is at first increased due to residual compressive stresses at the root of the notch; but, as the depth of the notch continues to increase, the tensile strength of the wire falls below the strength of unnotched wires (see reference (d)).

b. The rate of notching depth is obviously dependent upon cable load, sheave radius and cable life for a given number of stress reversals. These parameters must be segregated before the effects of core material can be evaluated. In all of the discussion that follows, the sheave size was maintained at 24 inches pitch diameter.

Some normalization of notching data with respect to cable life is required, for at a given load the outer layer wires of the dacron and nylon core ropes show a greater depth of notch than the fiber core ropes as a result of their increased longevity. The effect of life can be illustrated by graphing the depth of notch data obtained for cable sections subjected to a spectrum of deadload weights and engaging speeds at the NAVAIRENGCEN TC11 site (see reference (d)) and located 120 feet aft of the port terminal.

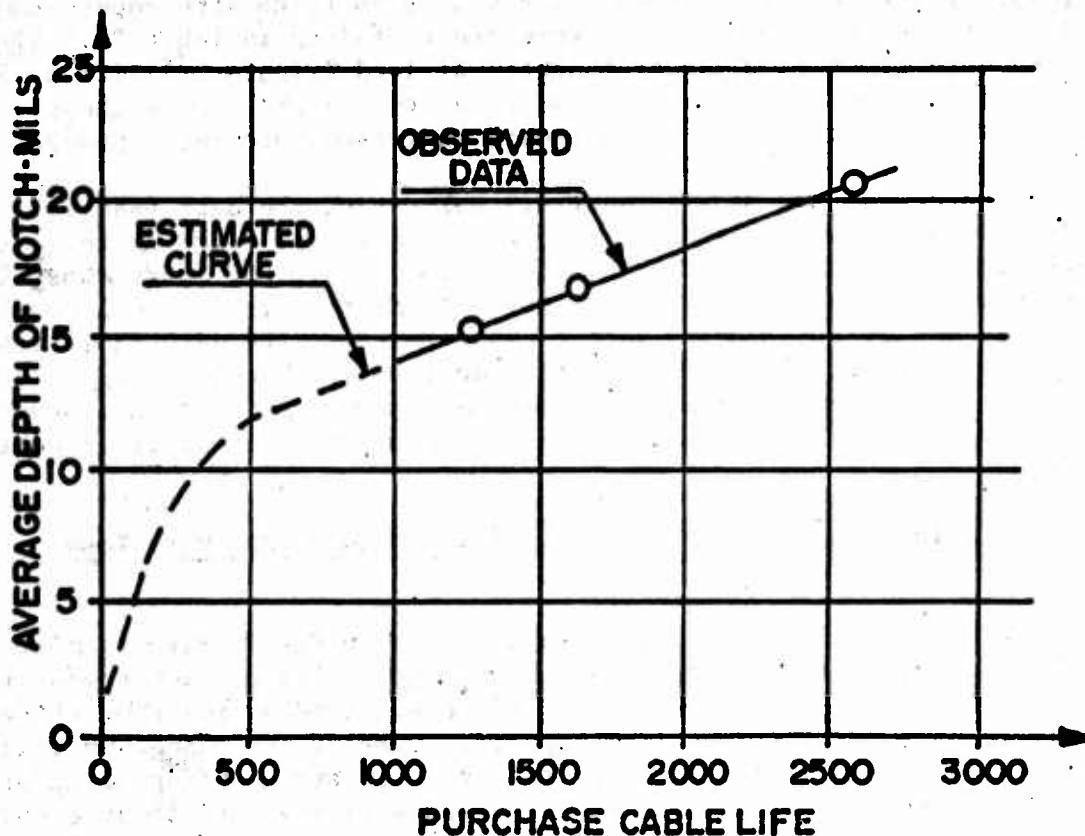


Figure 3
Outer Layer Wire Notch Depth
Vs. Purchase Cable Life
TC11 Deadload Spectrum Program

The relation between notching depth and rope life is entirely unknown for the initial number of cycles, but most likely follows the indicated curve. The wire undoubtedly suffers extensive deformation under the nearly infinite contact and fretting stresses, but the rate of deformation must diminish as the contact area is enlarged or else the wire would not survive. The degree of the initial portion of notch depth-life curve will depend upon cable load and number of stress reversals, and is probably most severe in arresting engine service, that is, the usage indicated in Figure 3. However, when a wire rope is cycled to failure, only the initial point (zero notch, zero life) and the final depth of notch at a known number of cycles is available. The average rate of depth of notch calculated over the entire rope life will not correspond to the theorized rate when the rope life is small, but will yield an increasingly better approximation as longer rope lives are achieved.

c. Data relating depth of notch and life for dacron, nylon, polypropylene and fiber core 1-3/8 6 x 25 FW LL RS wire ropes subjected to four stress reversals per cycle are contained in Table 21. The average rate data plots as a linear function of load (Figure 22) with great conformity between dacron, nylon and fiber core ropes. Only the polypropylene core rope exhibits a slightly increased notching depth per cycle.

At ten stress reversals per cycle, the data (see Table 22) is less voluminous, but the average rate of notching depth again appears to be proportional to cable load (Figure 23). Here the differences between wire ropes with differing cores are more distinct, but are undoubtedly influenced by the shorter rope lives. However, the data shows that dacron core wire rope offers some reduction in average notching rate while polypropylene core wire rope again produces the highest average rate with very little difference between nylon core and fiber core wire ropes.

5. Influence of Number of Wires on Round Strand Wire Rope Performance.

a. The fatigue life of a wire rope under flexure is also influenced by the construction of the strand. This parameter was investigated briefly by a limited number of sheave bending tests on three different ropes from one manufacturer. Each of the ropes subscribed to the basic round strand construction of a six stranded rope with an inner ring and then an outer ring of wires successively laid about a core wire, the voids between the inner and outer layers of wires occupied with a set of filler wires. The ropes differed in the quantities of wires contained in each ring, being in increasing order for the outer layer 10, 12 and 14 wires, and 5, 6 and 7 wires for the inner ring and filler ring (Figures 71 through 73).

b. Each of the three constructions were purchased from the same manufacturer at the same time in order to reduce or eliminate, as much as possible, any variations in manufacturing practices and wire material properties. The following tabulations, listing the rope breaking strengths, metallic areas, wire strengths and wire torsions show that the ropes can be considered as equivalent in all phases except for construction.

Table 2
Physical Properties
1-7/16 6 x 21, 6 x 25 & 6 x 29 FW LL RS FC
Wire Ropes

<u>Construction</u>	<u>WRI Reel No.</u>	<u>Metallic Area Sq. In.</u>	<u>Breaking Strength Pounds</u>
6 x 21	C-6523	.818	201,200
6 x 25	C-6525	.831	198,800
6 x 29	C-6521	.842	201,600

Table 3
Wire Strengths and Torsions
1-7/16 6 x 21, 6 x 25 & 6 x 29 FW LL RS FC

<u>Construction</u>	<u>Wire Type</u>	<u>No. of Wires per Strand</u>	<u>Wire Dia. Inches</u>	<u>Wire UTS Psi</u>	<u>Wire Torsions (8" Gage Length)</u>
6 x 21	OL	10	.1060	280,300	28.23
	IL	5	.0975	267,000	29.22
	Ctr	1	.0702	284,100	41.80
	FW	5	.0417	307,800	75.00
6 x 25	OL	12	.0911	271,600	31.62
	IL	6	.0972	274,700	24.20
	Ctr	1	.1010	288,100	30.00
	FW	6	.0410	272,500	88.50
6 x 29	OL	14	.0804	276,900	36.29
	IL	7	.0939	274,500	30.00
	Ctr	1	.1280	261,100	20.00
	FW	7	.0379	292,600	81.43

c. Fatigue data for the 1-7/16 6 x 21, 6 x 25 and 6 x 29 FW LL RS FC wire ropes is listed in Tables 15, 16 and 17 and is shown in Figures 32, 33 and 34, respectively. These ropes exhibit an exponential decrease in life for an increasing number of stress reversals in the "F" region (Figure 35) and in most cases, display an exponentially increasing life with respect to an increase in the number of wires in the strand (Figures 36 through 38).

The effect of the number of wires in the strand upon transition load is, in most cases, difficult to determine due to the limited amount of data. Approximate transition loads are given in Table 4 below.

Table 4
"F" to "H" Region Transition Loads
1-7/16 6 x 21, 6 x 25 & 6 x 29 FW LL RS FC Ropes

<u>No. of Stress Reversals</u>	<u>T - Approximate Transition Load - Pounds</u>		
	<u>6 x 21 Rope</u>	<u>6 x 25 Rope</u>	<u>6 x 29 Rope</u>
4	105,000	105,000	110,000
8	105,000	105,000	110,000
10	$\bar{T} < 100,000$	$\bar{T} < 100,000$	105,000

The apparent trend is to gain an increase in transition load relative to an enlargement in the number of wires in a strand. It is generally true that the flexibility of a rope will also vary directly as a function of wire quantity and thereby wire size. Previous fatigue tests of a 1/3/8 6 x 31 LL Modified Seale wire rope, a more flexible construction, have also demonstrated small increases in transition loads (reference (d)).

6. The Effects of Wire Size on Round Strand Rope Abrasion Resistance

a. A fleet purchase cable must be a compromise of many factors. It must include good resistance to abrasion as well as fatigue. Unfortunately, while an increase in the number of wires in a strand results in a greater degree of rope flexibility and thereby longer life under flexure, it will also cause a decrease in the abrasion resistance properties of the outer layer wires. These effects at the present time cannot be completely defined by numerical calculation as the distribution of flexural stresses in a wire moving around a sheave is unknown, but the reduction of wire strength has been shown to be proportional to the loss of cross-sectional area (reference (d)).

b. Inspection of abraded wires has shown that remaining cross-section of an abraded wire can be closely approximated by the area enclosed by a circle and its chord.

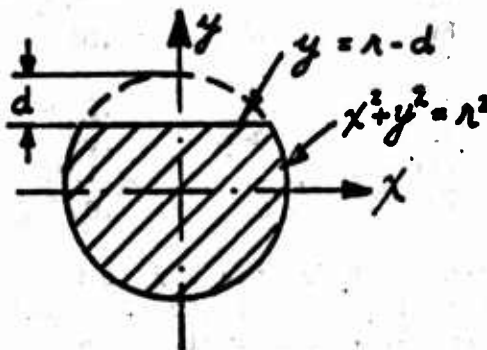


Figure 4
Wire Geometry for Calculation
of Abrasive Wire Area

The area A in terms of the wire radius r and the depth of abrasion d is the integral evaluated across the shaded area, that is,

$$A = \int dx dy$$

$$A = \pi r^2 - \int_{-r}^r dx \int_{(r-d)}^{\sqrt{r^2-x^2}} dy$$

$$A = \pi r^2 + (r-d)r - r^2 \sin^{-1} \frac{d}{r}$$

where

$$r = \sqrt{d(2r-d)}$$

c. Remaining cross-sectional areas for the outer layer wires of 1-7/16 6 x 21, 6 x 25 and 6 x 29 FW LL RS fiber core wire ropes are given in Figure 40 as a function of the depth of abrasion. The effect upon the total strand area, considering that all of the outer layer wires are abraded to the same depth, is found to be negligible among these ropes as shown in Figure 41. Thus, the effects of area reduction and corresponding strength reduction are not really significant among these three ropes. However, since the 6 x 29 construction offers a significant increase in sheave oriented fatigue, this construction should be considered as a possible purchase cable for fleet use.

7. Fatigue Tests of Variable Strength Round Strand Wire Ropes

a. Most of the wires used in purchase cables exhibit ultimate tensile strengths of 280,000 to 290,000 psi with reduction in areas slightly in excess of 50%. Data shown in reference (d) gives the results of analytical investigations relating wire strength to fatigue, particularly on the Five-Sheave Tester. An empirical expression was derived relating fatigue life with the parameters wire strength, rope size, sheave size and cable load combined into a dimensionless ratio and reduction in area. As an extension of this work, a limited number of tests was performed on two ropes, PW Reel 49117 and BE Reel 3-908-A9, with wire strengths supposedly differing from the mean tensile strength.

b. Single wire data presently available on these two ropes is completed in Table 5.

Table 5
Single Wire Properties
Variable Strength 1-3/8 6 x 25 FW LL RS FC Ropes

<u>Reel No.</u>	<u>No. of Wires per Strand</u>	<u>Wire Type</u>	<u>Wire Dia. Inches</u>	<u>Wire UTS Psi</u>	<u>Wire RA %</u>	<u>Wire Torsions</u>
PW 49117	12	OL	.0895	294,000	51.7	30.1
	6	IL	.0970	291,800	49.5	27.7
	1	Ctr.	.1010	292,300	51.5	28.0
	6	FW	.0400	-	-	70.3
BE3-908-A9	12	OL	.0888	270,100	-	-
	6	IL	.0950	271,800	-	-
	1	Ctr.	.0995	261,100	-	-
	6	FW	.0400	274,600	-	-

The wire strengths are seen to differ only slightly from the normal 280,000 to 290,000 psi range.

c. The limited number of fatigue tests (Tables 19 and 20 and Figures 42 through 44) show that both ropes exhibit increased life with respect to standard ropes at four stress reversals. This conforms to the pattern noted in reference (d). However, at ten stress reversals, the reduced strength rope is equivalent with the standard rope in the "F" region, while testing of the PW rope has not been accomplished. The lack of extended testing and/or incomplete single wire data precludes any in-depth analysis.

8. Fatigue Tests of Non-Rotating Wire Ropes

a. The non-rotating wire ropes are characterized by a reduced modulus of elasticity relative to the 6 x 25 FW LL RS fiber core construction, a greater metallic area per unit diameter (due to the smaller volume of core material) and a higher degree of interstrand notching due to the increased angle of contact caused by the alternating directional lays of the outer and inner strands. To investigate these effects, six specimens, each of 1-1/4 18 x 7 fiber core non-rotating wire rope and 1-1/4 12 x 6/6 x 30 polypropylene core non-rotating wire rope (Figures 74 and 75), were cycled to failure around 24 inch P.D. sheaves under four reversals of stress per cycle. Pertinent fatigue data is contained in Table 6 below:

Table 6
Fatigue Data for Non-rotating Wire Rope
24 Inch P.D. Sheaves
Four Stress Reversals per Cycle

<u>Wire Rope Type</u>	<u>Mfg.</u>	<u>Cable Load Pounds</u>	<u>Cycles at Failure</u>
1-1/4 18x7, P/N A92791-33	CFI	56,000	4600
		70,000	4254
			2509
			2777
			2440
1-1/4 12x6/6x30, P/N A92791-50	ACCO	56,000	2698
		70,000	5049
			5028
			2466
			3784
	2645		
	3608		

The 12 x 6/6 x 30 construction shows a slight advantage in bending fatigue with respect to the 18 x 7 rope. Although both ropes are nominal 1-1/4 inch diameter ropes, the former rope contains significantly more metallic area (.792 square inches versus .671 square inches) and thereby exhibits a correspondingly higher breaking strength. Elastic moduli for the two ropes are essentially equivalent: 10.7×10^6 psi for the 12 x 6/6 x 30 construction and 10.5×10^6 psi for the 18 x 7 rope.

b. While the tensile strength of the wires from the two non-rotating wire ropes was not investigated, previous tests of other ropes from a number of manufacturers has established that most wires exhibit an average ultimate tensile strength of 285,000 psi (reference (d)). With this strength, the fatigue data for these ropes can be compared against that obtained for 1-3/8 6 x 25 FW LL RS FC, 1-3/8 6 x 30 LL FS Type G FC and 1-3/8 6 x 31 LL Modified Seale FC wire ropes by recourse to the non-dimensional Drucher-Tachan β parameter (reference (h)). This function is defined as

$$\beta = \frac{2T}{UDd}$$

where T = nominal cable load, pounds.
 U = average ultimate tensile strength of wires, psi.
 D = pitch diameter of sheave, inches.
 d = nominal rope diameter, inches.

Fatigue data for these ropes and the non-rotating ropes is presented in Figure 45. The high stresses incurred by inter-strand contact during sheave bending of the non-rotating ropes are decisive and preclude a high fatigue life for these ropes, especially under severe conditions as characterized by a high β factor.

c. The initial failures of the 1-1/4 12 x 6/6 x 30 rope were predominantly located in the inner strands where they could not be observed, while the early signs of impending rope failure for the 1-1/4 18 x 7 rope were congregated in the outer strands. Thus, while the former rope is superior in breaking strength and sheave oriented fatigue, the 18 x 7 rope offers the important advantage of broken wire observation.

B. Wire Rope Properties

1. Fiber Core Ropes

a. The typical response for fiber or synthetic core wire rope under increasing load consists of several parts.

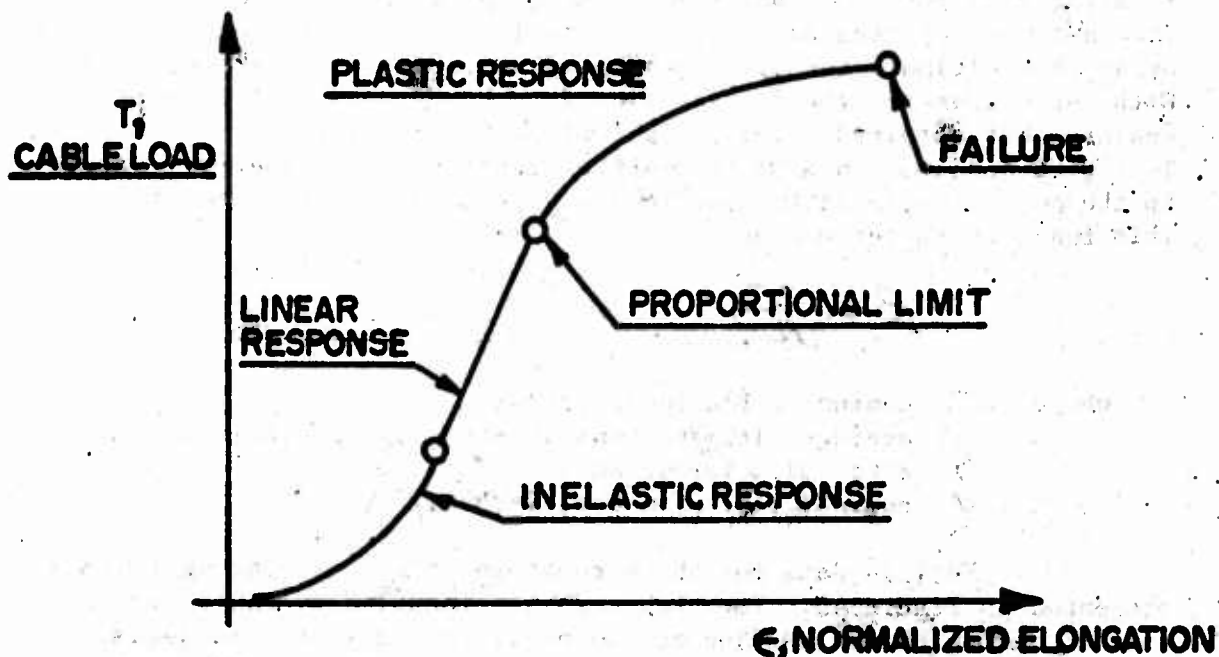


Figure 5
Typical Load - Strain Response
for 6 x 25 FW LL RS Fiber
or Synthetic Core Wire Rope

Phase 1: An initial inelastic response, commonly called "permanent or constructional stretch" which is caused by the progressive adjustment of the individual wires to their proper working positions and the seating of the strands in the core of the rope. The response is very non-linear. Thus, wire rope is one of many materials that possess a stress-strain curve that is totally, or in part, concave towards the stress axis. For these materials, waves carrying the larger strains will propagate faster than those carrying smaller strains, and when the faster waves overtake the slower ones, shock waves appear (Cristescu, reference (1)).

Phase 2: A region of linear response where the extension varies directly with the load. The response is truly elastic when the loading path and relaxation path coincide and the rope does not display any viscoelasticity, that is dependence upon time.

Phase 3: When the load is increased beyond the proportional limit, the wire rope response becomes plastic due to the essentially plastic condition of the metal. The rope as a whole behaves like a plastic body; it exhibits strain hardening and relaxes elastically with a non-recoverable strain.

b. Plots of normalized elongation versus cable load for three 1-3/8 6 x 25 FW LL RS FC wire ropes with varying wire ductilities are presented in Figures 46 through 48. Data for a 1-7/16 and a 1-1/2 6 x 25 FW LL RS FC wire rope are shown in Figures 49 and 51, respectively.

The load elongation relations for the initial inelastic phase can be expressed by equations of the form

$$T = A_0 \epsilon + B_0 \epsilon^3$$

where T is cable load, pounds
 ϵ is wire rope strain, inch/inch
 and A_0 and B_0 are constants.

The coefficients were determined by the method of least squares (reference (j)) and are tabulated below.

Table 7
Wire Rope Response Coefficients
for Initial Inelastic Phase
6 x 25 FW LL RS FC Wire Ropes

<u>Rope Type</u>	<u>Wire Rope Elongation Coefficients</u>			<u>Load Range</u> <u>Pounds</u>
	<u>RA-%</u>	<u>A₀</u>	<u>B₀</u>	
1-3/8 XIP Wires	49.5	4.817×10^6	68.273×10^9	$0 \leq T \leq 33,000$
1-3/8 Red. Str. OL Wires	54.3	2.532×10^6	55.105×10^9	$0 \leq T \leq 31,000$
1-3/8 Extra Str. Wires	44.9	3.684×10^6	107.457×10^9	$0 \leq T \leq 29,000$
1-7/16 XIP Wires	52.4	3.021×10^6	99.170×10^9	$0 \leq T \leq 33,000$
1-1/2 XIP Wires	52.8	4.007×10^6	175.515×10^9	$0 \leq T \leq 31,000$

All the 1-3/8 ropes possess similar geometries, that is, equivalent lay angles and radii. In general, there appears to be an increase in elongation relative to an increase in wire ductility. The choice of a core material undoubtedly influences initial rope elongation; but as the "fiber core" is only defined in broad terms, it is difficult to segregate the influences of wire properties from the effects of core properties.

c. In Phase 2, the rope elongation varies directly with load. The following rope properties were determined for increasing load.

Table 8
Wire Rope Phase 2 Properties
6 x 25 FW LL RS FC Wire Ropes

<u>Rope Type</u>	<u>Rope Area Inches²</u>	<u>Modulus Psi</u>	<u>Avg. Wire UTS Psi</u>	<u>Proportional Limit Load Pounds</u>	<u>Proportional Limit Stress Psi</u>
1-3/8 XIP Wires	.792	12,600,000	297,400	105,000	133,000
1-3/8 Red Str. OL Wires	.792	12,100,000	260,600	100,000	126,000
1-3/8 Extra Str. Wires	.792	13,800,000	326,300	115,000	145,000
1-7/16 XIP Wires	.862	13,800,000	283,300	111,000	129,000
1-1/2 XIP Wires	.910	13,700,000	271,900	115,000	127,000

All the moduli were found to vary between 12,000,000 and 14,000,000 psi which are compatible with the handbook values for the 6 x 25 FW LL RS fiber core construction. The proportional limit expressed in terms of rope stress is essentially a function of wire strength (Figure 6). As in the case of a 1-7/16 6 x 25 FW LL RS fiber core wire rope, the proportional limit can be increased by loading the rope beyond the original limit (Figure 50) with a corresponding decrease in plastic strain.

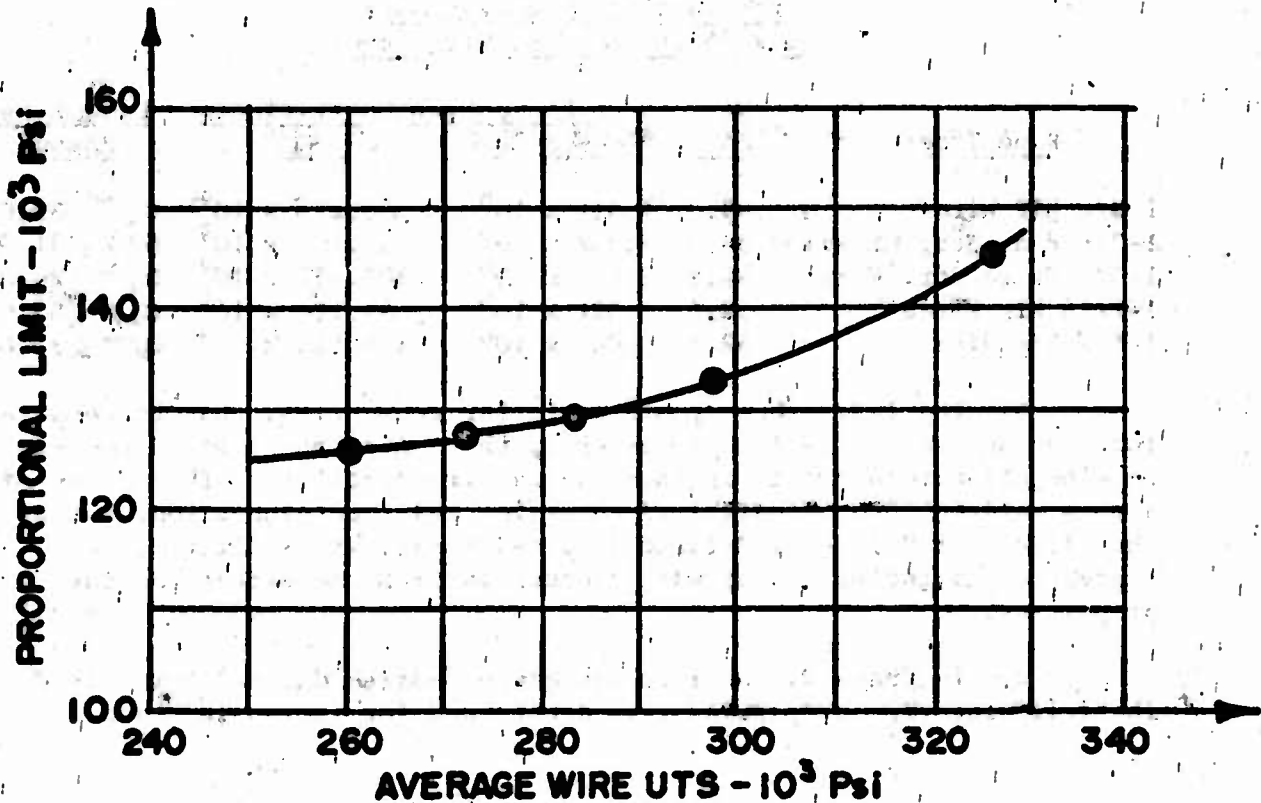


Figure 6
Wire Rope Proportional Limit
Vs. Average Wire UTS
6 x 25 FW LL RS FC Construction

d. For Phase 3, the rope stress can be related to plastic strain by the power expression.

$$\sigma = A \epsilon_p^B$$

where σ = rope stress, psi
 ϵ_p = plastic strain, inch/inch
 A and B are constants

The constitutive relations are given in Table 9.

Table 9
Wire Rope Phase 3 Constitutive Relations

<u>Rope Type</u>	<u>Avg. Wire RA - %</u>	<u>Stress-Strain Law</u>
1- 3/8 XIP Wires	49.5	$\sigma = 131,900 \epsilon_p^{.1584}$
1-3/8 Red. Str. OL Wires	54.3	$\sigma = 129,600 \epsilon_p^{.1736}$
1-3/8 Extra Str. Wires	44.9	$\sigma = 153,400 \epsilon_p^{.1458}$
1-7/16 XIP Wires	52.4	$\sigma = 128,700 \epsilon_p^{.1923}$
1-1/2 XIP Wires	52.8	$\sigma = 123,800 \epsilon_p^{.1853}$

and the exponent B (the strain hardening exponent) for these ropes is plotted as function of wire ductility in Figure 7, showing a general increase in strain hardening exponent as a function of ductility.

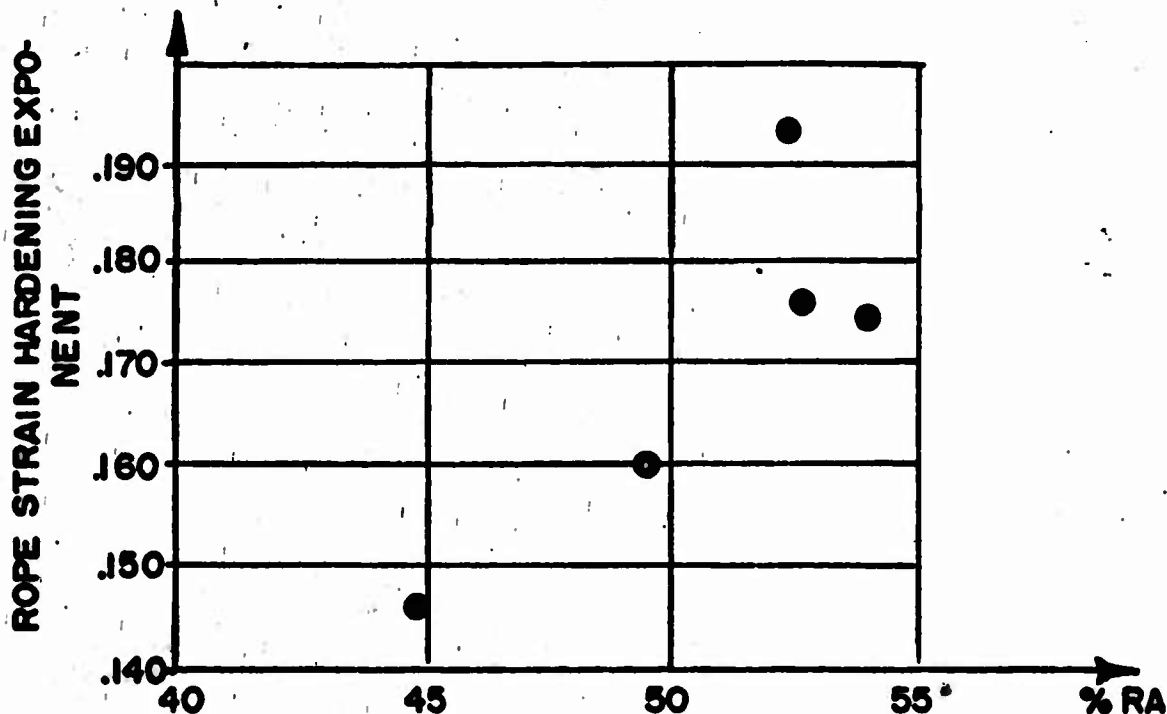


Figure 7
Wire Rope Strain Hardening Exponent
Vs. Average Wire Ductility
6 x 25 FW LL RS FC Construction

e. It is well known that the application of a tensile load upon most wire ropes with fixed ends will produce a torque. Gibson, et. al. (reference (k)) have shown that the torque is proportional to cable load and wire rope geometry. Figures 52 through 54 show the observed relation for torque as a function of cable load for several 6 x 25 FW LL RS fiber core ropes. It is observed that the torque is unrelated to wire strength, but does show an increase with respect to rope size.

2. Synthetic Core Ropes

a. Synthetic core ropes exhibit the same general shape for their load-strain relations as fiber core wire ropes. However, in general, the initial inelastic or constructional stretch effect is more pronounced for synthetic core ropes as indicated in Figures 55 and 56 and as well as in Table 10 below.

Table 10
Wire Rope Response Coefficients
for Initial Inelastic Phase
6 x 25 FW LL RS Synthetic Vs. Fiber Core
Wire Ropes

<u>Wire Rope Core</u>	<u>Rope Elongation Coefficients</u>		<u>Load Range</u> <u>Pounds</u>
	<u>A₀</u>	<u>B₀</u>	
Dacron	.318 x 10 ⁶	27.419 x 10 ⁹	0 ≤ T ≤ 43,000
Nylon	1.923 x 10 ⁶	19.224 x 10 ⁹	0 ≤ T ≤ 60,000
Fiber *	4.817 x 10 ⁶	68.273 x 10 ⁹	0 ≤ T ≤ 33,000

* Fiber core rope with production (XIP) wires.

b. The wire rope elongation in the Phase 2 region appears to be independent of core material as both nylon and dacron core ropes display moduli within the 12,000,000 to 14,000,000 psi range associated with the 6 x 25 FW LL RS fiber core construction.

Table 11
Wire Rope Phase 2 Properties
6 x 25 FW LL RS Synthetic Vs. Fiber Core
Wire Ropes

<u>Wire Rope Core</u>	<u>Rope Area</u> <u>Inches²</u>	<u>Rope Modulus</u> <u>Psi</u>	<u>Rope Proportional</u> <u>Limit - Pounds</u>
Dacron	.792	12.56 x 10 ⁶	120,000
Nylon	.792	13.87 x 10 ⁶	111,000
Fiber *	.792	12-14 x 10 ⁶	105,000

*Fiber core with production (XIP) wires.

However, the substitution of dacron or nylon core for fiber core in a 6 x 25 FW LL RS wire rope produces an increase in the rope proportional limit, with dacron core effecting a significant rise and nylon core causing only a moderate increase. The proportional limit is related to wire rope fatigue, as Figure 8 shows a general increase in "F" range to "H" range transition load with respect to increasing rope proportional limit.

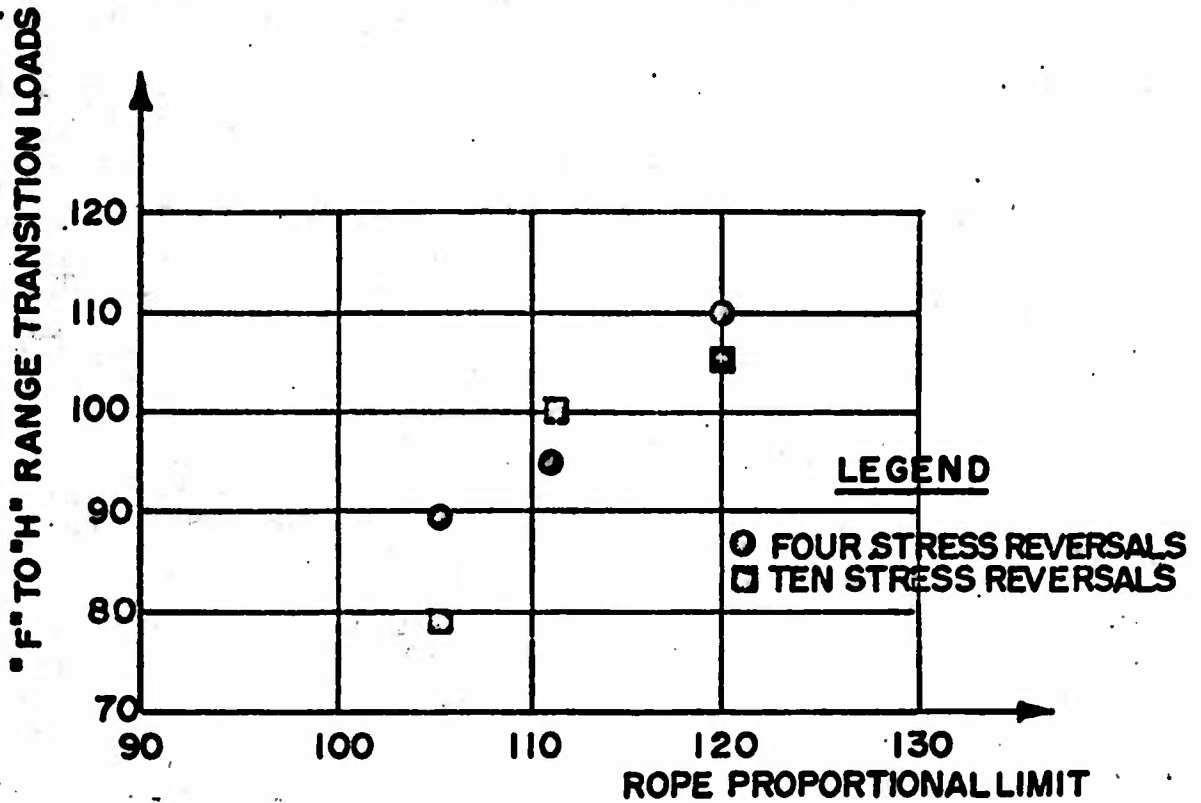


Figure 8
Wire Rope Fatigue "F" to "H" Range
Transition Load
Vs. Rope Proportional Limit
1-3/8 6 x 25 FW LL RS Construction

c. The wire rope Phase 3 constitutive relations (Table 12) are essentially similar for dacron, nylon and fiber core 6 x 25 FW LL RS ropes except that the synthetic core curves are displaced upwards with respect to the stress axis.

Table 12
Wire Rope Phase 3 Constitutive Relations
6 x 25 FW LL RS Synthetic and Fiber Core
Wire Ropes

<u>Wire Rope Core</u>	<u>Stress-Strain Relation</u>
Dacron	$\sigma = 146,900 \epsilon^{.1527}$
Nylon	$\sigma = 144,700 \epsilon^{.1583}$
Fiber *	$\sigma = 131,900 \epsilon^{.1584}$

*Fiber core rope with production (XIP) wires.

The similarity between the values for the strain hardening exponents suggests that the wire ductilities for the three ropes may not greatly differ.

d. The observed cable torque-load data for 1-3/8 6 x 25 FW LL RS dacron core wire rope is presented in Figure 57. A comparison with the data for fiber core rope of the same construction shows that the torque build-up is not influenced by the choice of core material.

e. The variations of rope diameter and rope lay as a function of cable load for the first and thirtieth cycles of a 0 to 100,000 pound loading are presented in Figures 58 through 69 for three 1-3/8 6 x 25 FW LL RS wire ropes with fiber, dacron and nylon cores. The rope geometry is not constant, as the rope exhibits a longitudinal extension coupled with a lateral contraction which is largely recoverable after the load has been relieved, but does become significant with respect to life on an accumulative basis. Both nylon and dacron core ropes demonstrate a greater degree of lateral contraction under cable load than does fiber core rope, and thereby possess a reduction in transverse stiffness. There is very little difference in the lateral contraction between dacron and nylon core ropes until a cable loading of 30,000 pounds is applied; but when the loading is further increased, the nylon core rope demonstrates a somewhat higher degree of lateral stiffness than does the dacron core rope.

f. It is shown in Appendix A that the angle between the tangent vector of an OL wire in a strand and the centerline of the rope is equal to the sum of the rope lay angle and the strand lay angle. This combined angle was measured as a function of load during the tensile loading of a 1-3/8 6 x 25 FW LL RS nylon core wire rope. The rope lay angle was determined in the usual way, that is from measurements of the rope pitch and the diametrical contraction, again with both parameters expressed as a function of cable load. After the rope lay angle had been calculated, the strand lay angle was attained by a simple subtraction. The results, contained in Figure 70, show that the strand lay angle varies proportionately with the rope lay angle with respect to increasing cable load.

VII. REFERENCES

- (a) R. Black, Report NAEC-ENG-7543, "Mark 7 Arresting Gear Purchase Cable and Deck Pendant Development Program, January 1966 through June 1968"
- (b) P. Gibson, et. al., Battelle Memorial Institute Report, "Analytical and Experimental Investigation of Aircraft Arresting Gear Purchase Cable", 3 July 1968
- (c) A. M. Freudenthal, Aspects of Cumulative Damage in Fatigue Design, Report AFML-TR-67-112
- (d) R. Black, Report NAEC-ENG-7625, "Mark 7 Arresting Gear Purchase Cable and Deck Pendant Development Program, July 1968 through June 1969"
- (e) E. N. da C. Andrade, "On the Viscous Flow in Metals and Allied Phenomena", Proc. Royal Soc. (London), 84 (1910), p. 1
- (f) F. C. Monkman and N. J. Grant, "An Empirical Relationship between Rupture Life and Minimum Creep Rate in Creep Rupture", Proc. ASTM, 56 (1957), p. 593
- (g) C. D. Daiello, Report NAEC-ENG-7461, "Investigations and Test of Wire Rope Core Materials for Aircraft Arresting Engine Purchase Cable", p. 38
- (h) Drucker, D. and Tachan, H., "A New Design Criteria for Wire Rope", Journal of Applied Mechanics, Vol. 12, No. 1, March 1945
- (i) Cristescu, N., "Dynamic Plasticity", John Wiley & Sons, Inc., 1967
- (j) R. Black, Report NAEC-ENG-7683, "A Study in Terminal Bending of Uniform and Encapsulated Wire Rope with Linear and Non-Linear Constitutive Equations"
- (k) P. Gibson, et. al., "Torsional Properties of Wire Rope", Wire and Wire Products, November 1970
- (l) P. Gibson, et. al., "The Continuation of Analytical and Experimental Investigation of Aircraft Arresting-Gear Purchase Cable", 7 April 1970

Table 13
Fatigue Data
1-3/8 6 x 25 FW LL RS Polypropylene Core Wire Rope
P/N 414465-5
24 Inch P.D. Sheaves
BE Reel 3-900-A8A

<u>Cable Load Pounds</u>	<u>Number of Stress Reversals</u>	<u>Cycles at Failure</u>	<u>Cable Load Pounds</u>	<u>Number of Stress Reversals</u>	<u>Cycles at Failure</u>
60,000	4	10996*	75,000	8	3521
75,000		11857*	100,000		1605
100,000		7132	110,000		1855
110,000		7924	75,000	10	1070
		4789	100,000		2371
		4900	110,000		2596
		4087			1003
		4782			1023
		2140			606
		2185			1149
	1847		492		
	2791		526		
				412	
				270	

*Data from reference (1).

Table 14
Fatigue Data
1-3/8 6 x 25 FW LL RS Dacron Core Wire Rope
P/N 414465-35
24 Inch P.D. Sheaves
BE Reel 3-900-B8A

<u>Cable Load Pounds</u>	<u>Number of Stress Reversals</u>	<u>Cycles at Failure</u>	<u>Cable Load Pounds</u>	<u>Number of Stress Reversals</u>	<u>Cycles at Failure</u>
40,000	4	15815*	75,000	8	5045
60,000		18398*	100,000		5134
75,000		13862	110,000		3145
90,000		13321	75,000		3011
100,000		8569	100,000	668	
110,000		8341	110,000		
		8523	75,000	10	3724
		8903	100,000		3970
		4467	110,000		4053
		6598	100,000		4054
	6728	110,000		2146	
	6518	110,000		2170	
	5195			2038	
	5718			1784	
	1863			608	
	1345			829	
				561	
				282	

*Data from reference (1).

Table 15
Fatigue Data
1-3/8 6 x 25 FW LL RS Nylon Core Wire Rope
P/N 414465-36
24 Inch P.D. Sheaves
BE Reel 3-900-C8A

<u>Cable Load Pounds</u>	<u>Number of Stress Reversals</u>	<u>Cycles at Failure</u>	<u>Cable Load Pounds</u>	<u>Number of Stress Reversals</u>	<u>Cycles at Failure</u>	
40,000	4	17091	75,000	8	4347	
↓		19494	↓		2574	
60,000		12650*	100,000		↓	2998
↓		13683*	↓	110,000	↓	184
75,000		9613	↓	↓	168	
↓		9096	75,000	10	3402	
90,000		9409	↓		3191	
↓		9774	100,000		↓	1810
100,000		8919	↓		847	
↓		9029	110,000		↓	2275
110,000		2600	↓		2085	
↓		4262	↓		145	
↓		2320	↓	276		
↓	3850	↓	96			
↓	1109	↓	254			
↓	1389	↓				

*Data from reference (1).

Table 16
Fatigue Data
1-7/16 6 x 21 FW LL RS FC Wire Rope
P/N 414455-37
24 Inch P.D. Sheaves
WRI Reel C-6523

<u>Cable Load Pounds</u>	<u>Number of Stress Reversals</u>	<u>Cycles at Failure</u>	<u>Cable Load Pounds</u>	<u>Number of Stress Reversals</u>	<u>Cycles at Failure</u>
60,000	4	10304*	75,000	8	3801
75,000		10304*	100,000		2377
100,000		6871	110,000	737	
110,000		8076	75,000	10	2740
		4632			2310
		4125			474
		3661			414
		3868			847
		1126			1035
		531			168
	584	115			
918	422				
			110,000		143

*Data from reference (1).

Table 17
Fatigue Data
1-7/16 6 x 25 FW LL RS FC Wire Rope
P/N 414465-30
24 Inch P.D. Sheaves
WRI Reel C-6525

<u>Cable Load Pounds</u>	<u>Number of Stress Reversals</u>	<u>Cycles at Failure</u>	<u>Cable Load Pounds</u>	<u>Number of Stress Reversals</u>	<u>Cycles at Failure</u>
60,000	4	12053*	60,000	8	6354
75,000		12281*	75,000		4655
100,000		8015	100,000	10	2198
110,000		7797	60,000		4508
	2487	75,000	3452		
	4452	100,000	2518		
	1892	110,000	738		
	1742		794		
	2457		706		
	1575		306		
	877		189		
	802		110		
			101		

*Data from reference (1).

Table 18
Fatigue Data
1-7/16 6 x 29 FW LL RS FC Wire Rope
P/N 414465-38
24 Inch P.D. Sheaves
WRI Reel C-6521

<u>Cable Load Pounds</u>	<u>Number of Stress Reversals</u>	<u>Cycles at Failure</u>	<u>Cable Load Pounds</u>	<u>Number of Stress Reversals</u>	<u>Cycles at Failure</u>
60,000	4	14611*	75,000	8	5087
75,000		15353*	100,000		2795
100,000		9230	110,000		2683
110,000		9999	75,000		1637
		4120	100,000		3255
		3686	110,000		3332
		3489	110,000		1402
		4097	110,000		1159
		3178		1163	
		3100		884	
	1033		395		
	2272		862		
			329		
			548		

*Data from reference (1).

Table 19
Fatigue Data
1-3/8 6 x 25 FW LL RS FC Wire Rope
P/N 414465-47
24 Inch P.D. Sheaves
BE Reel 3-908-A9

<u>Cable Load Pounds</u>	<u>Number of Stress Reversals</u>	<u>Cycles at Failure</u>	<u>Cable Load Pounds</u>	<u>Number of Stress Reversals</u>	<u>Cycles at Failure</u>
75,000	4	9528	75,000	8	4701
100,000		9569	100,000		1784
100,000		4404	110,000	650	
110,000		4333	75,000	10	2658
		3510			2995
		3733			472
		2278			280
		869			121
		556			197
		679			119
	687	160			
			110,000		94
					91

Table 20
Fatigue Data
1-3/8 6 x 25 FW LL RS FC Wire Rope
P/N 414465-39
24 Inch P.D. Sheaves
PW Reel 49117

<u>Cable Load Pounds</u>	<u>Number of Stress Reversals</u>	<u>Cycles at Failure</u>	<u>Cable Load Pounds</u>	<u>Number of Stress Reversals</u>	<u>Cycles at Failure</u>
75,000	4	9844	110,000	4	321
↓		9522			710
100,000		4388			786
↓		5011			455
↓		5100			823
		4872			1774

Table 21
Outer Layer Wire Notching Data
1-3/8 6 x 25 FW LL RS Construction
Dacron, Nylon, Polypropylene and Fiber Core
Four Stress Reversals Per Cycle

<u>Rope Core Material</u>	<u>Cable Load Pounds</u>	<u>Fatigue Region</u>	<u>Depth of Notch - Mils</u>		<u>Cycles at Failure</u>	<u>Notching Rate Mils/Cycle</u>	
			<u>Average Value</u>	<u>Std. Dev.</u>			
Dacron	60,000	F	13.875	2.610	13862	.001001	
			12.792	1.382	13321	.000960	
	75,000	F	9.708	-	8569	.001133	
			11.167	-	8341	.001339	
	90,000	F	13.478	2.042	8523	.001581	
			13.542	2.284	8903	.001521	
	100,000	F	11.604	-	6598	.001759	
			11.729	-	6518	.001799	
	110,000	H	12.125	-	4467	.002714	
			F	11.542	-	5718	.002019
			H	10.896	-	1863	.005849
			10.167	-	1345	.007559	
Nylon	40,000	F	11.875	1.825	19494	.000609	
			12.708	3.316	17091	.000744	
	75,000	F	11.417	2.283	9096	.001255	
			11.083	2.145	9613	.001153	
	90,000	F	13.208	1.956	9774	.001351	
			13.542	2.992	9409	.001439	
	100,000	H	14.458	2.377	8919	.001621	
			15.333	2.200	9029	.001698	
	110,000	H	15.250	2.691	4262	.003578	
			12.542	1.956	2600	.004824	
				13.750	2.069	2320	.005927
				13.667	2.697	3850	.003550
				12.500	2.670	1109	.011271
			13.392	3.303	1389	.009569	
Poly.	75,000	F	10.000	1.911	7132	.001402	
			12.917	1.792	7924	.001630	
	100,000	F	10.042	1.805	4789	.002097	
			12.625	2.081	4900	.002577	
	110,000	H	10.667	1.685	4087	.002610	
			11.917	2.717	4782	.002492	
				12.208	3.162	2140	.005705
				9.750	0.944	2185	.004462
			11.208	1.560	1847	.006068	
			11.792	1.888	2791	.004225	

Table 22
Outer Layer Wire Notching Data
1-3/8 6 x 25 FW LL RS Construction
Dacron, Nylon, Polypropylene and Fiber Core
Ten Stress Reversals Per Cycle

<u>Rope Core Material</u>	<u>Cable Load Pounds</u>	<u>Fatigue Region</u>	<u>Depth of Notch - Mils</u>		<u>Cycles at Failure</u>	<u>Notching Rate Mils/Cycle</u>	
			<u>Average Value</u>	<u>Std. Dev.</u>			
Dacron ↓	75,000	F	11.417	1.257	4054	.002816	
			10.875	1.746	4053	.002683	
			13.729	1.934	3724	.003687	
	100,000		16.292	3.150	2146	.007592	
		110,000	H	12.583	3.127	282	.044621
				16.705	3.791	829	.020151
Nylon ↓	75,000	F	13.583	1.998	3191	.004257	
			13.208	1.865	3402	.003882	
			16.875	3.012	2085	.008094	
	100,000	H	16.500	4.737	847	.019481	
		F	15.750	3.542	2275	.006923	
			15.792	2.670	1810	.008725	
Poly. ↓	75,000	F	13.917	2.701	2596	.005361	
			14.208	1.719	2371	.005992	
			14.125	2.173	1149	.012293	
	100,000	H	11.667	1.761	606	.019252	
		F	15.000	2.359	1023	.014663	
			16.083	2.339	1003	.016035	
	110,000	H	12.667	3.185	270	.046915	
			14.042	3.085	526	.026696	
			14.500	2.978	412	.035194	
Fiber ↓	70,000	F	10.833	2.396	3316	.003267	
	80,000	H	12.556	2.405	2612	.004807	
	110,000	H	12.083	2.882	35	.34523	
			14.194	3.763	54	.26285	

Table 23
Summary of Steady State Creep Data
"F" Region Fatigue
6 x 25 FW LL RS Wire Rope
with Dacron, Nylon and Fiber Cores

<u>Core Material</u>	<u>Tester</u>	<u>Mfg.</u>	<u>Cable Load Kips</u>	<u>Cycles at Failure</u>	<u>Strain Rate In./In./Cycle</u>	<u>Constant</u>	
Dacron ↓	2 Sheave ↓	BE ↓	75	8455	.0000005765	.005180	
			90	8523	.0000005851	.004987	
			100	4467	.0000011186	.004997	
	5 Sheave ↓		75	3724	.0000013619	.005072	
			100	2146	.0000026135	.005609	
Nylon ↓	2 Sheave ↓	BE ↓	40	17091	.0000001342	.002294	
			75	9409	.0000002147	.002020	
			90	8919	.0000002699	.002408	
Fiber ↓	2 Sheave ↓		WRI ↓	70	8716	.0000002374	.002069
				80	6123	.0000004032	.002469
				90	5044	.0000004407	.002223
	5 Sheave ↓	60		2759	.0000008819	.002433	
		80		2612	.0000009166	.002394	
		BE ↓		60	3521	.0000006492	.002351
				75	2658	.0000008741	.002323

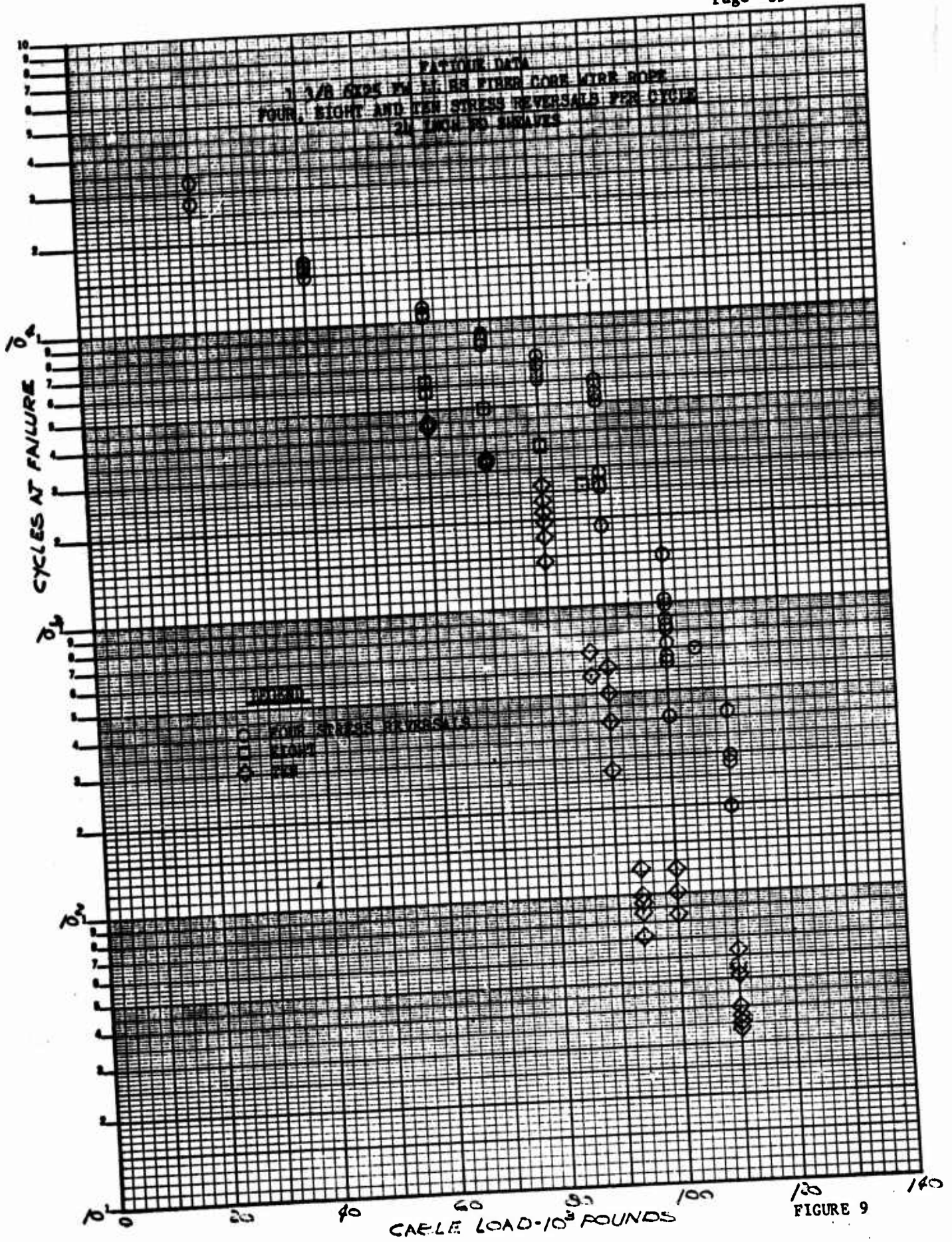


FIGURE 9

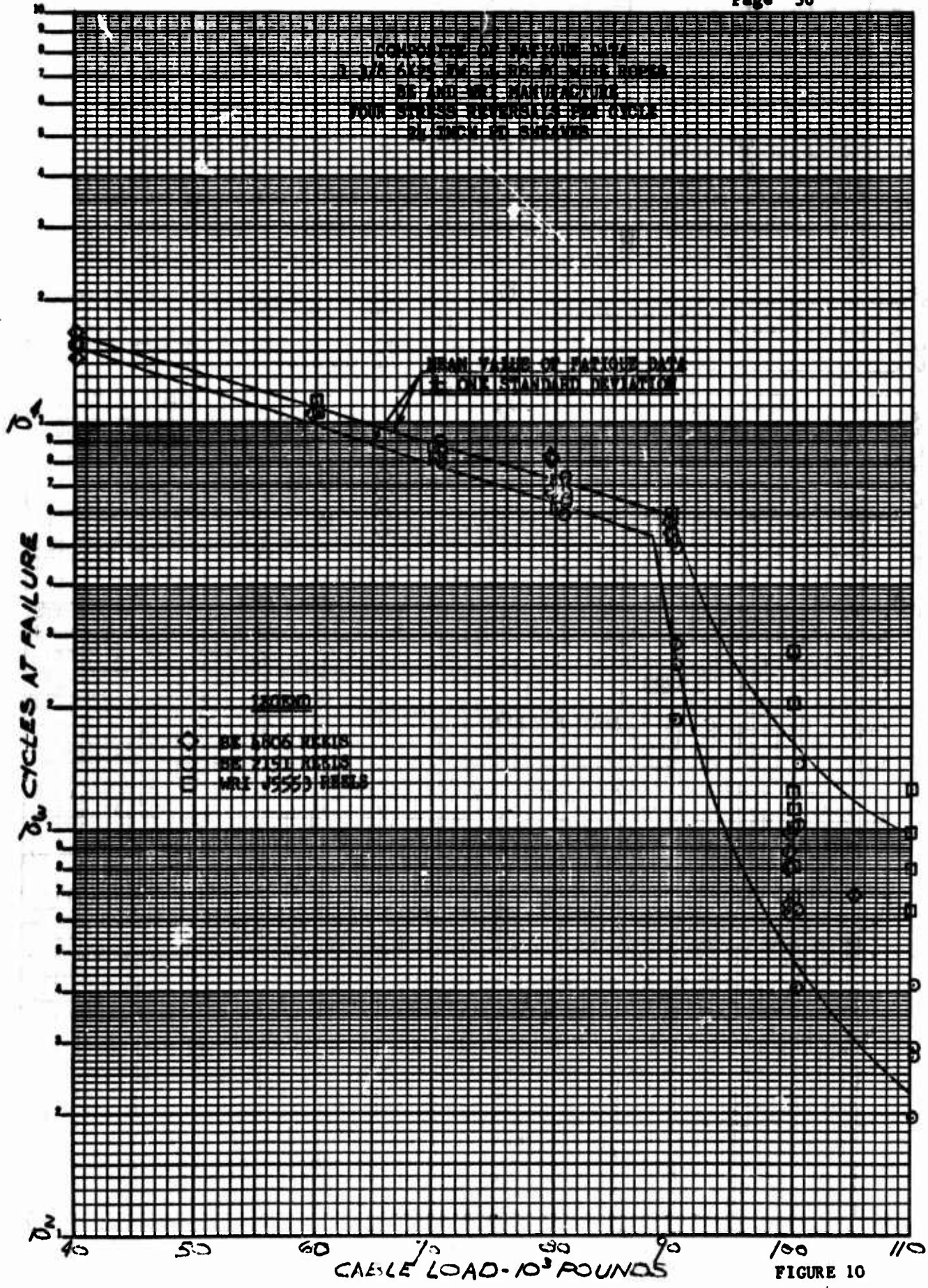


FIGURE 10

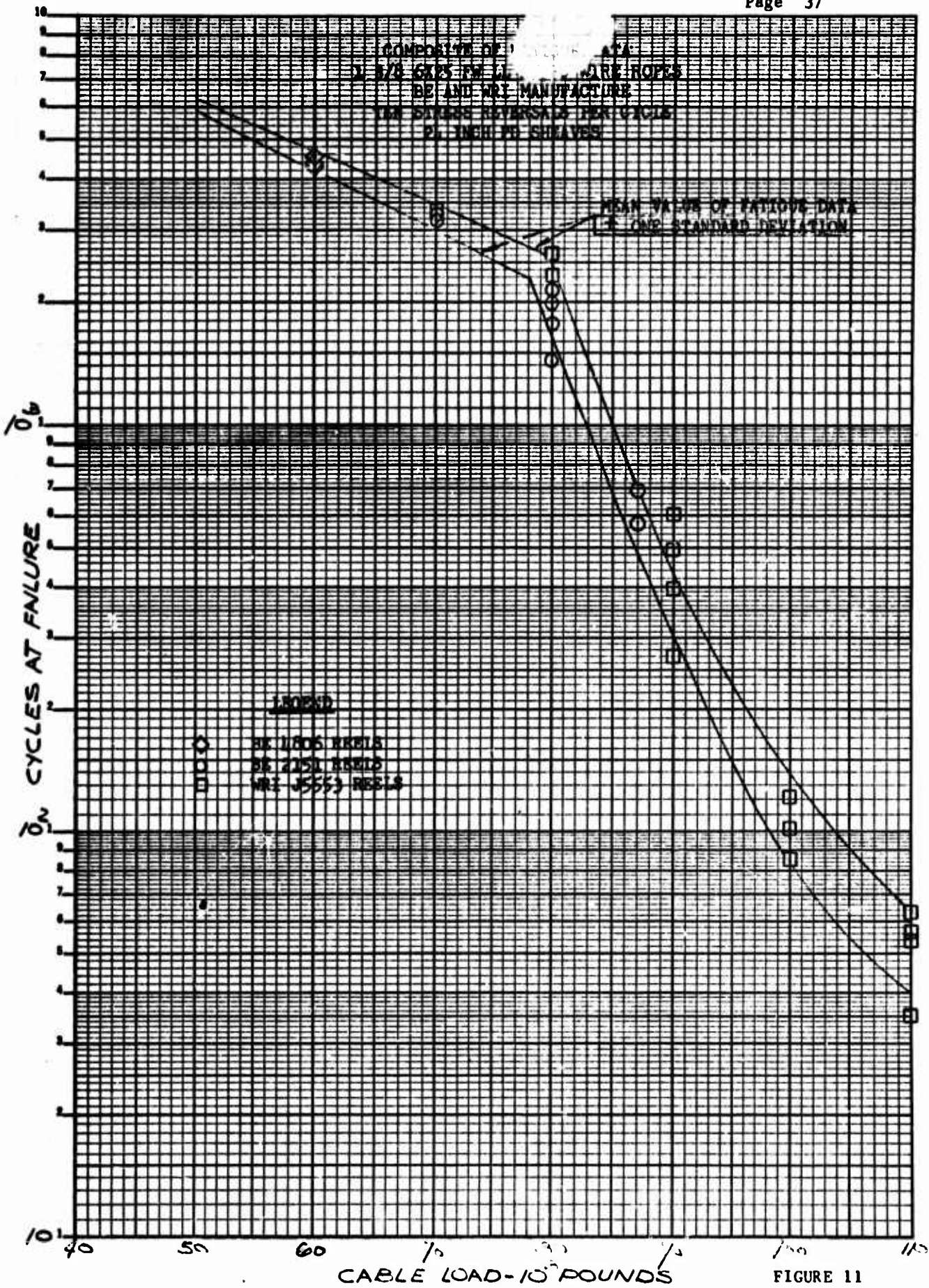


FIGURE 11

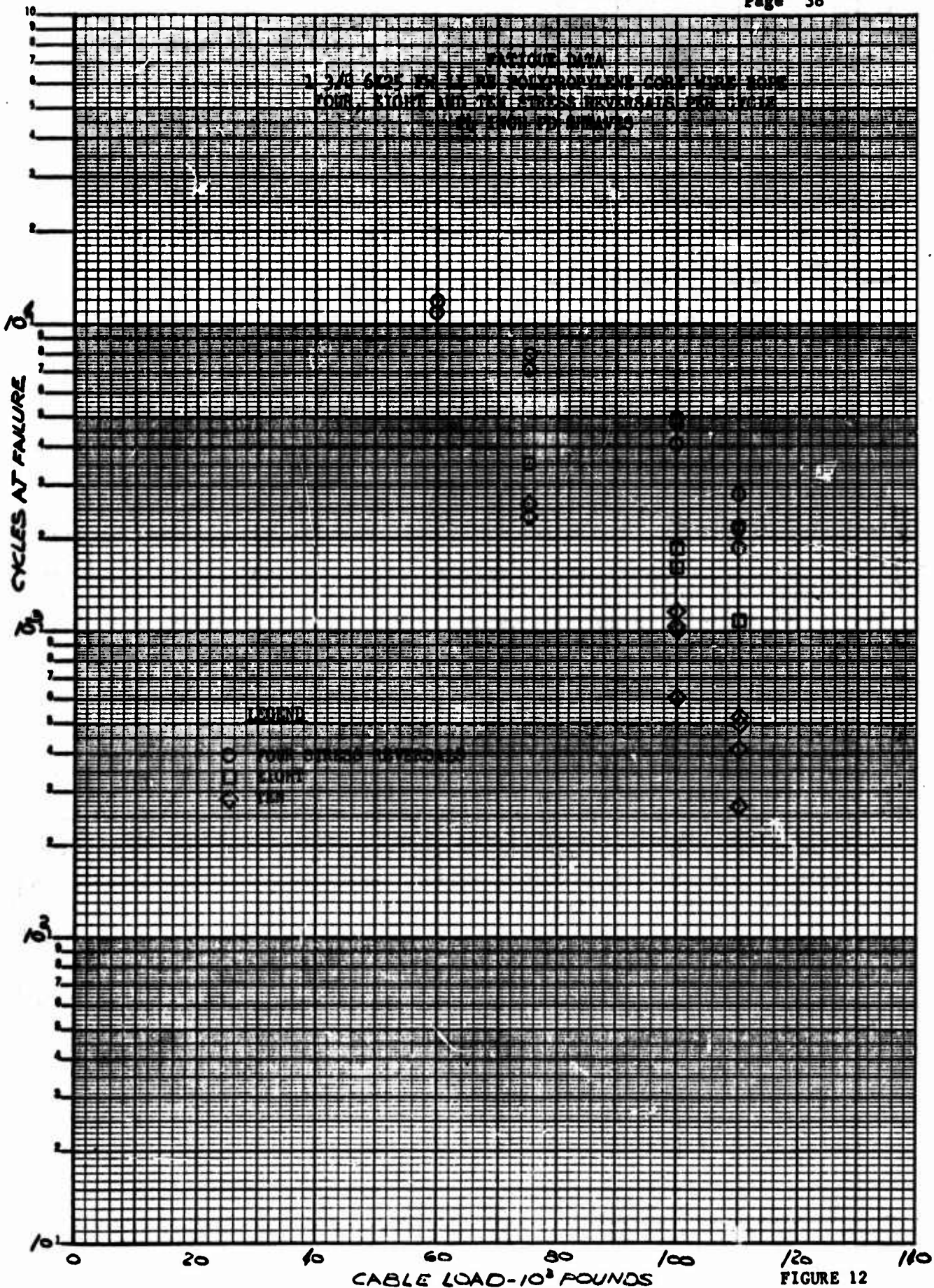


FIGURE 12

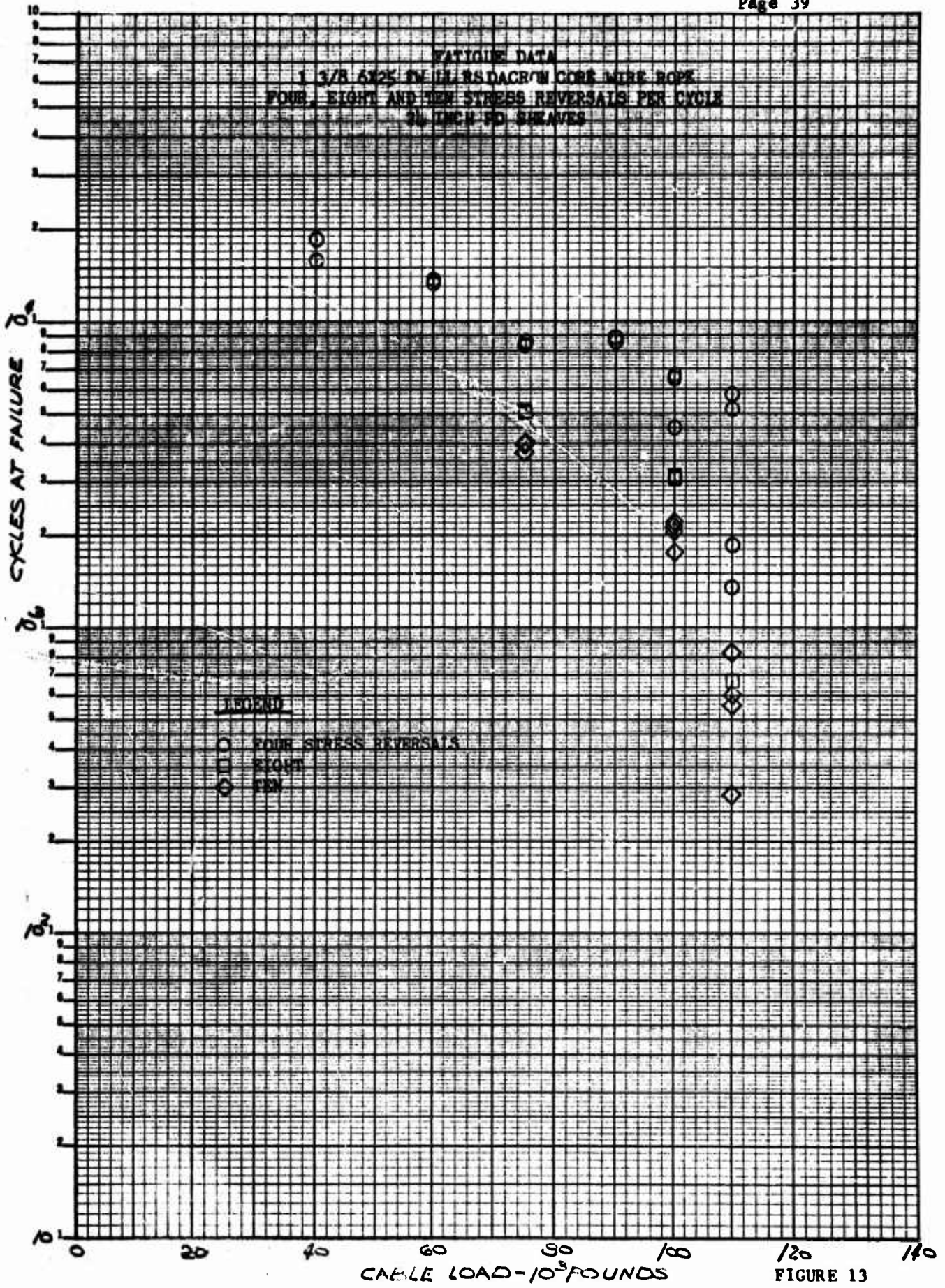


FIGURE 13

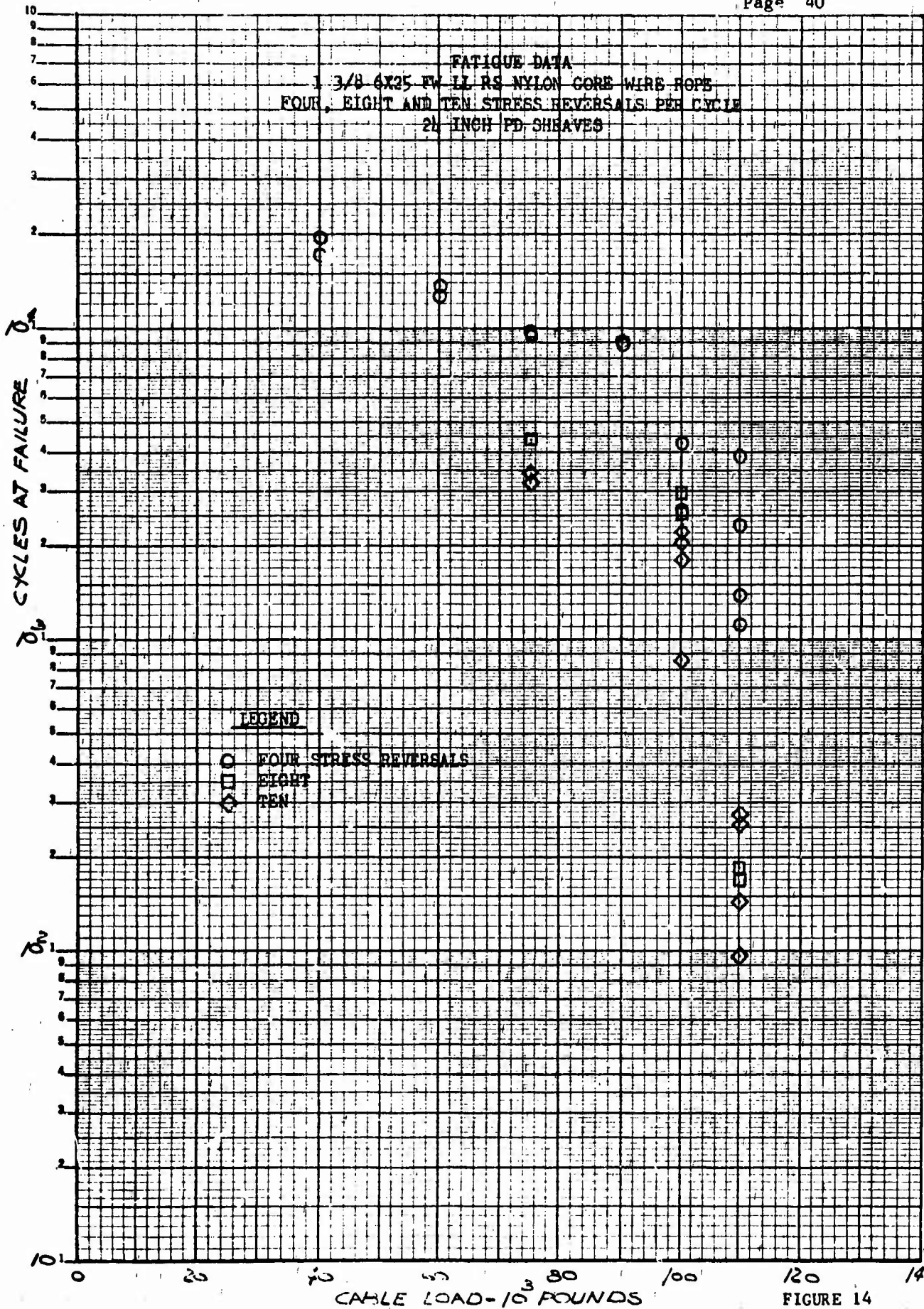


FIGURE 14

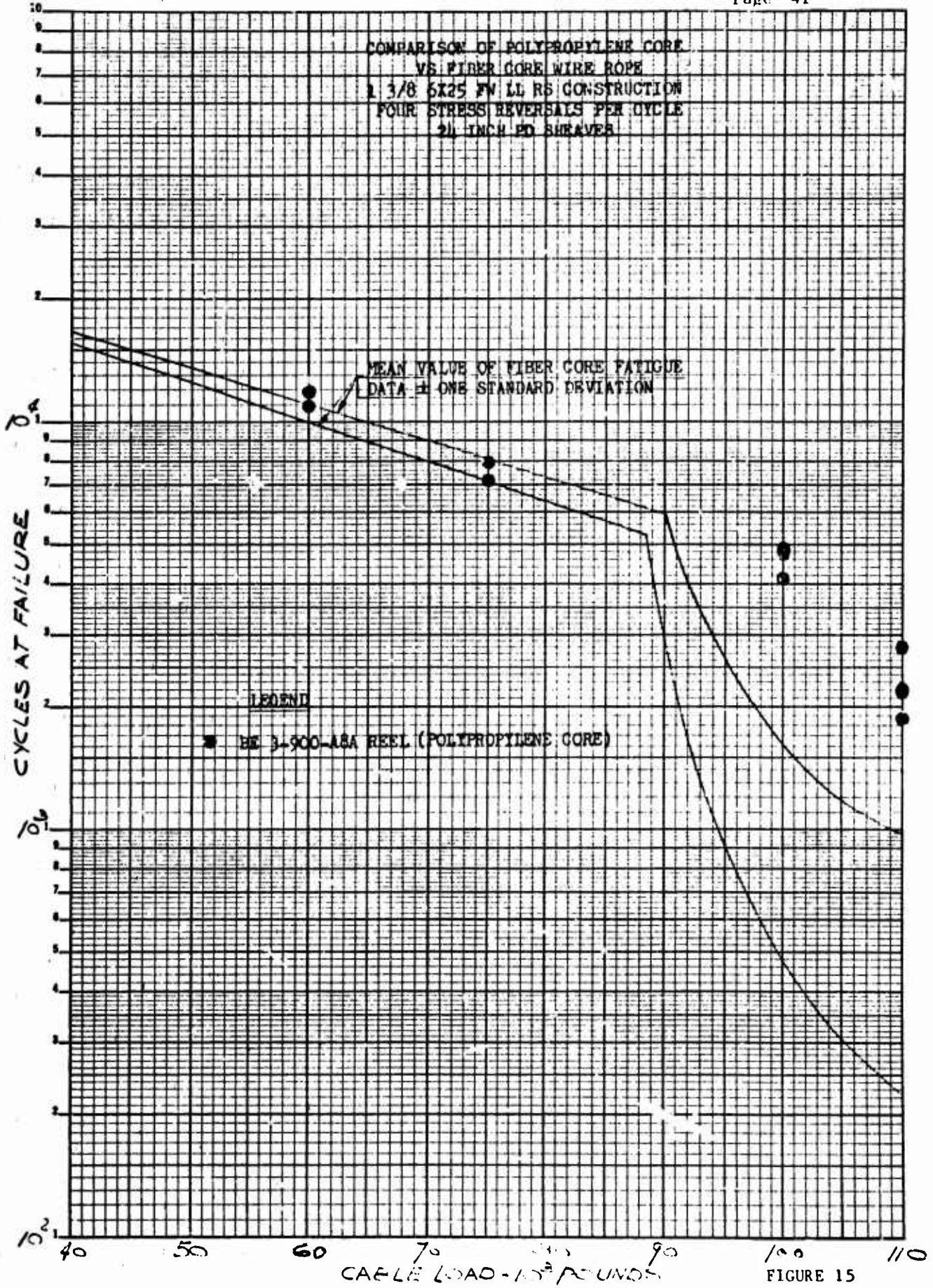
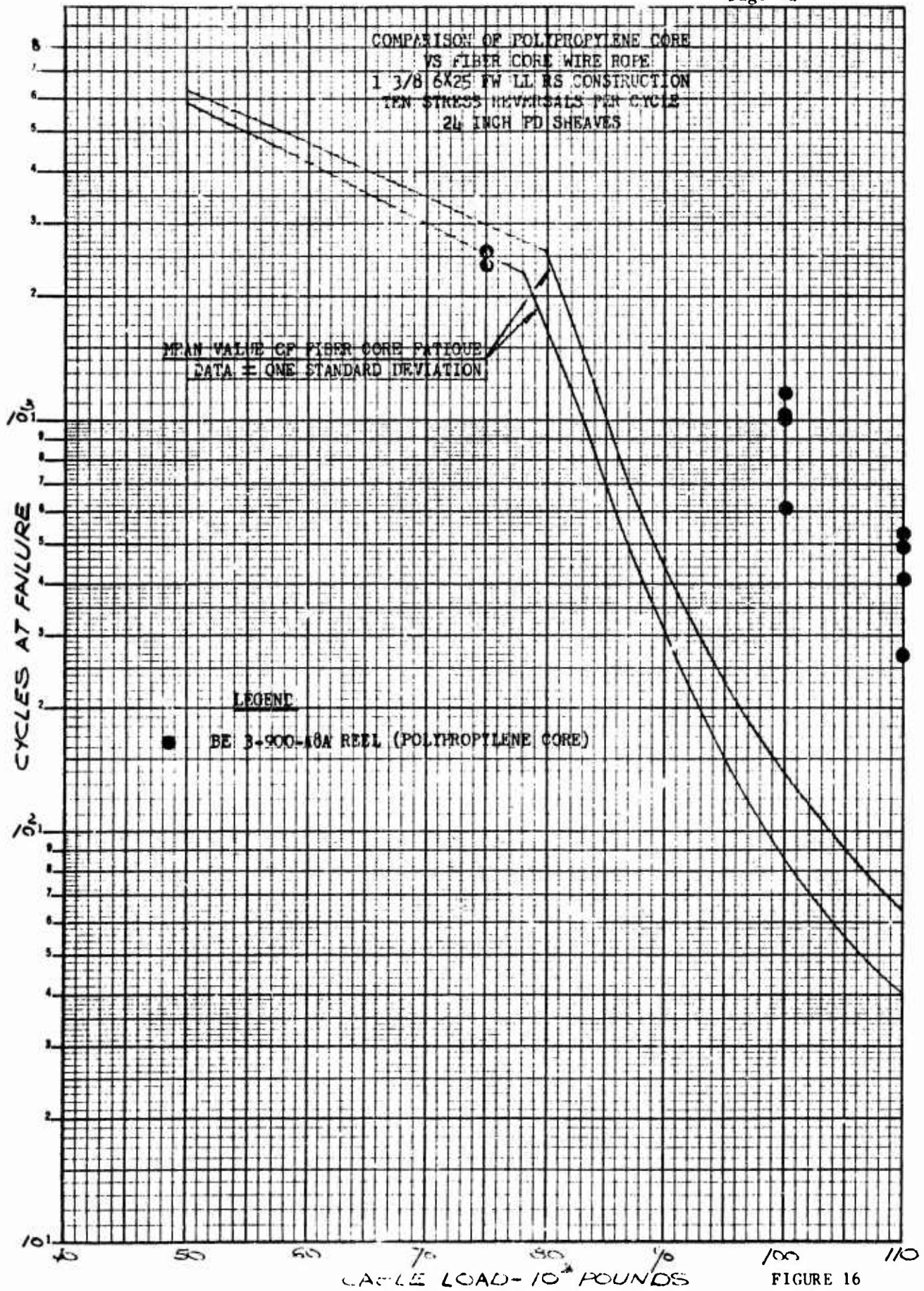


FIGURE 15



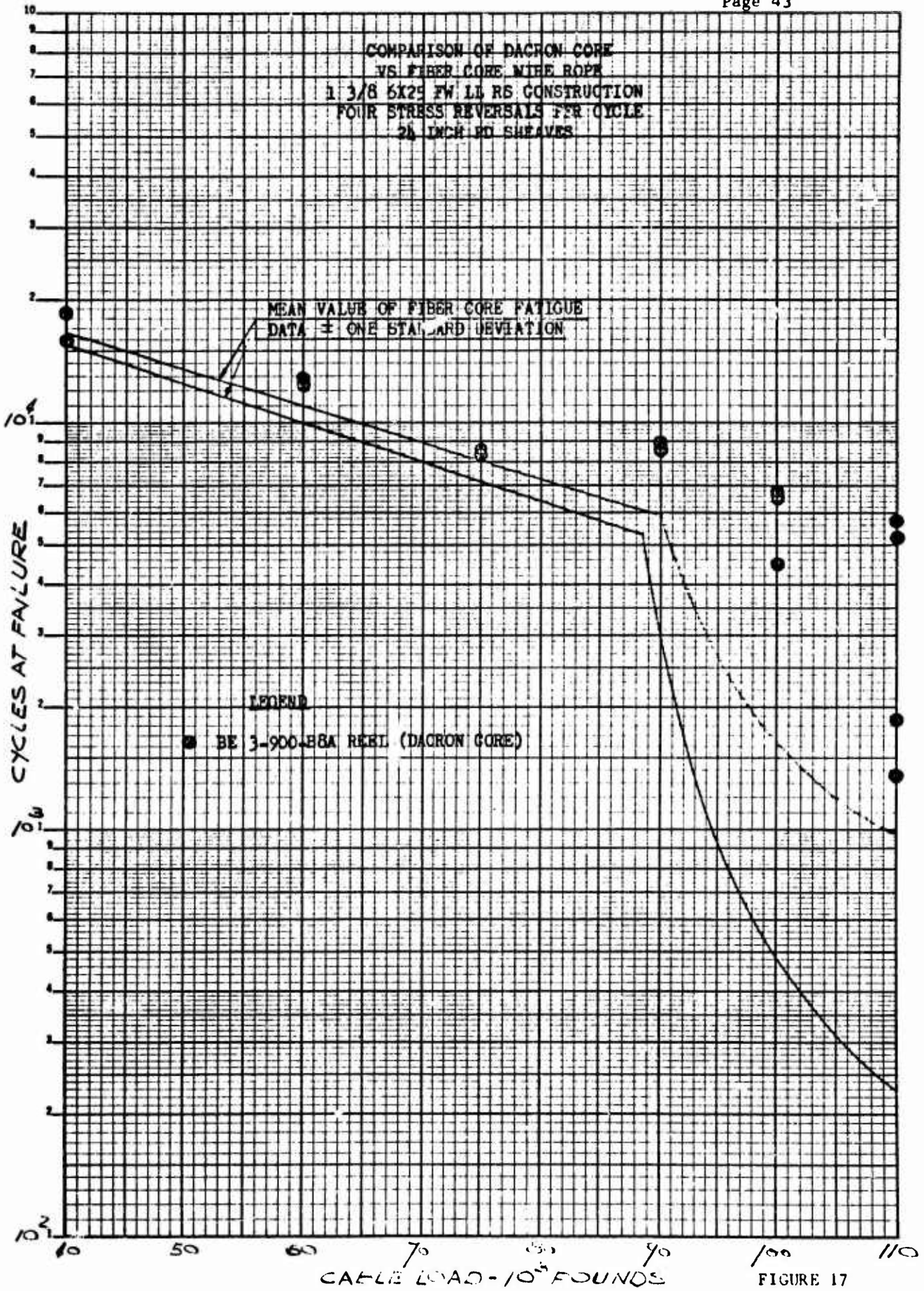


FIGURE 17

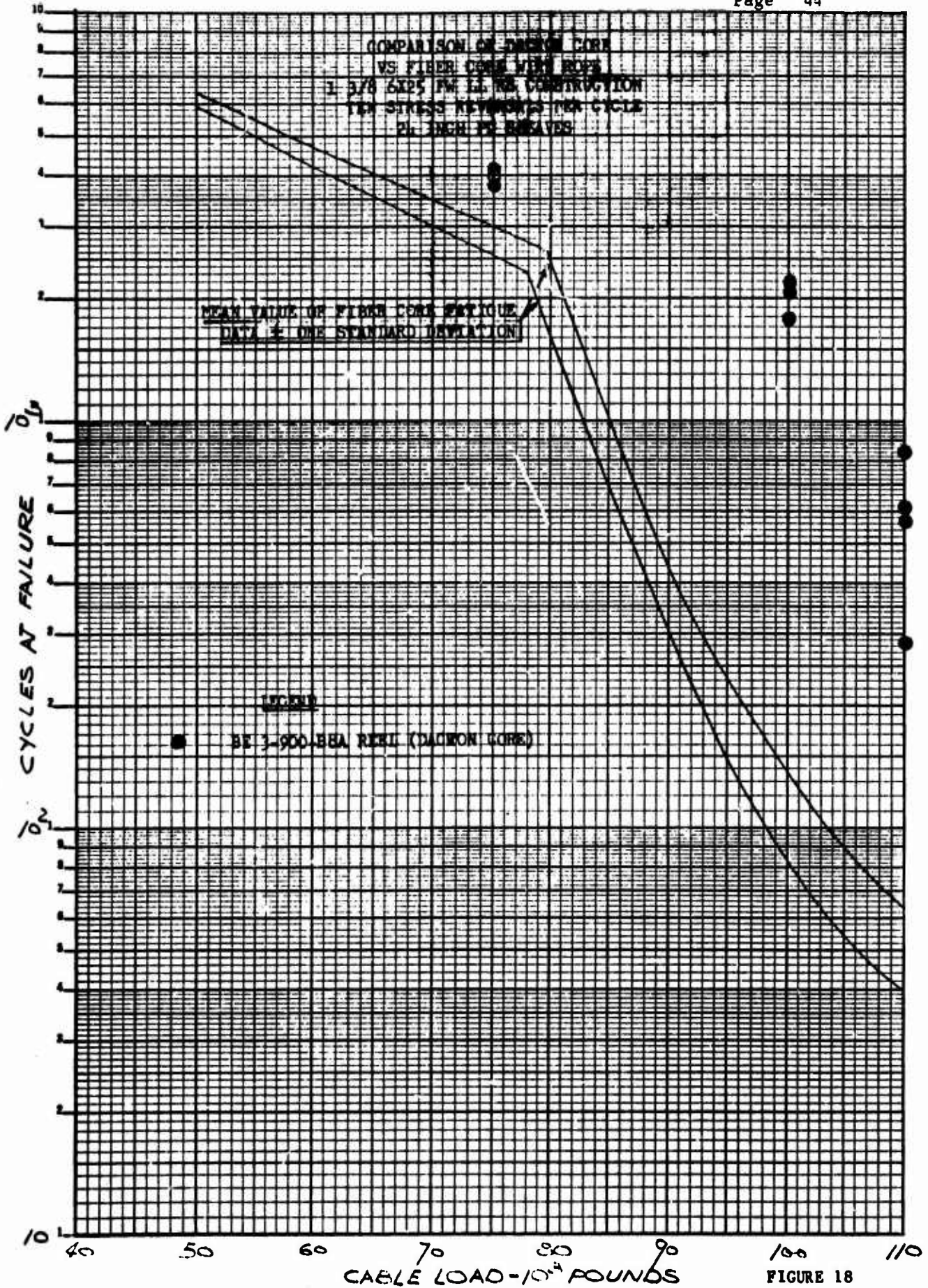


FIGURE 18

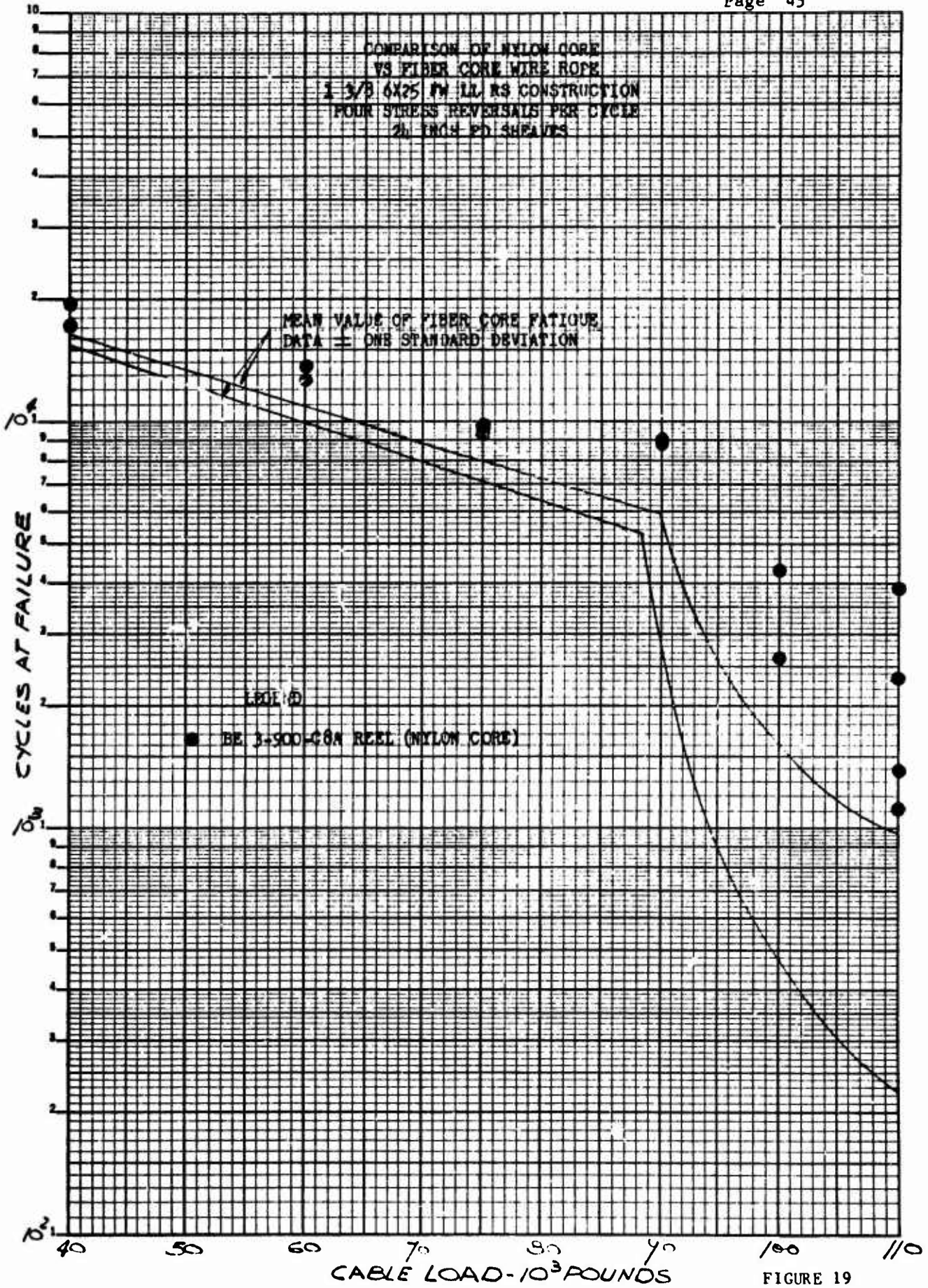


FIGURE 19

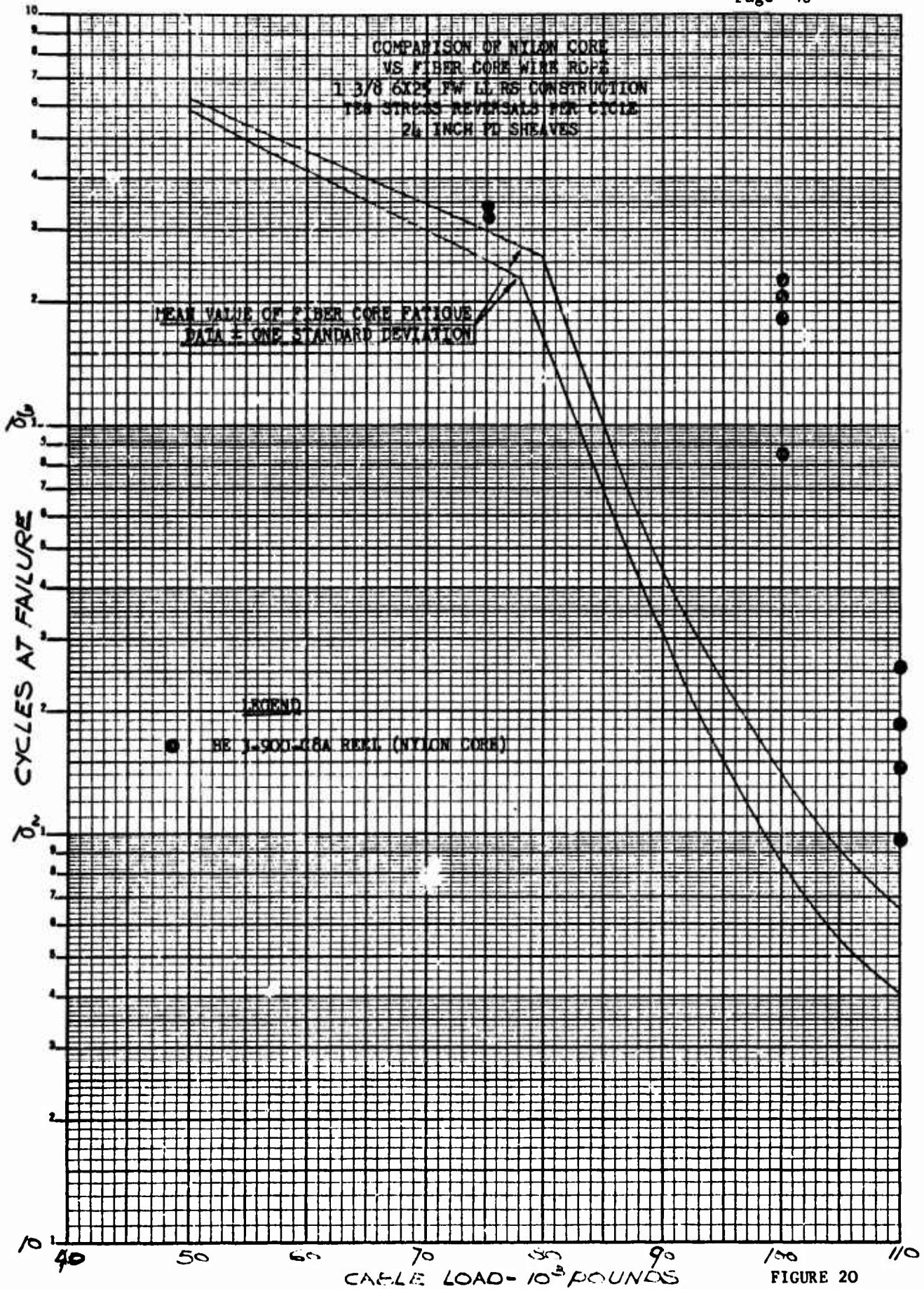


FIGURE 20

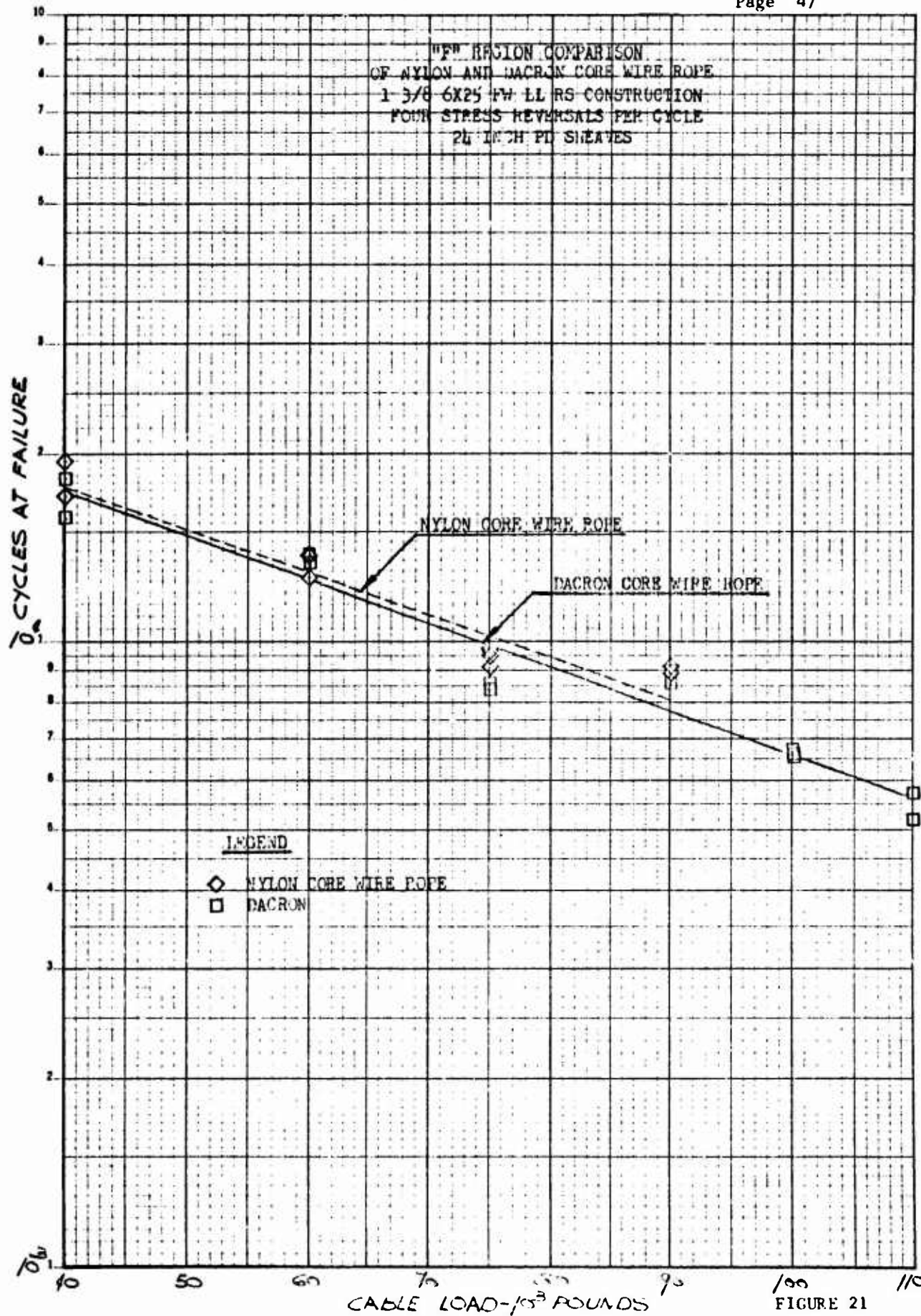


FIGURE 21

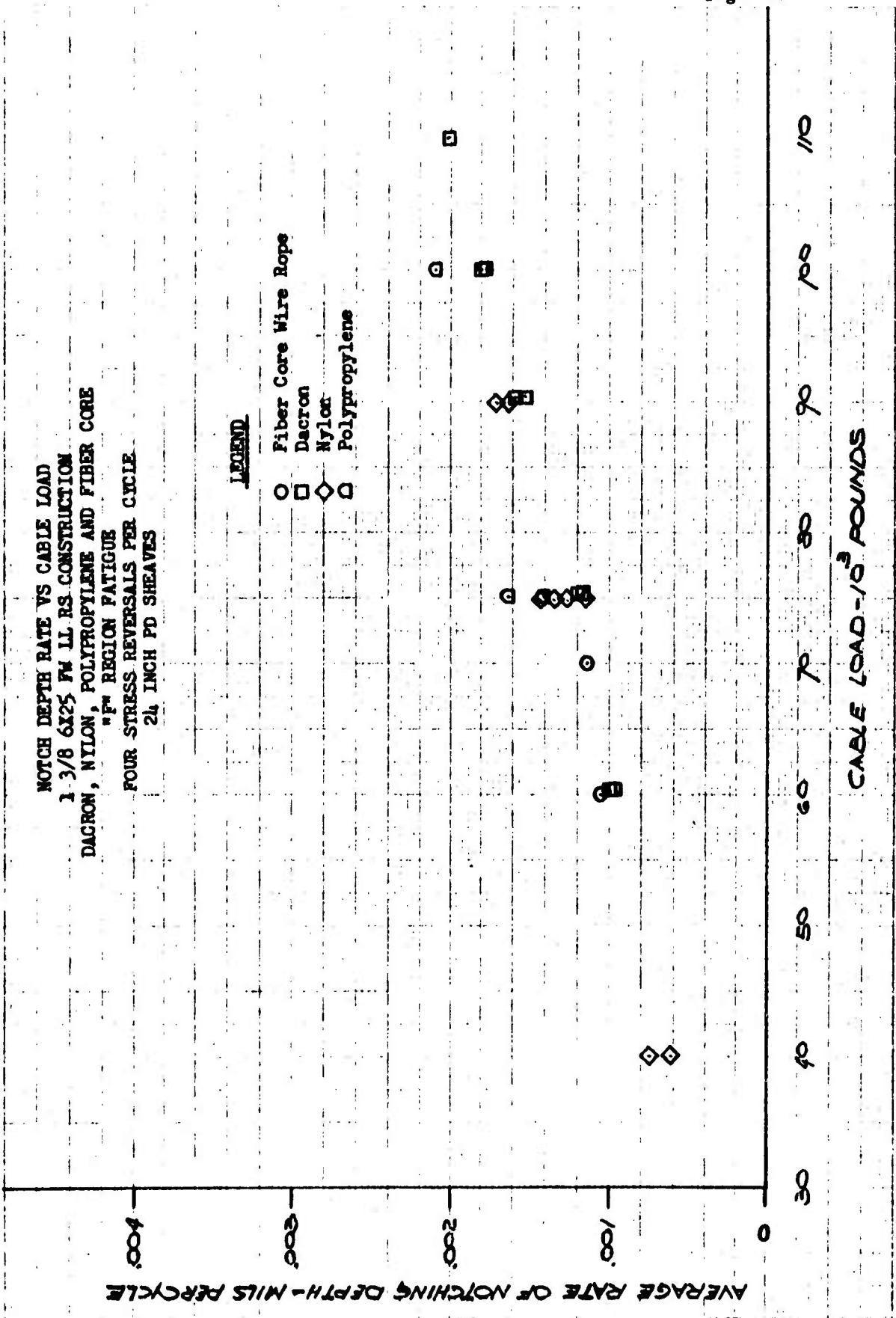


FIGURE 22

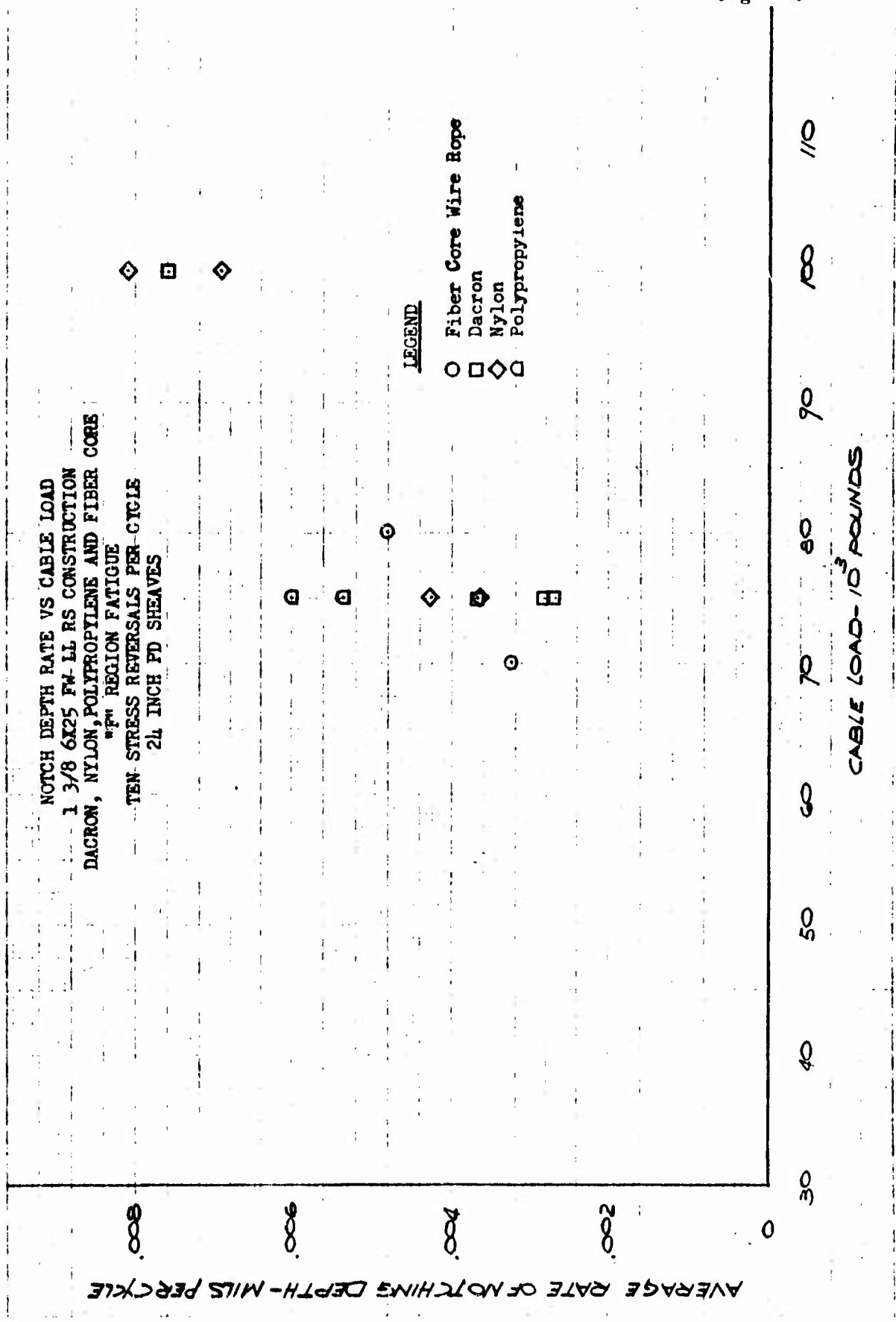


FIGURE 23

TOTAL CYCLIC STRAIN
1 3/8 6X25 FW LL RS
FIBER CORE WIRE ROPE
FOUR STRESS REVERSALS PER CYCLE
2 1/2 INCH PD SHEAVES

LEGEND

- 70000 Pound Cable Load
- 80000
- ◇ 90000

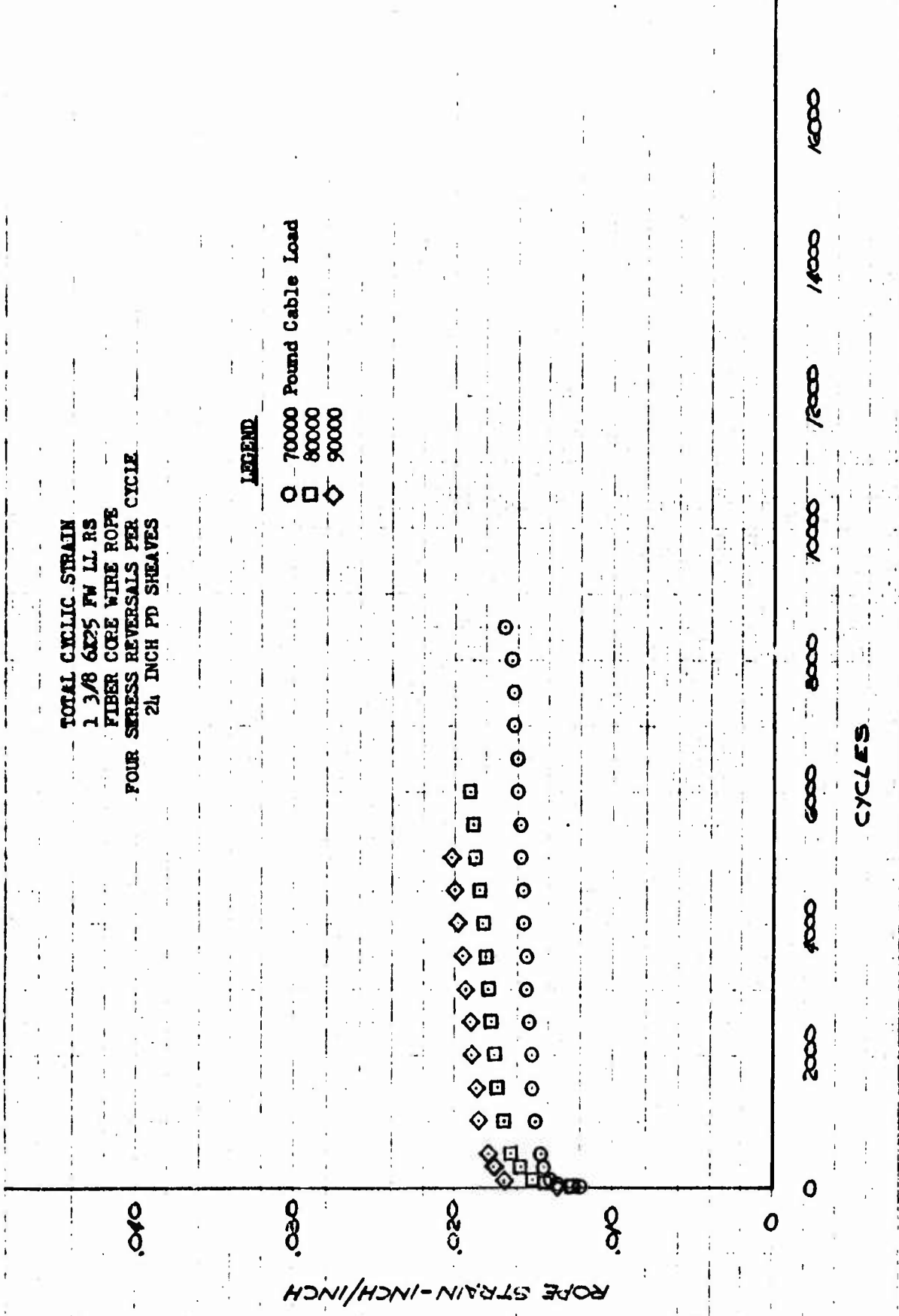


FIGURE 24

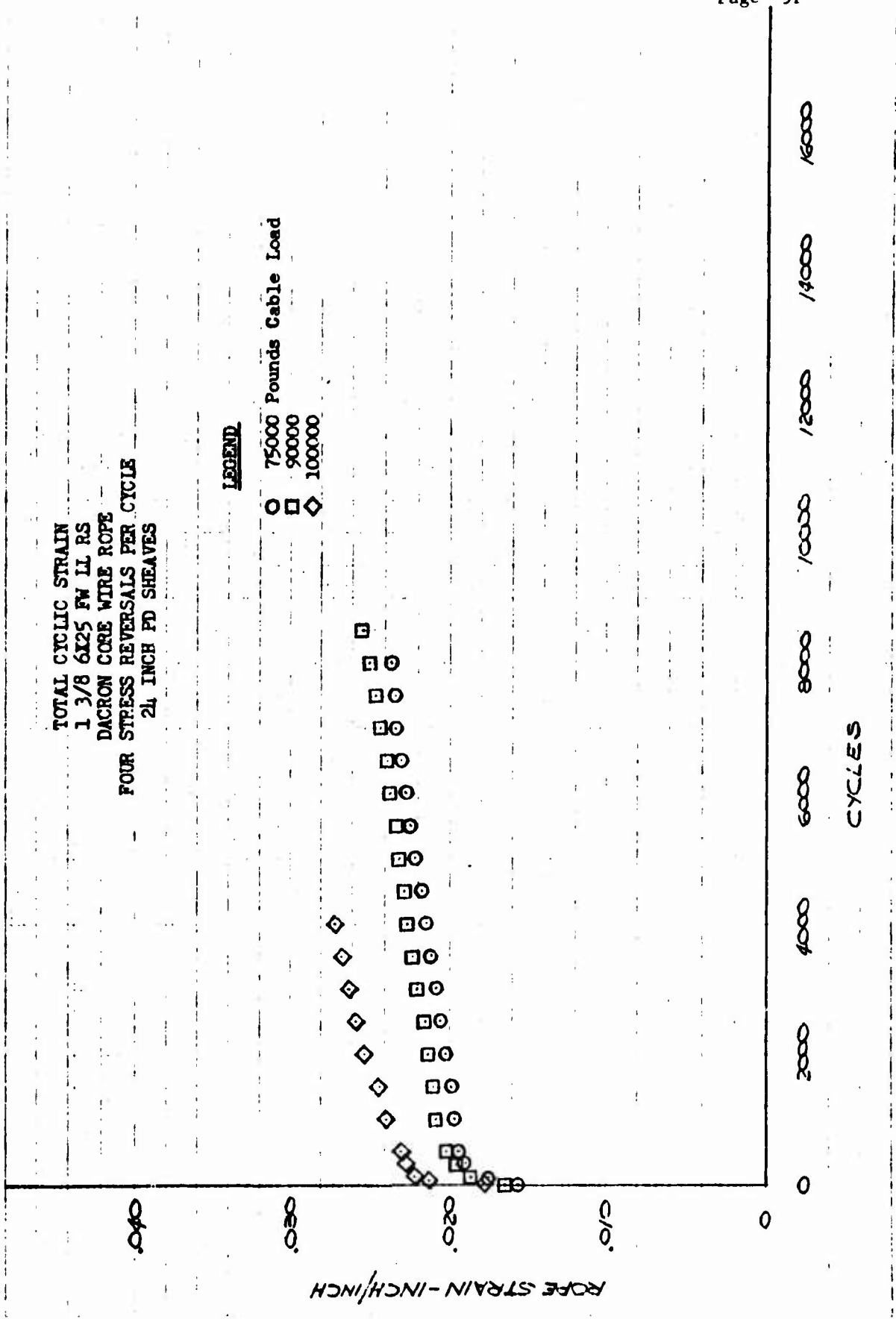


FIGURE 25

TOTAL CYCLIC STRAIN
 1 3/8 6x25 FW LL RS
 NYLON CORE WIRE ROPE
 FOUR STRESS REVERSALS PER CYCLE
 2 1/2 INCH PD SHEAVES

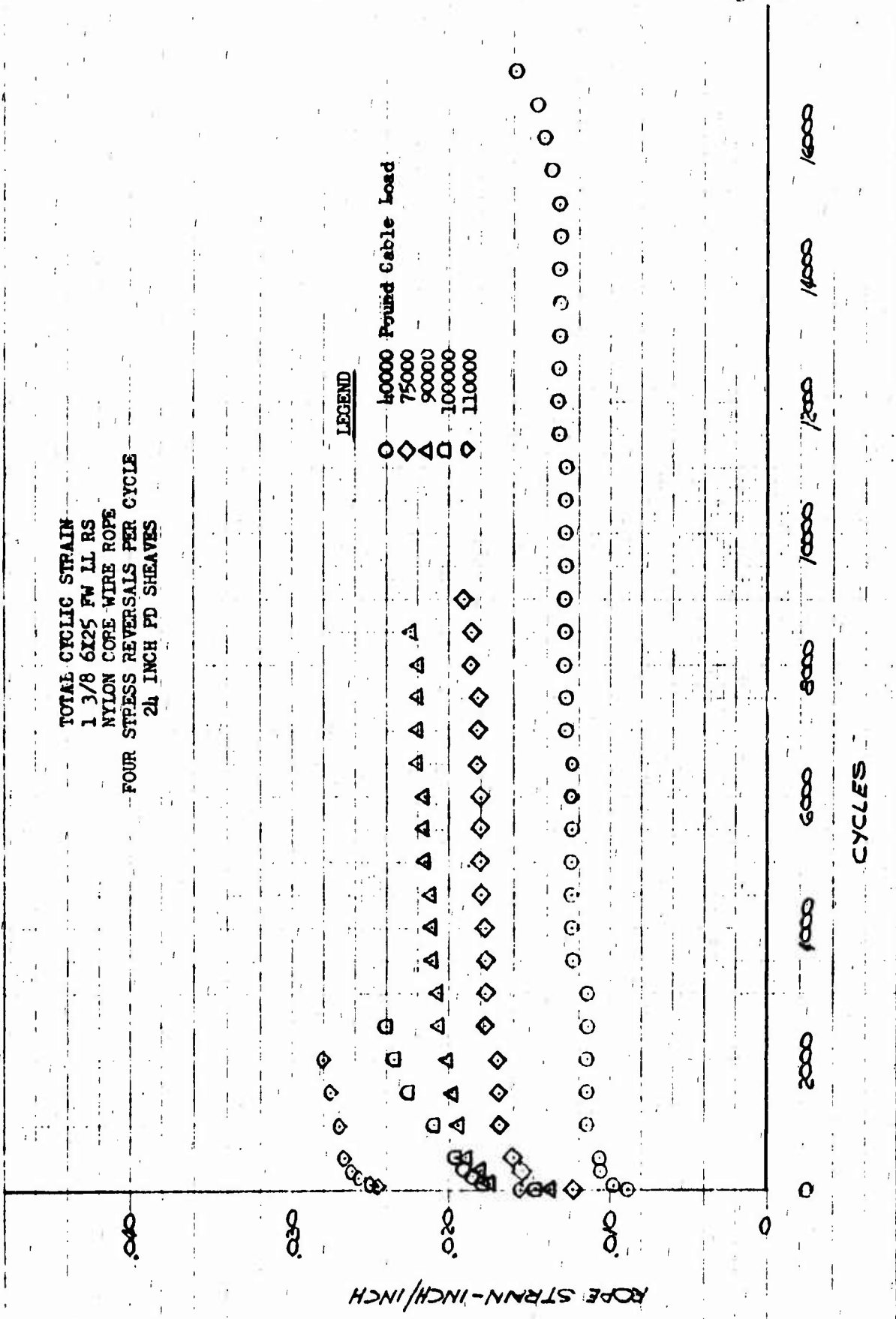


FIGURE 26

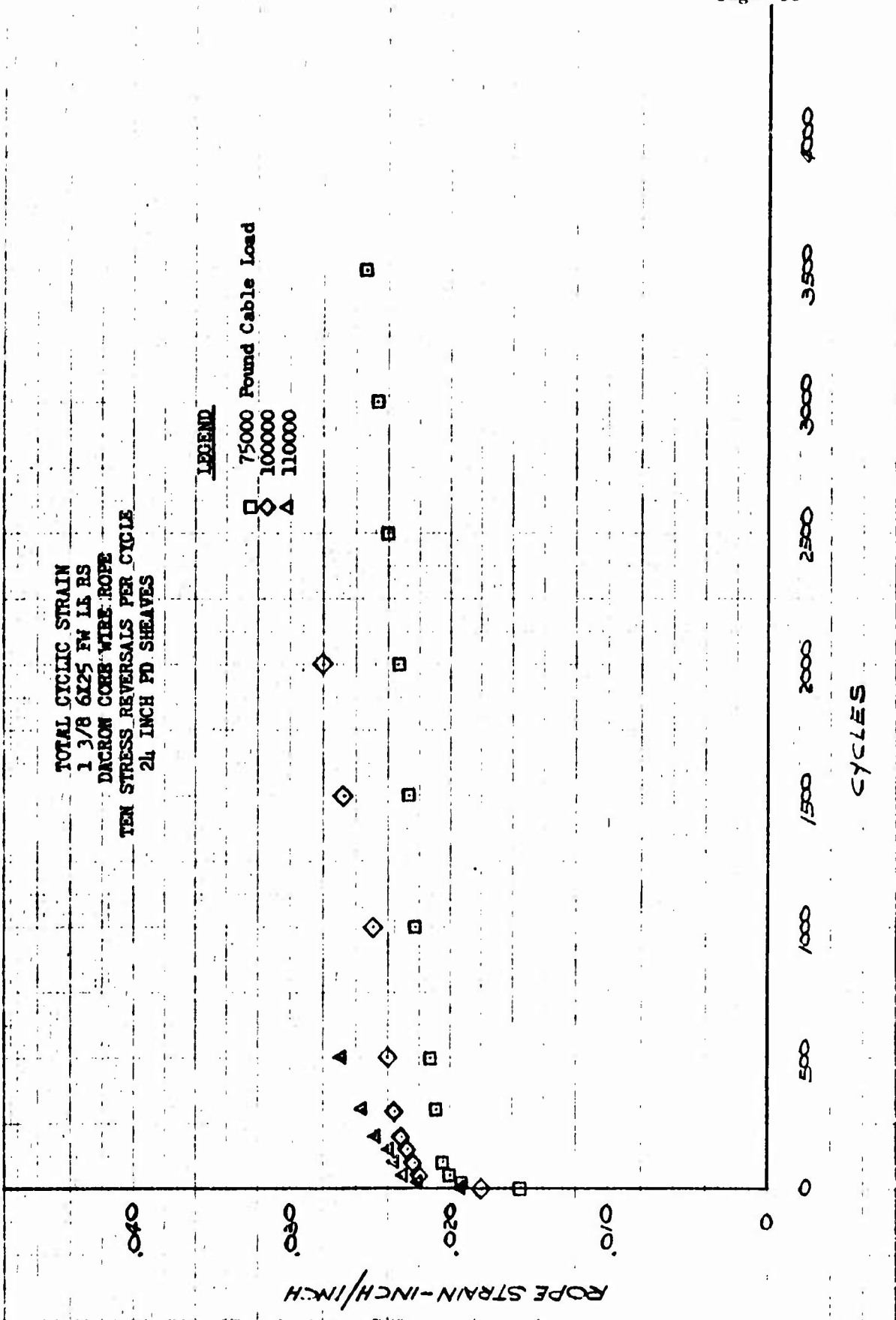


FIGURE 27

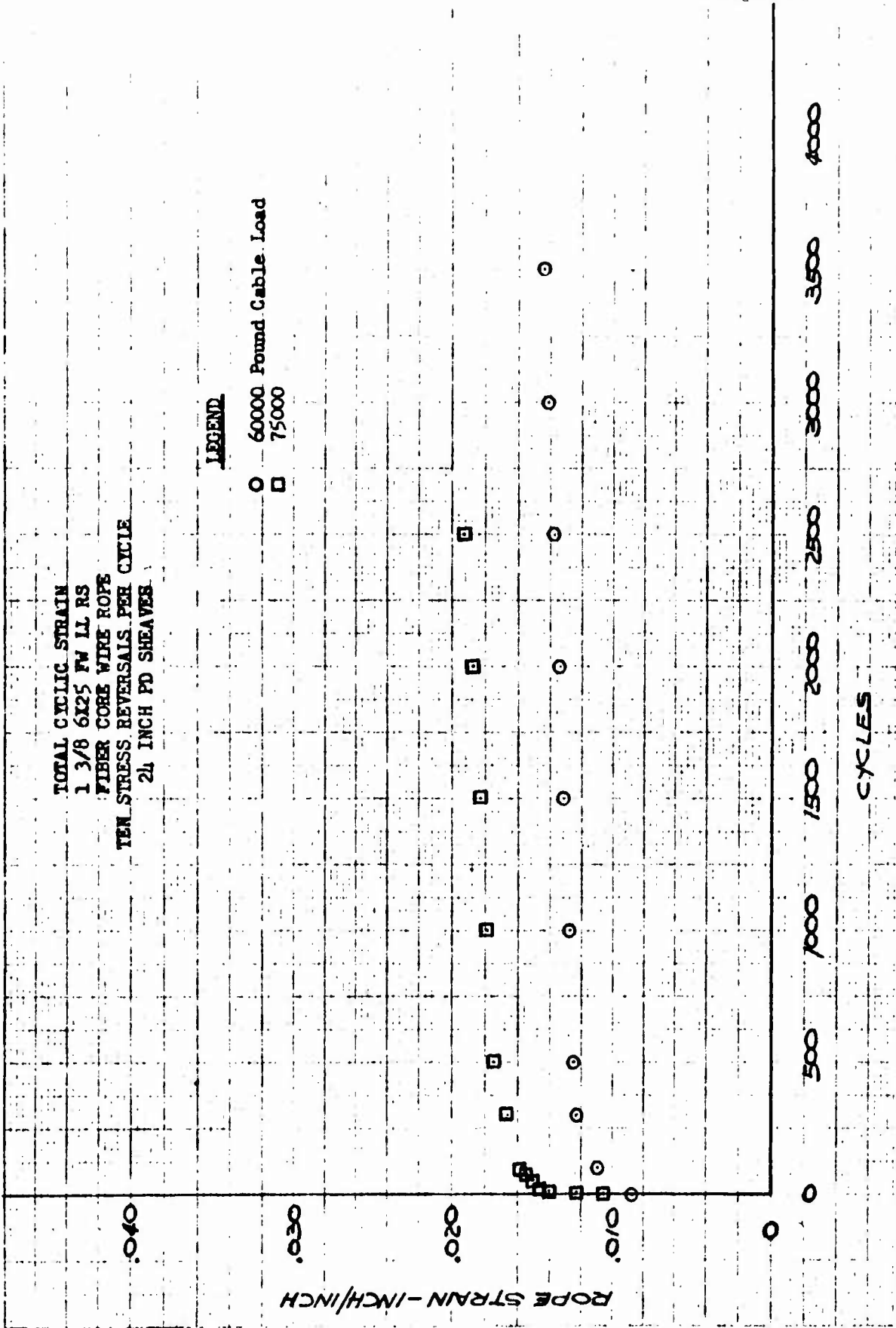


FIGURE 28

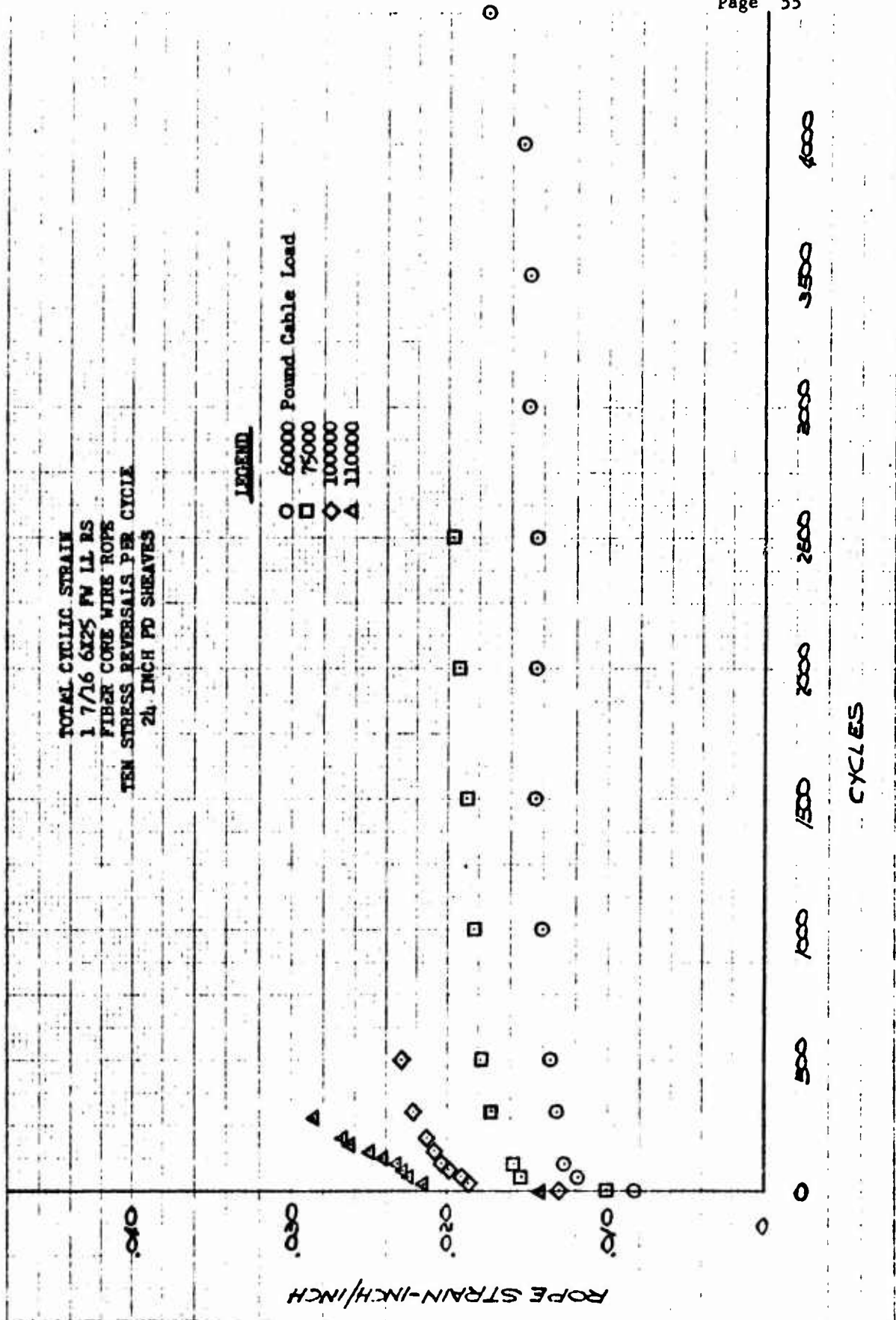


FIGURE 29

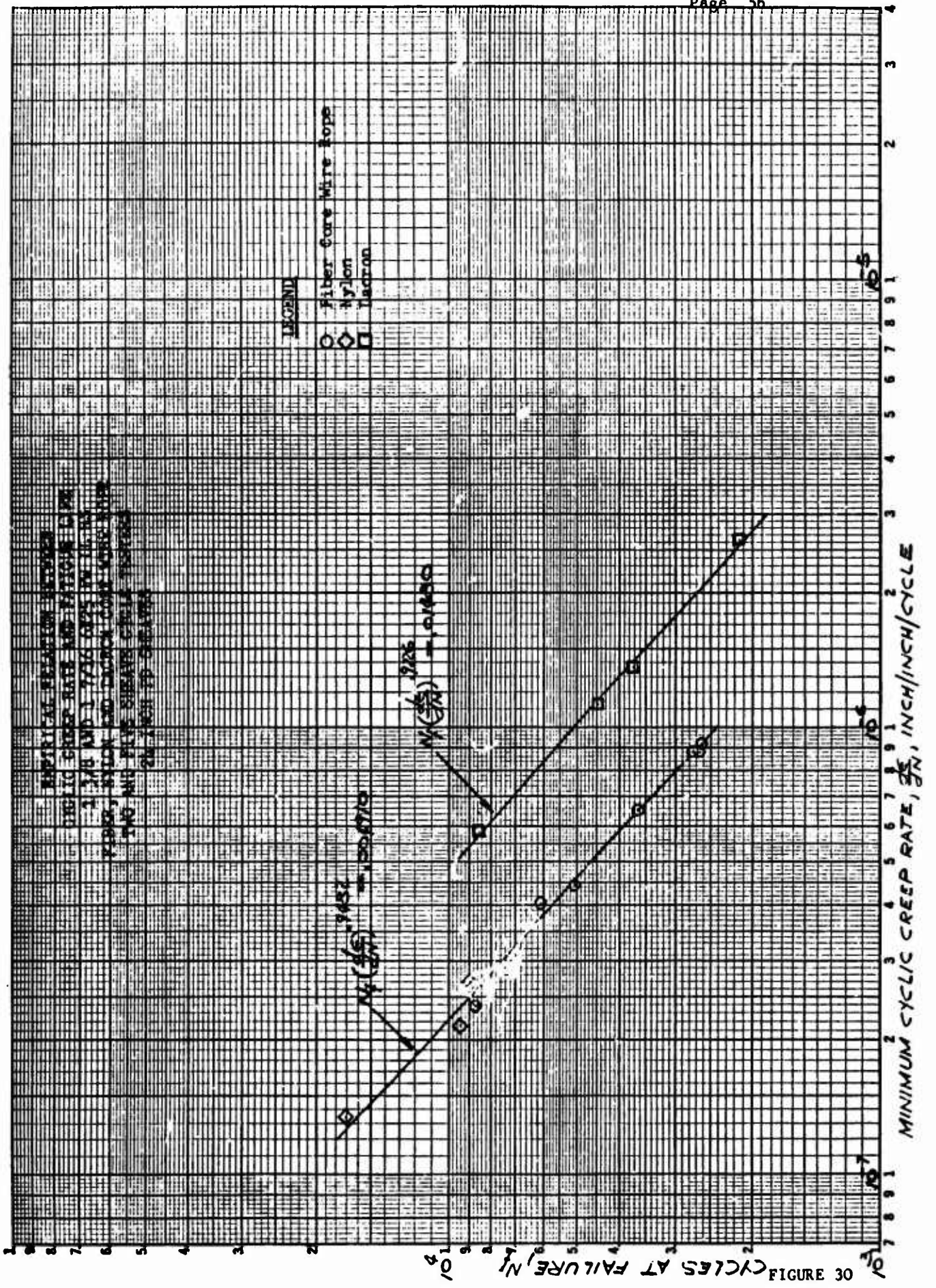


FIGURE 30

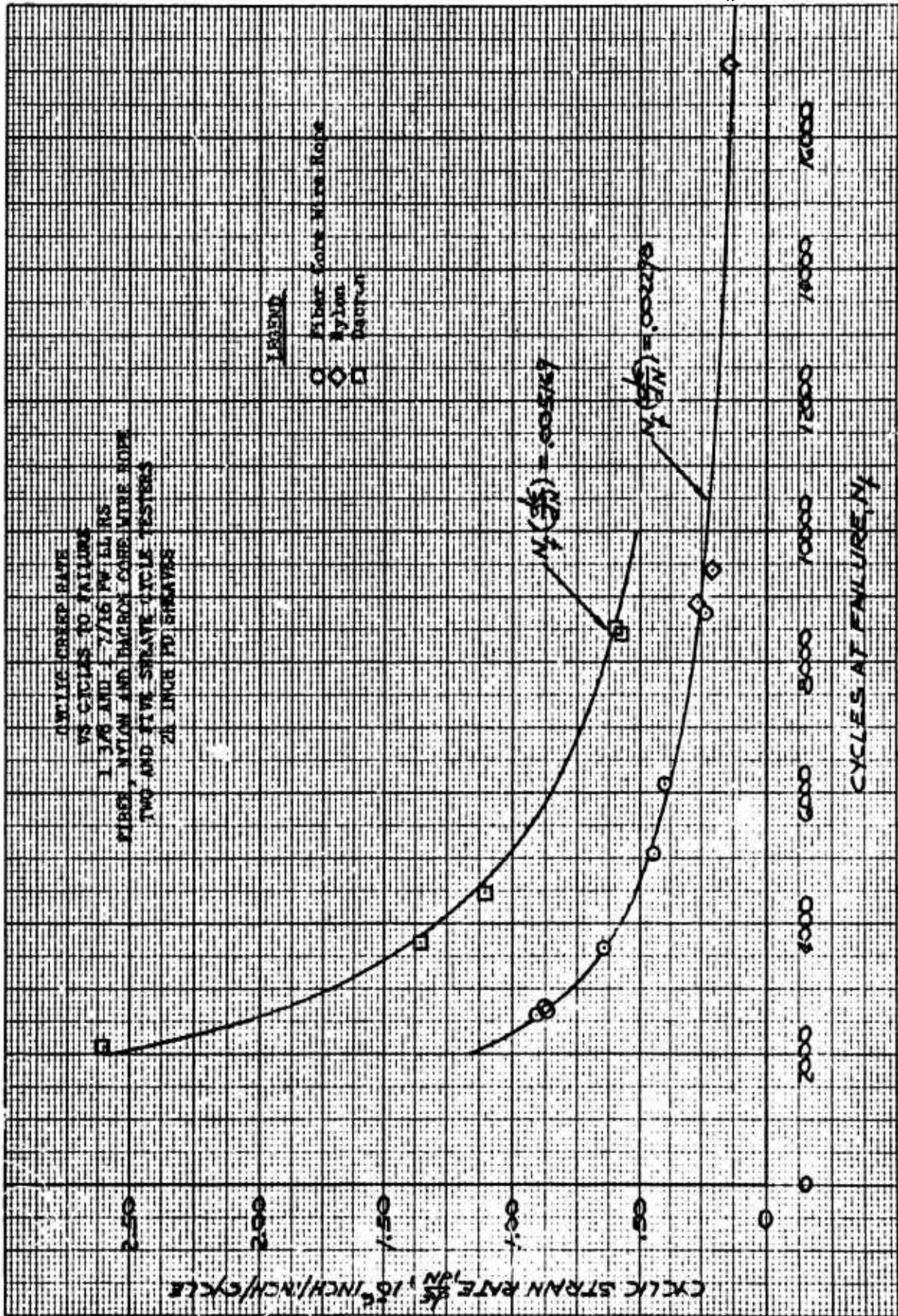
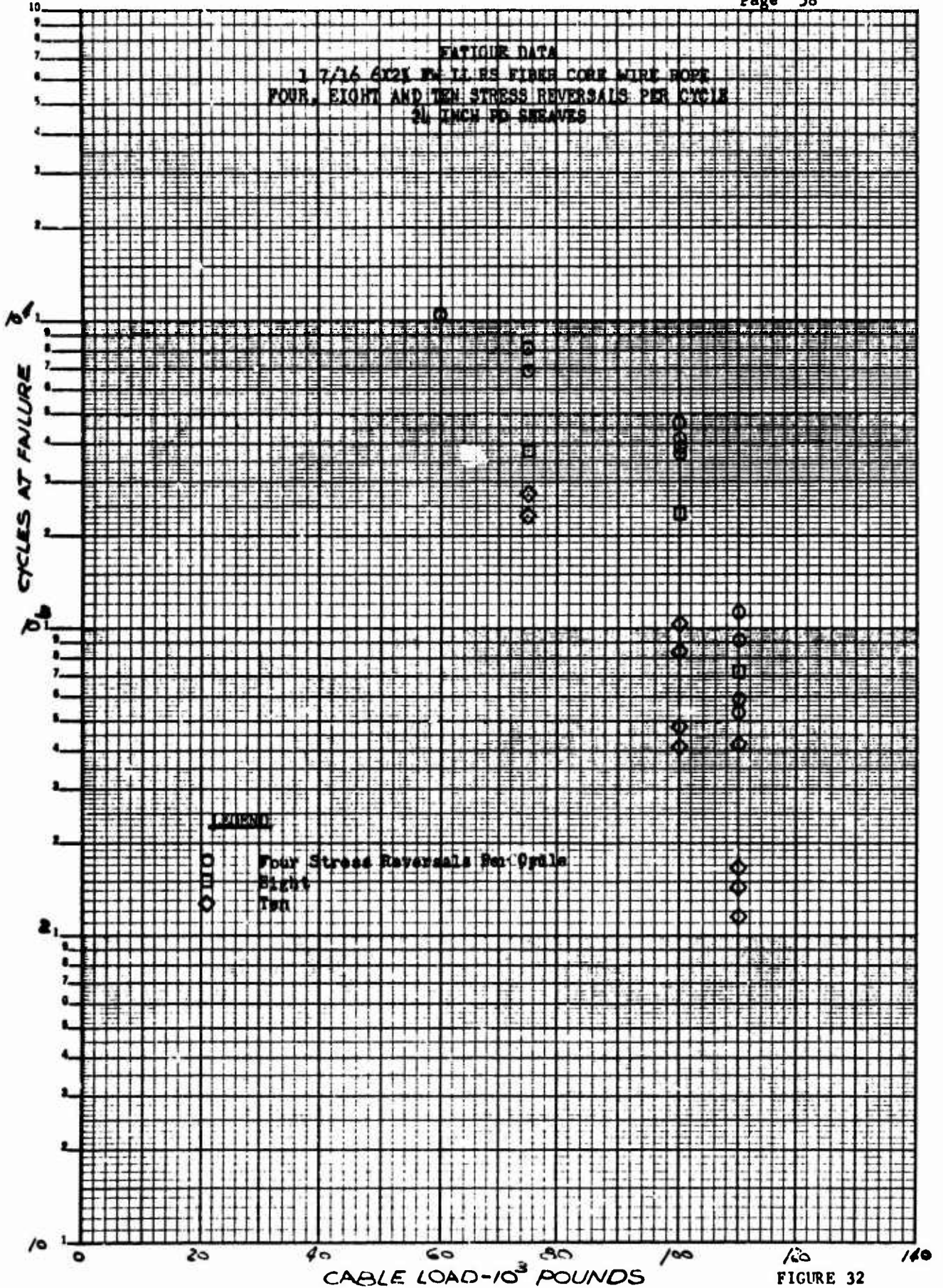


FIGURE 31



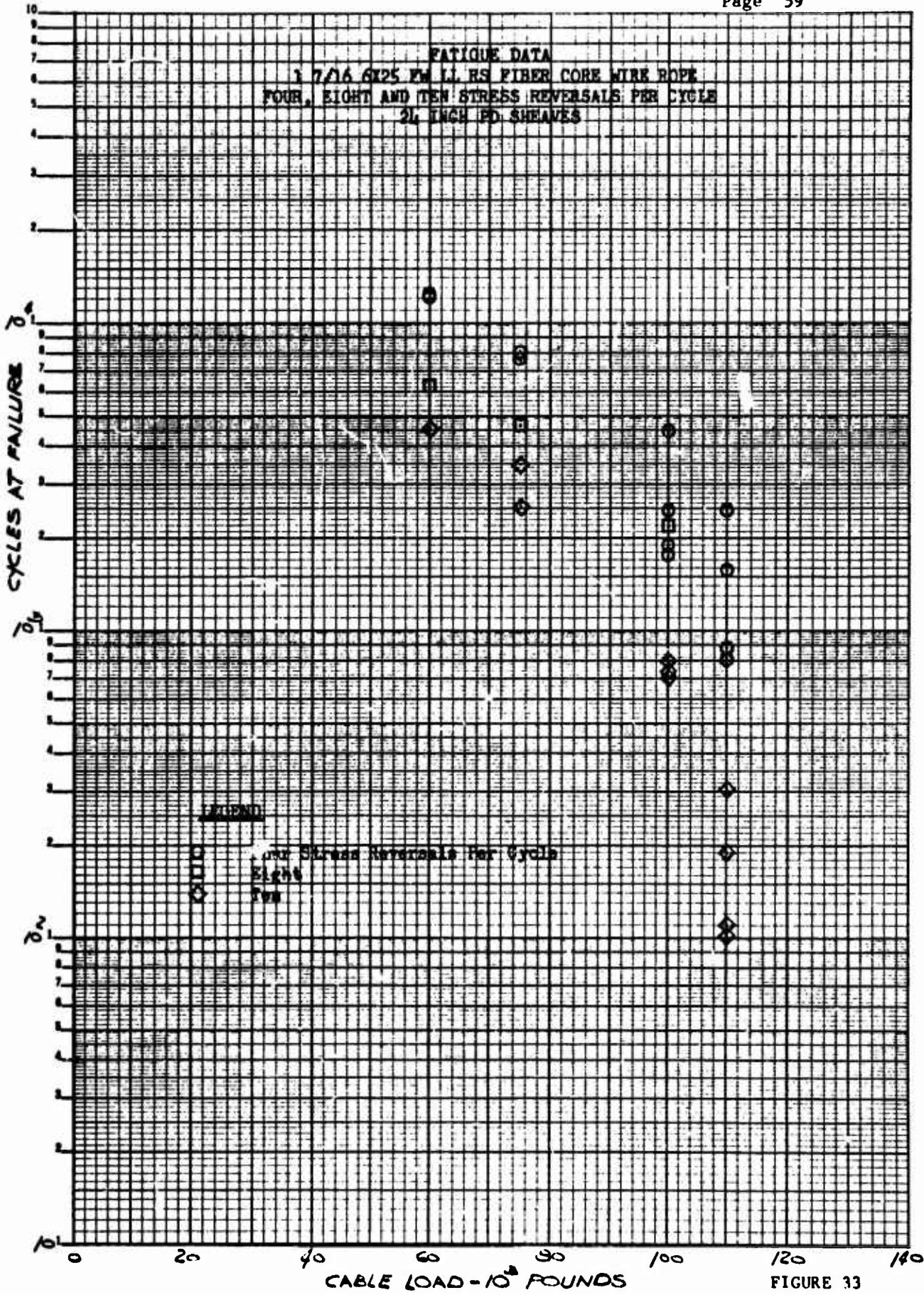


FIGURE 33

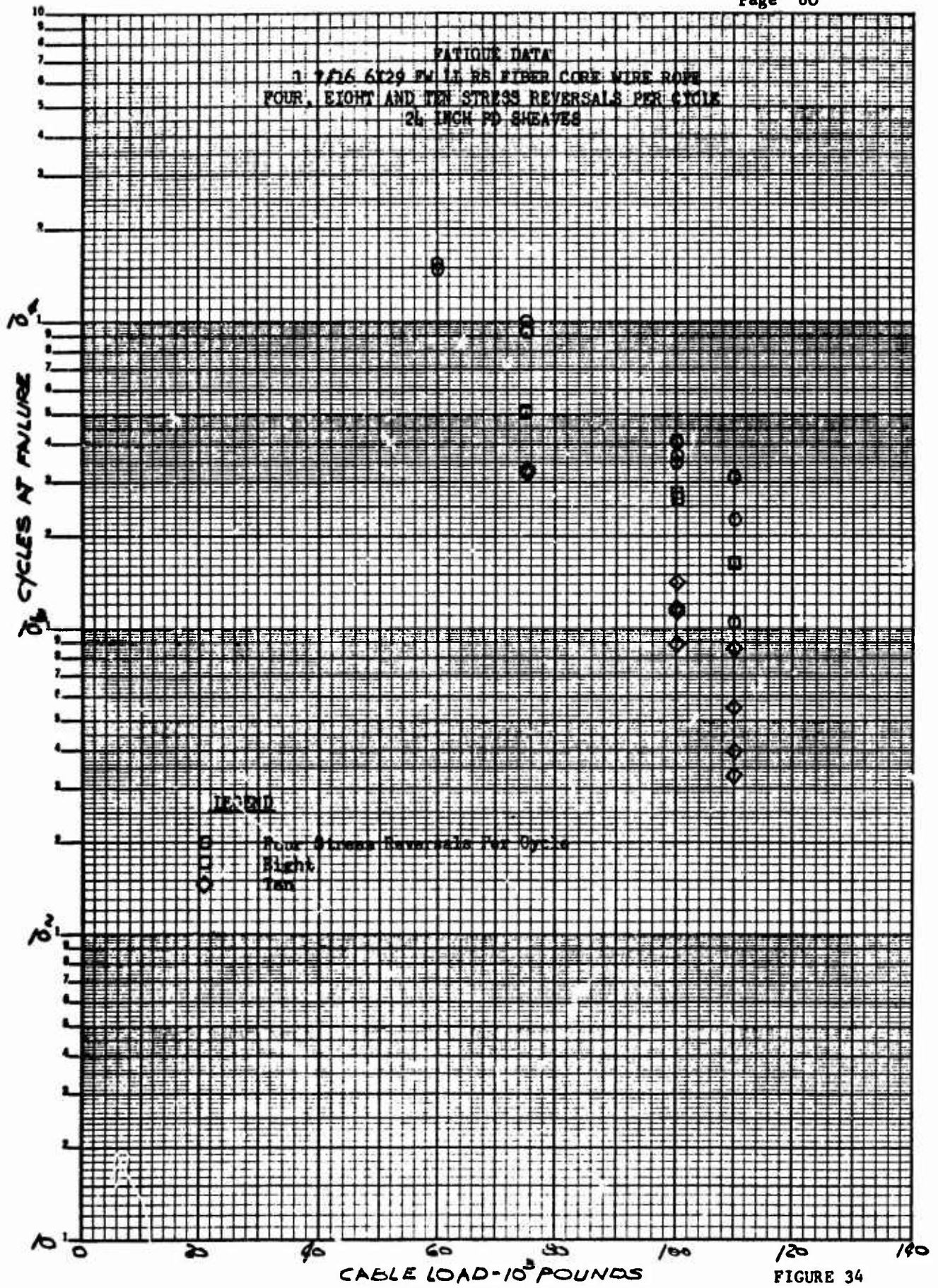


FIGURE 34

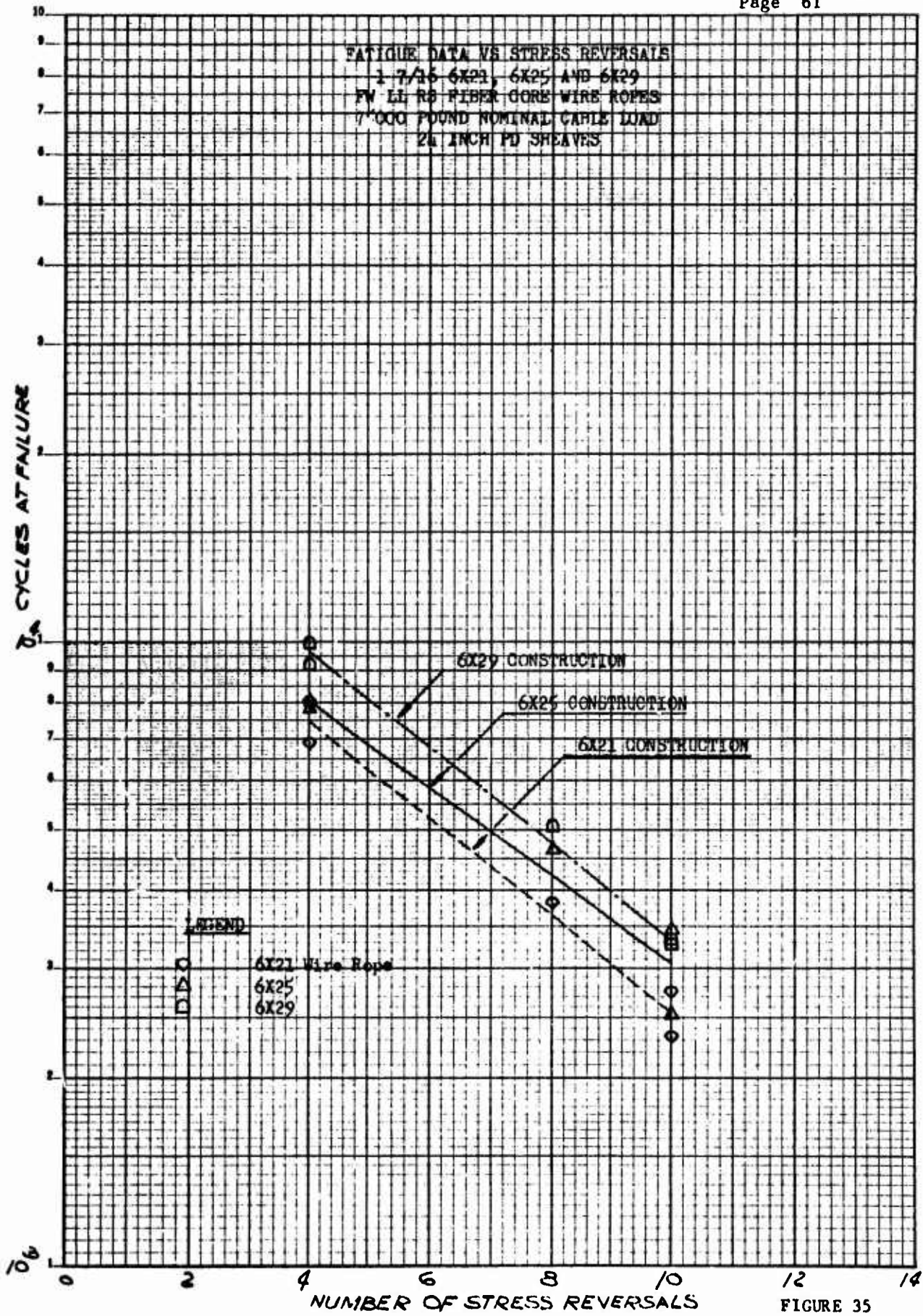
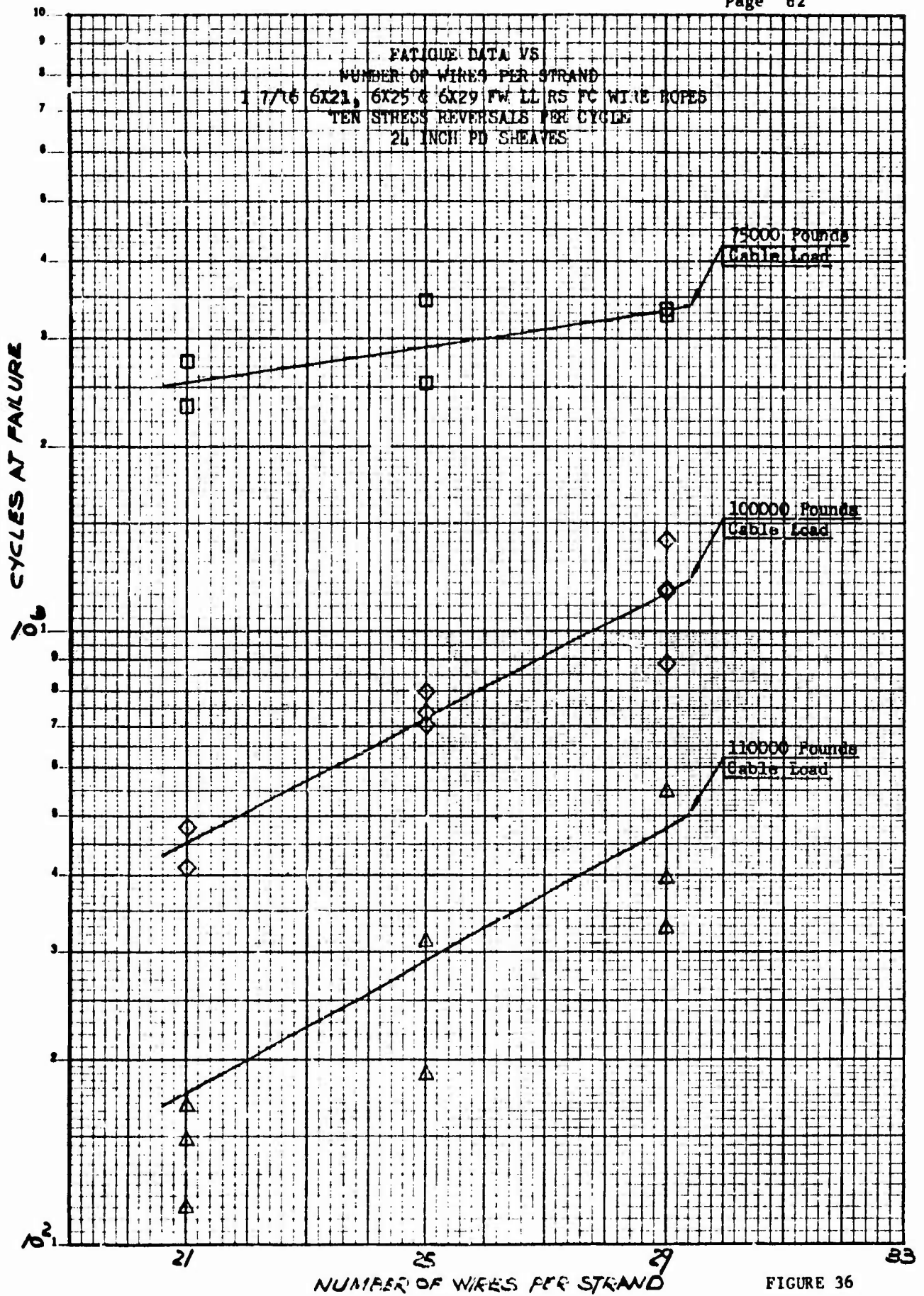


FIGURE 35



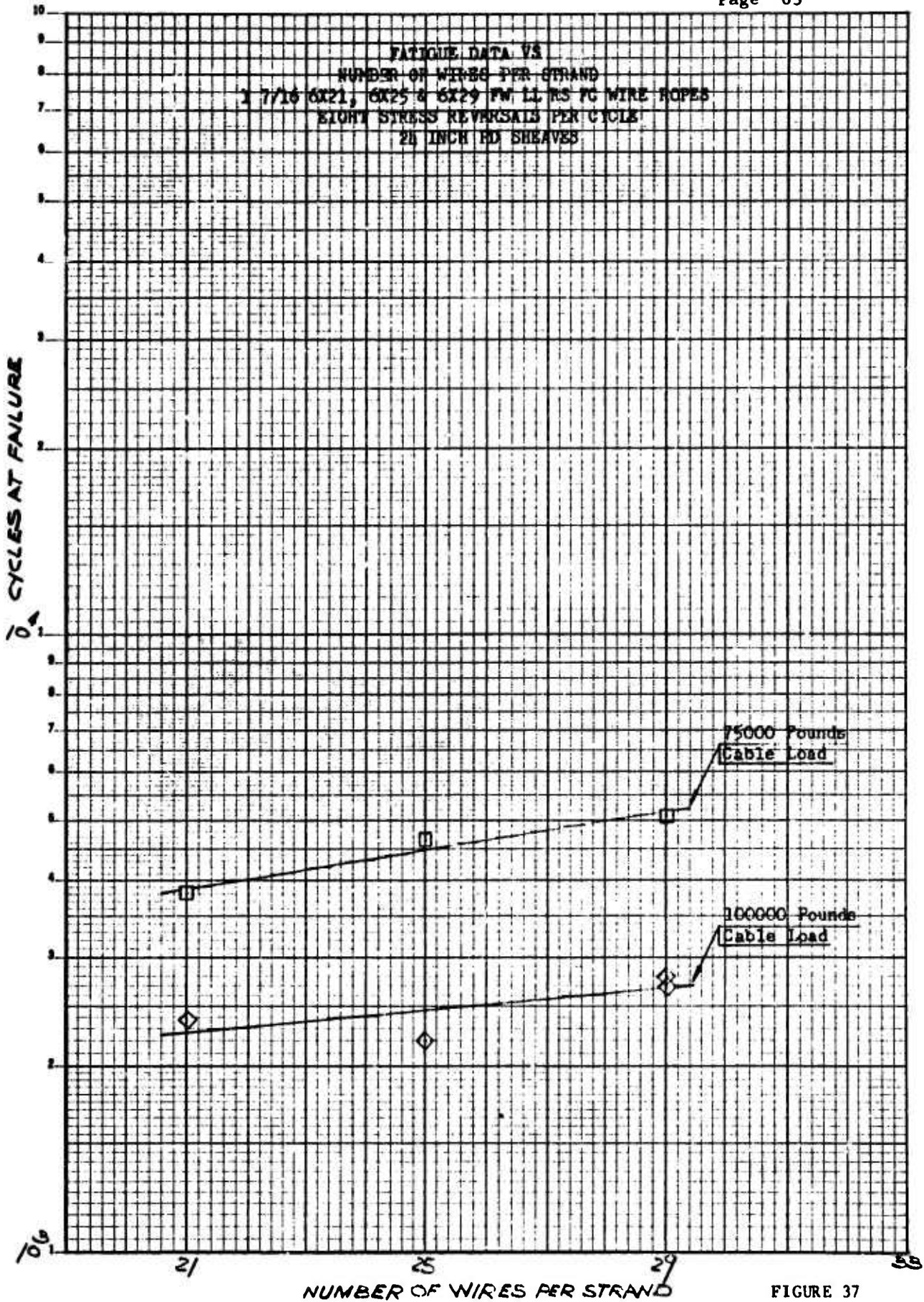


FIGURE 37

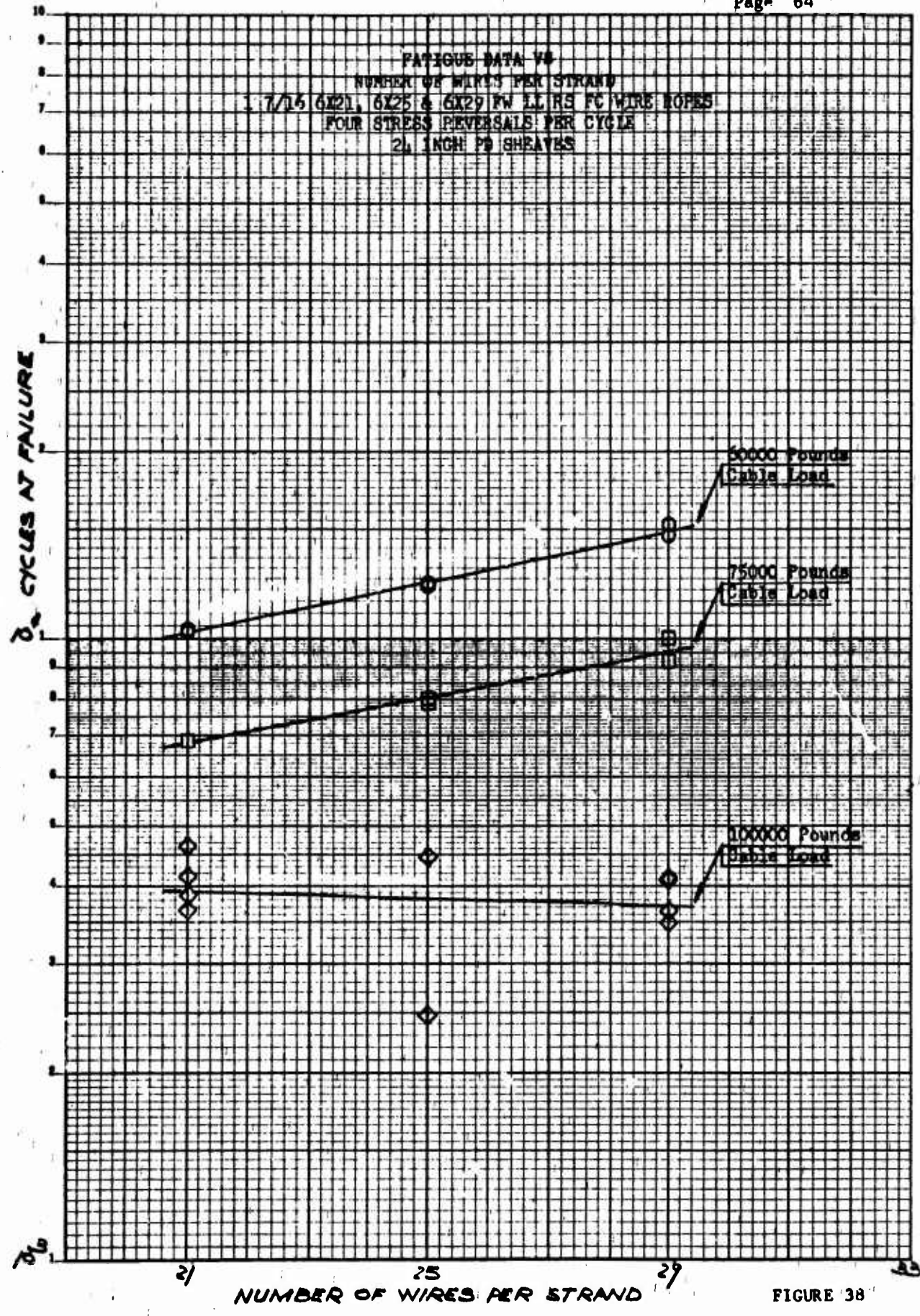


FIGURE 38

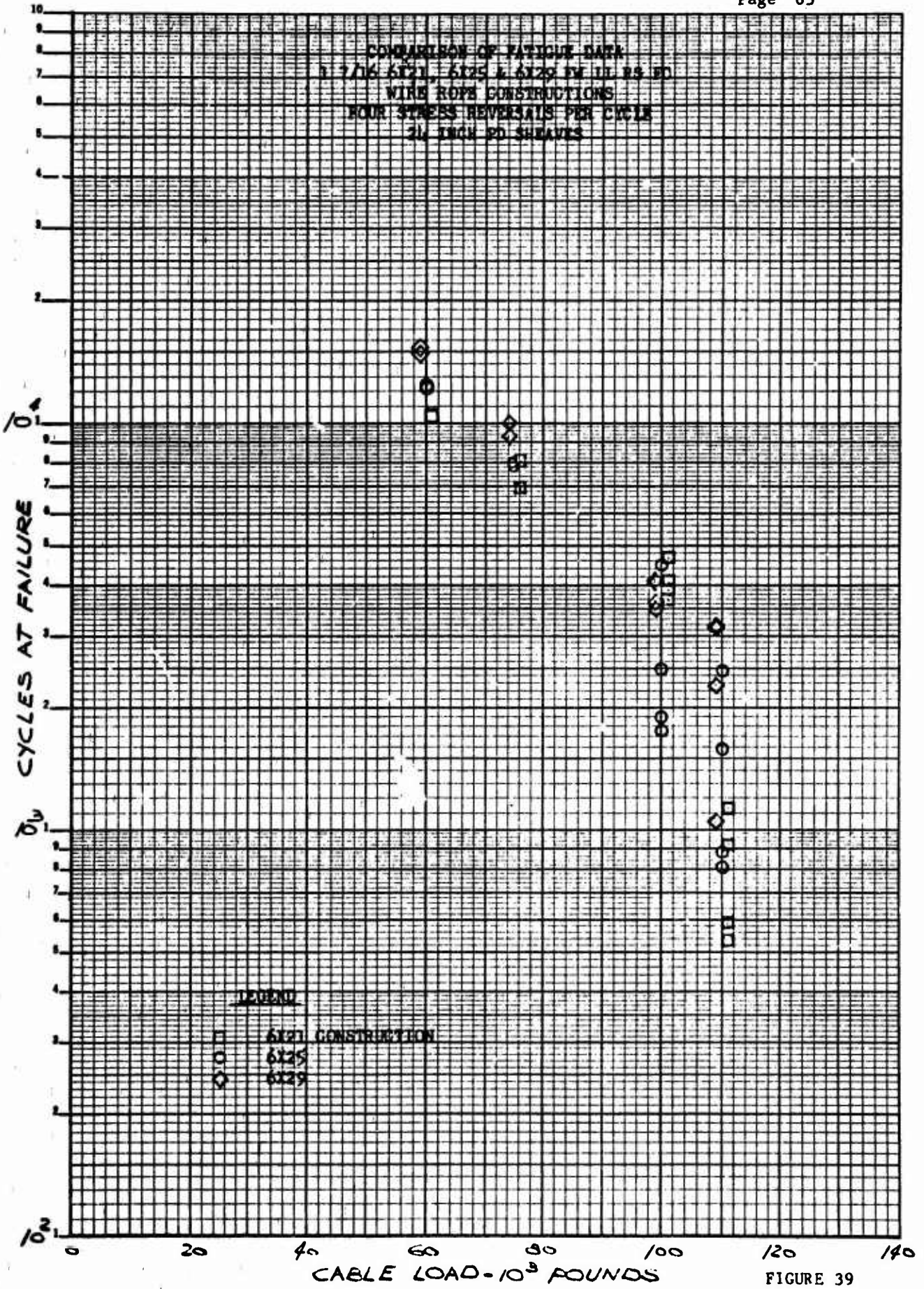


FIGURE 39

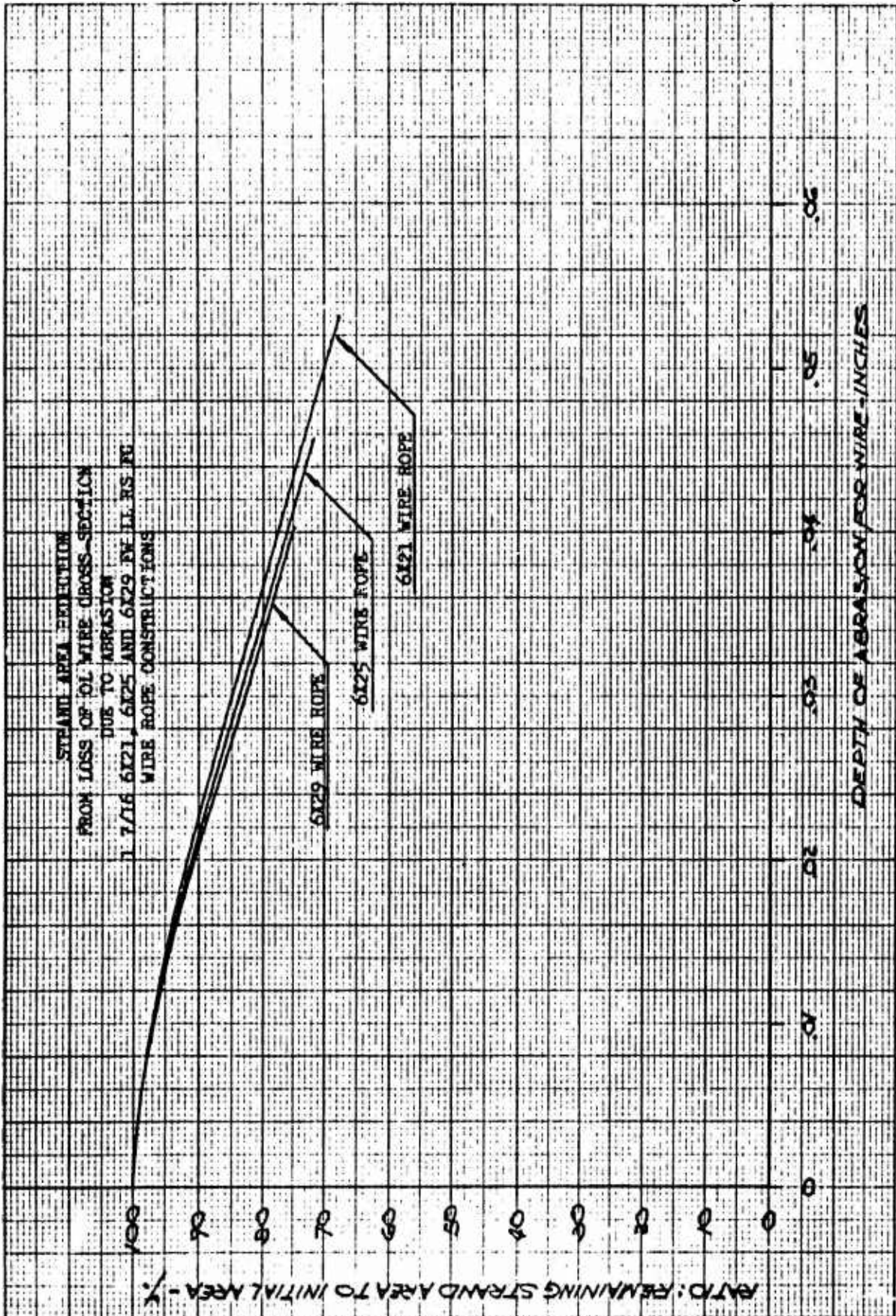


FIGURE 40

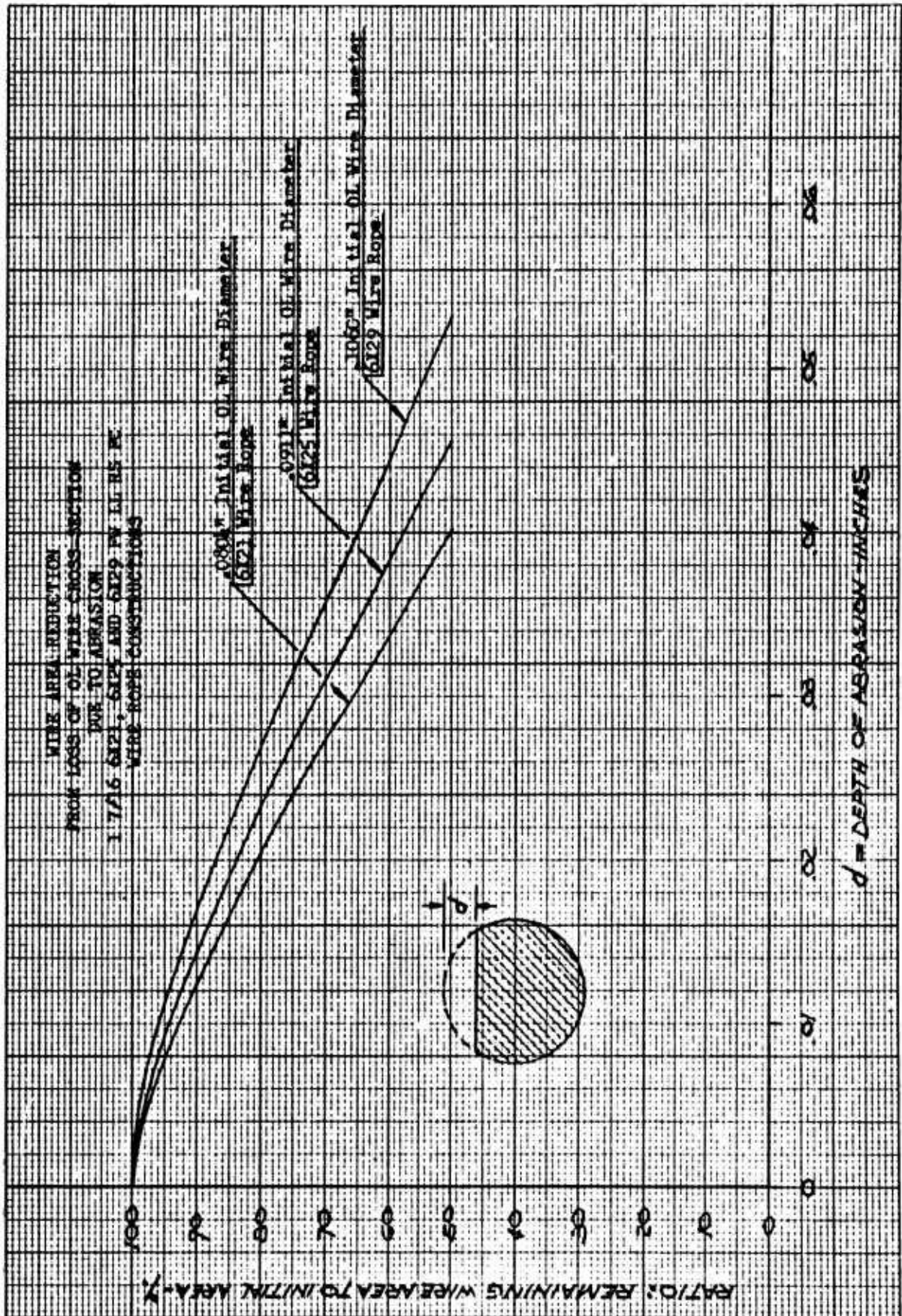


FIGURE 41

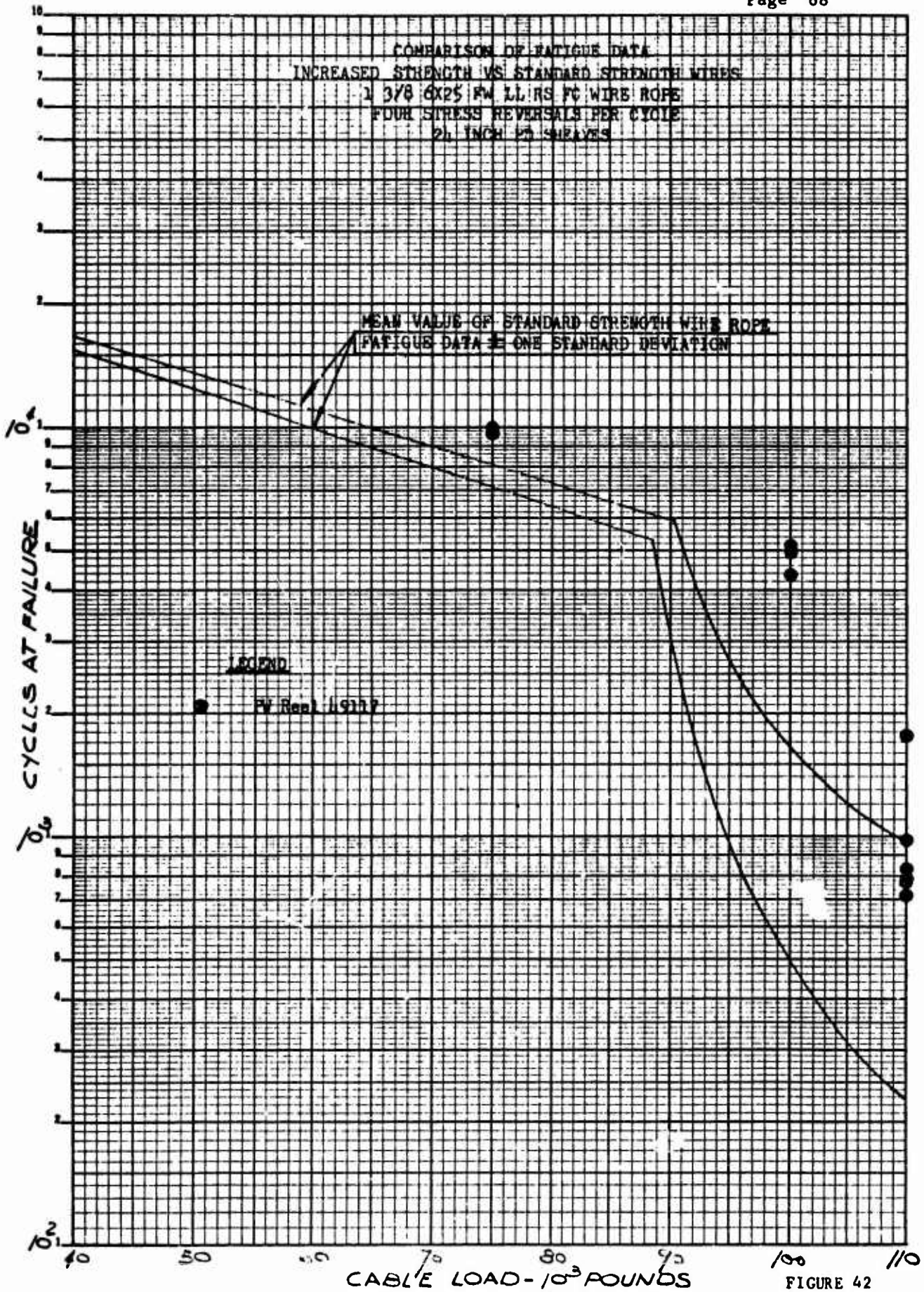


FIGURE 42

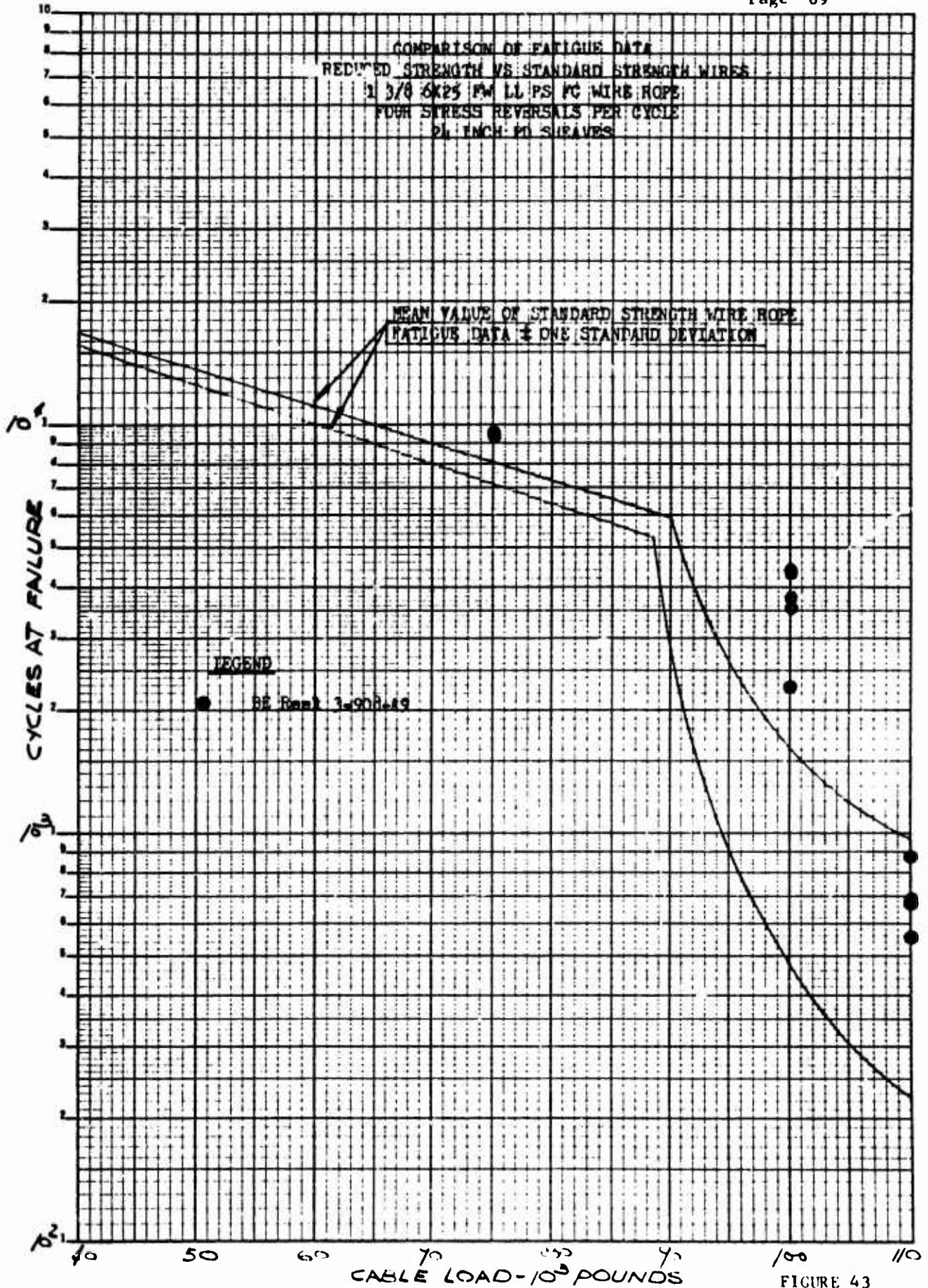


FIGURE 43

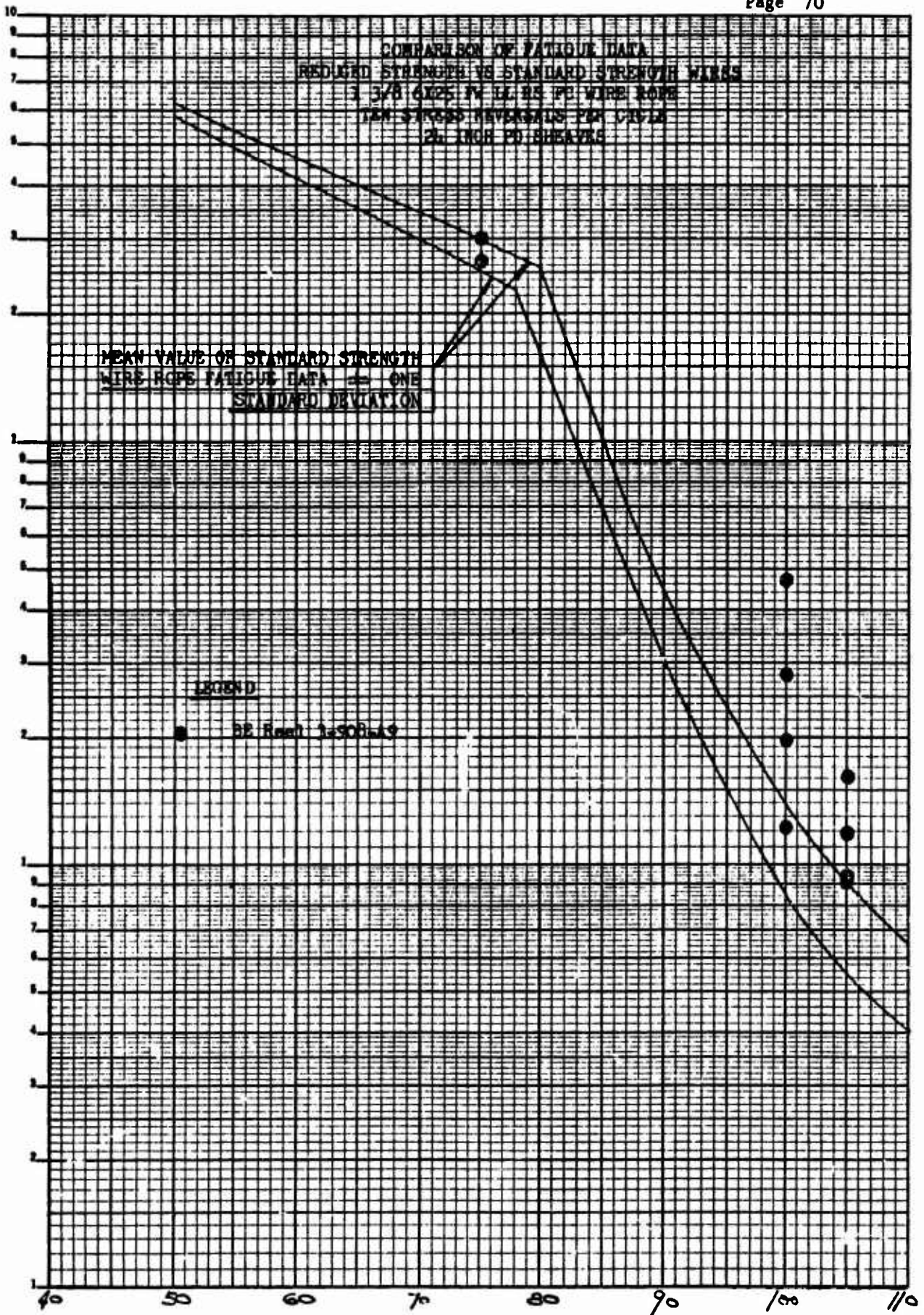


FIGURE 44

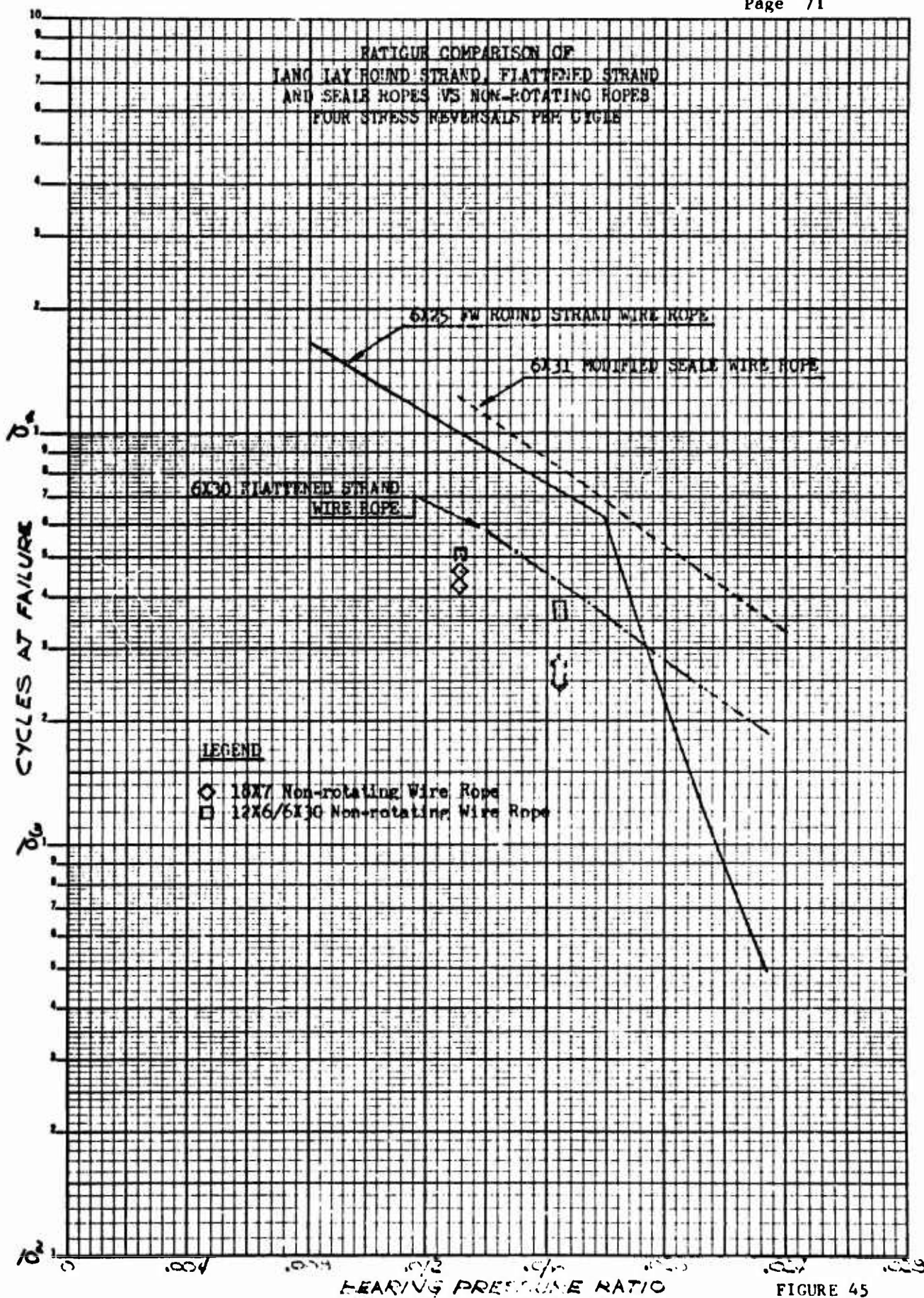


FIGURE 45

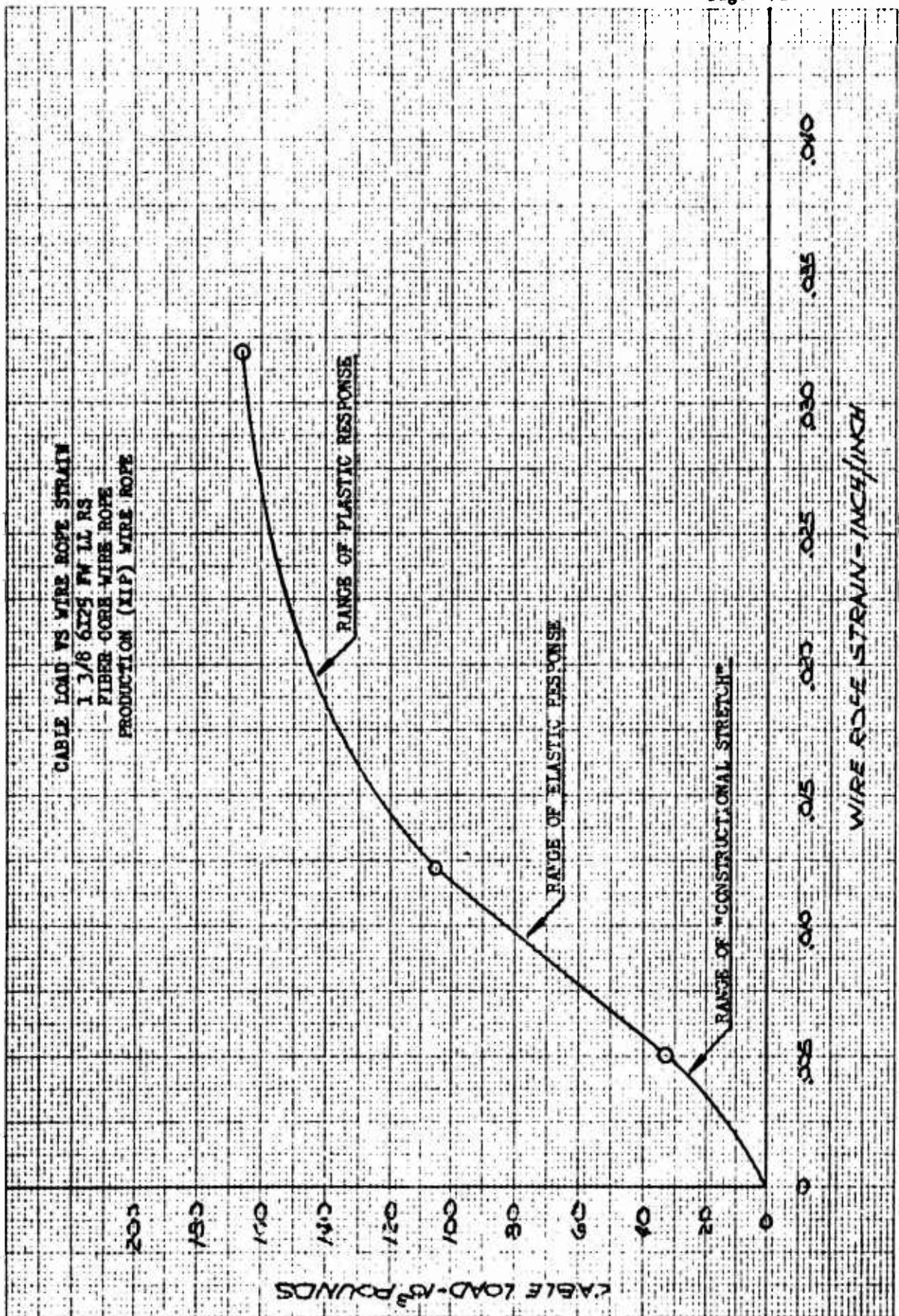


FIGURE 46

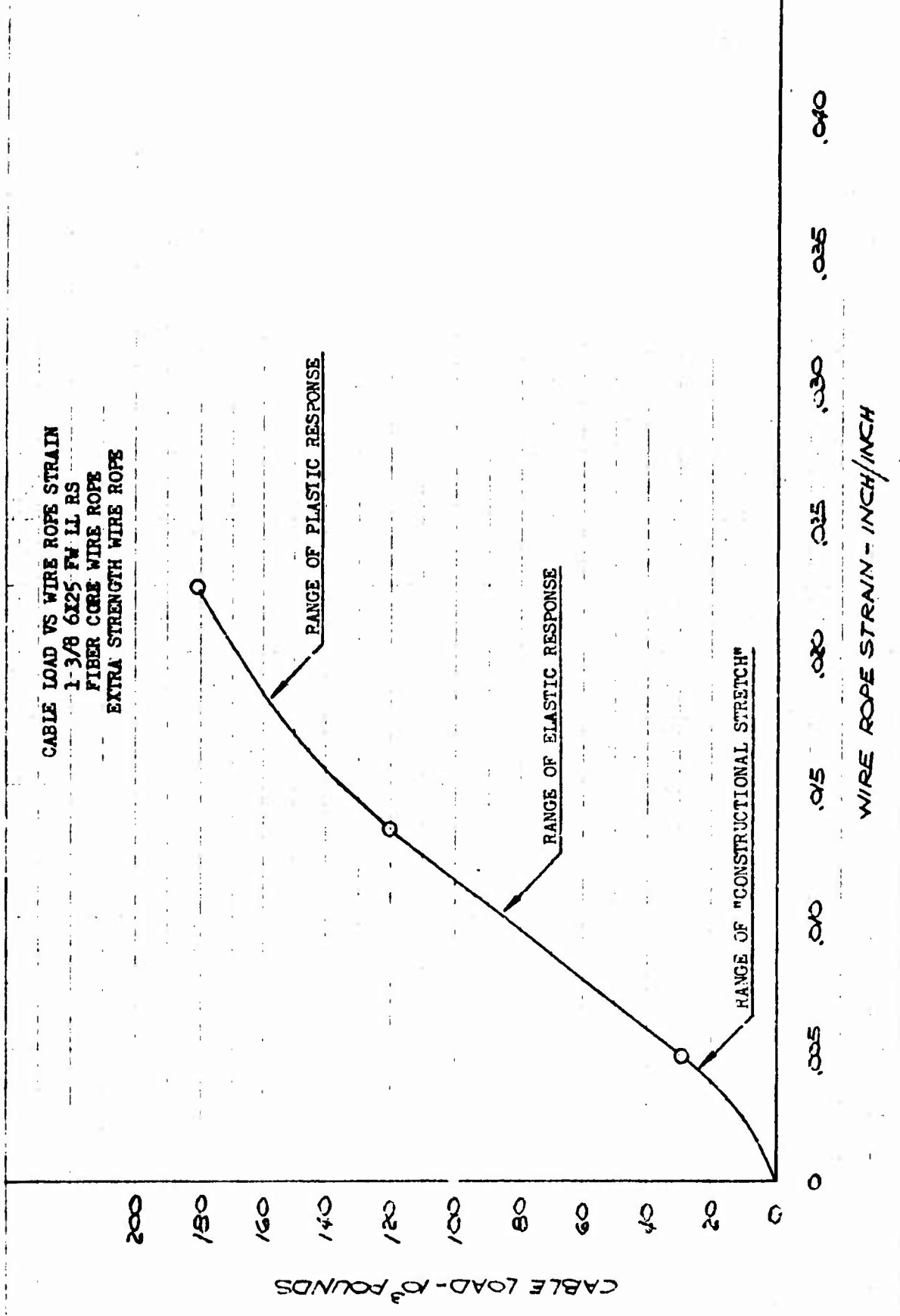


FIGURE 47

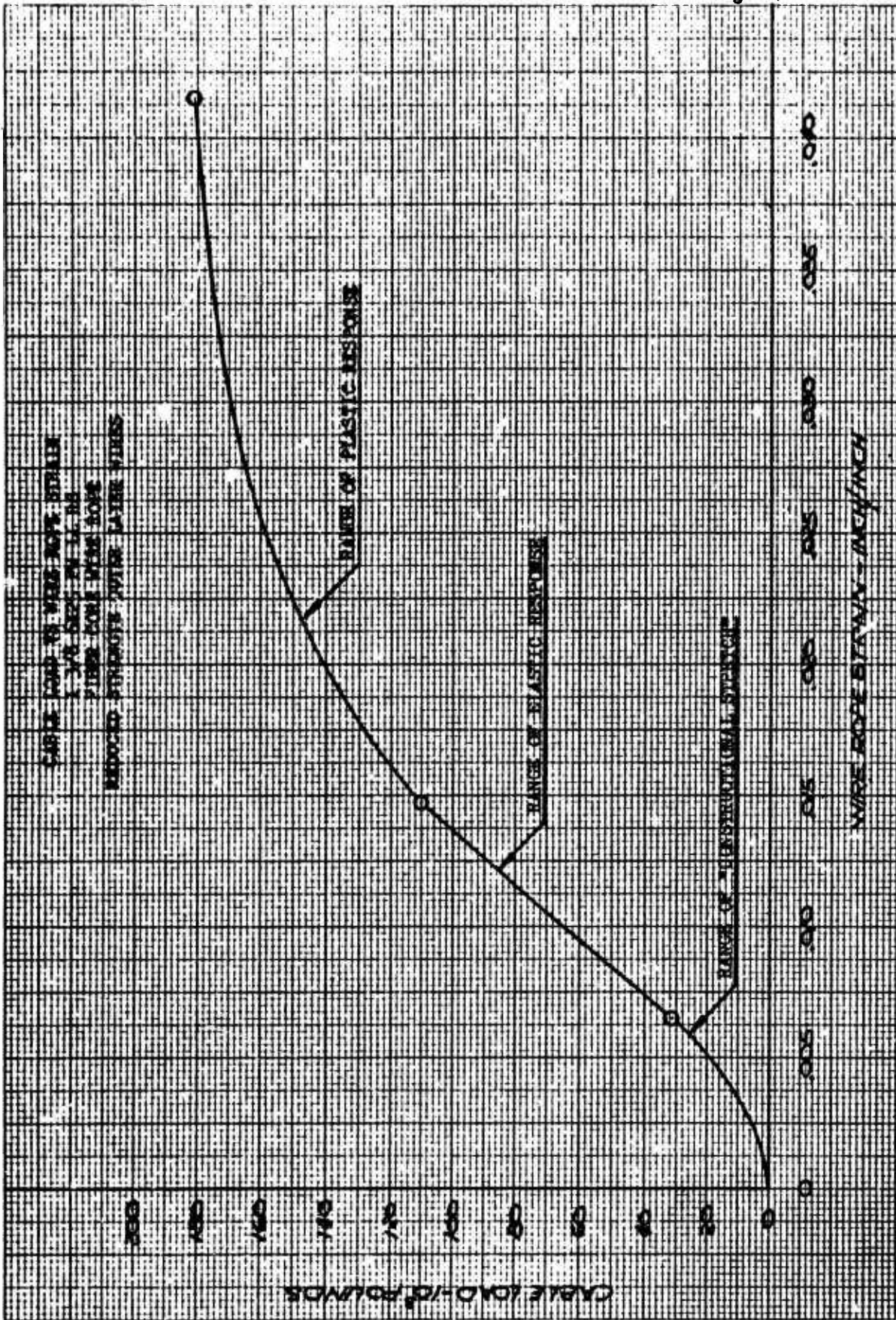


FIGURE 48

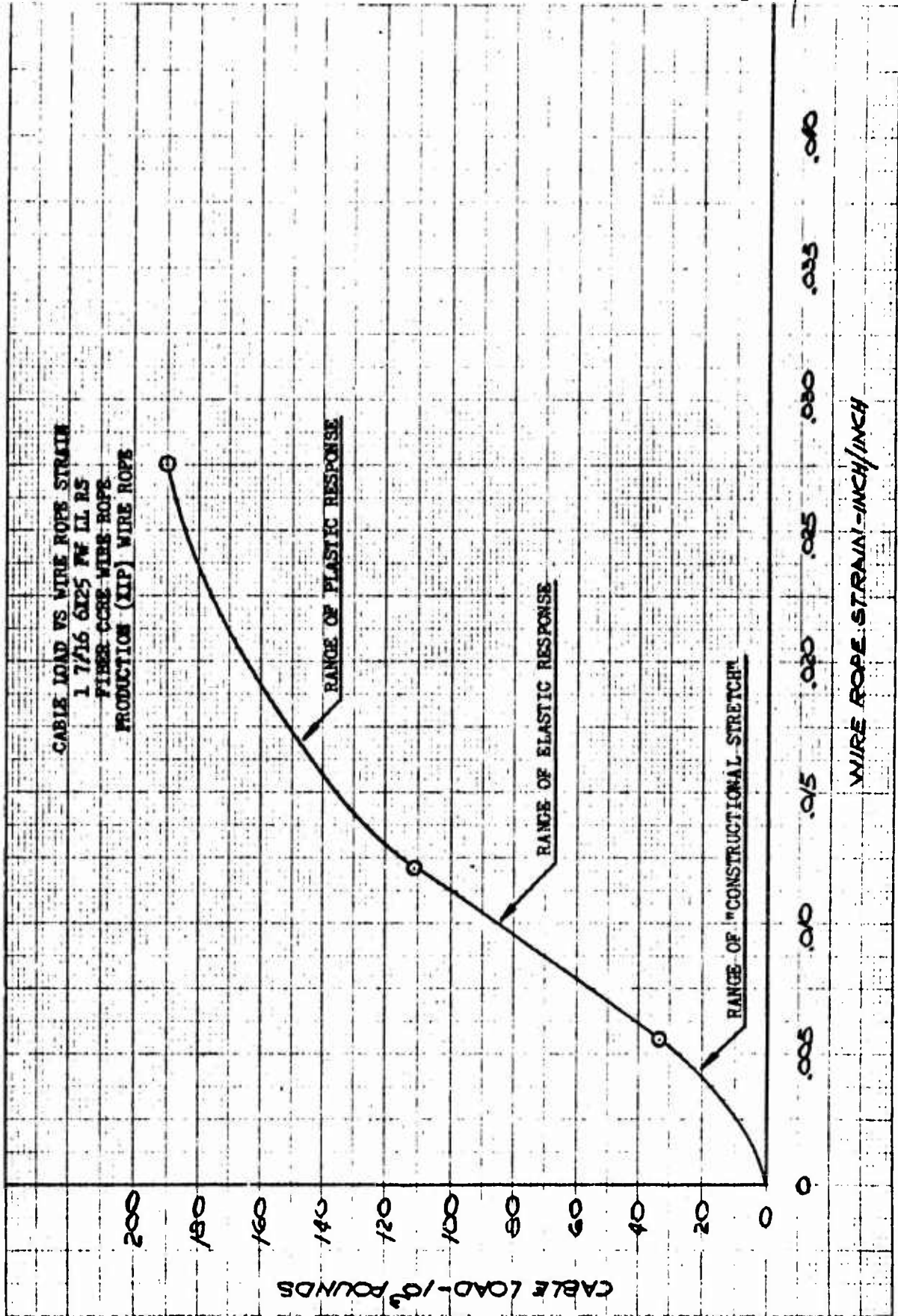


FIGURE 49

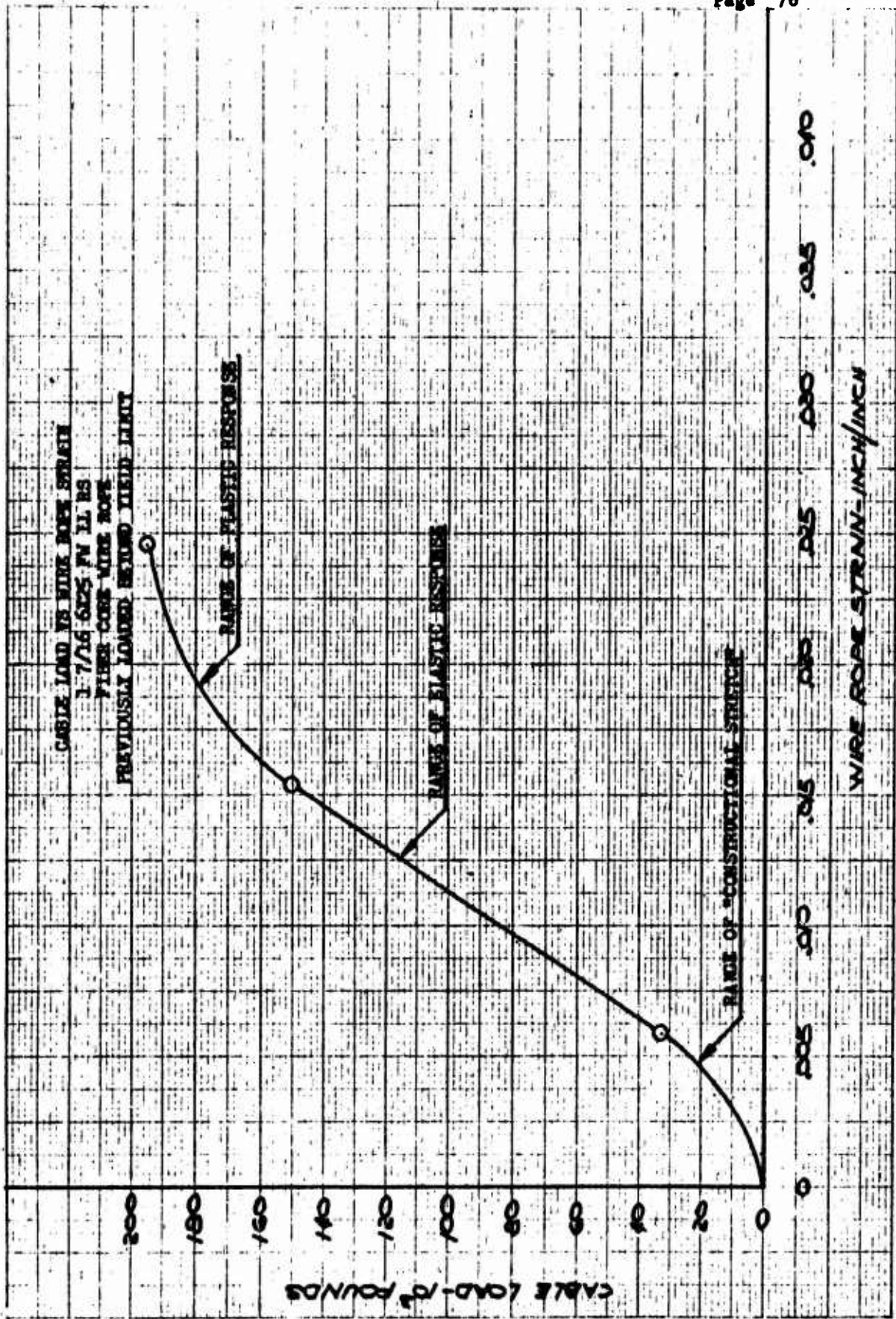


FIGURE 50

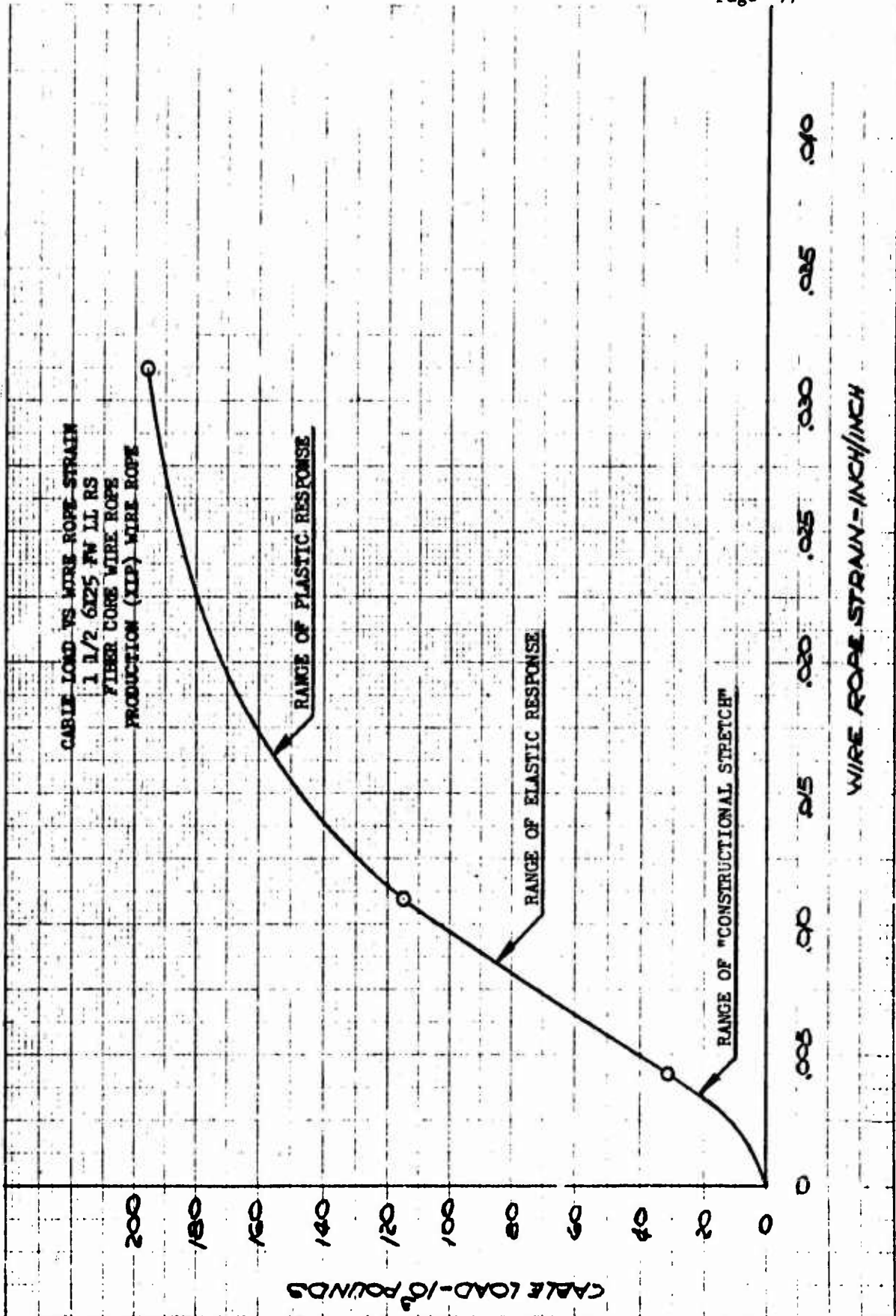


FIGURE 51

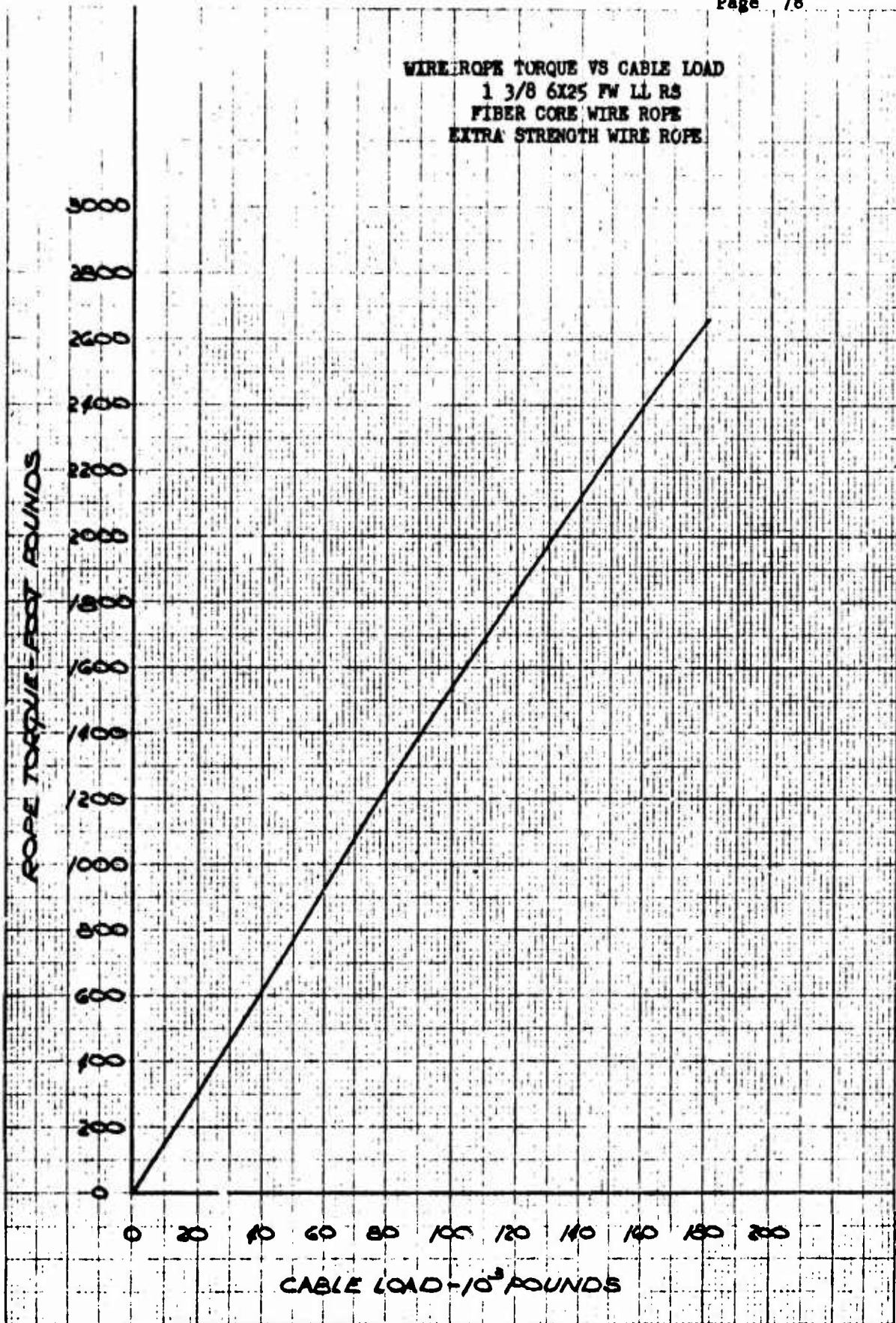


FIGURE 52

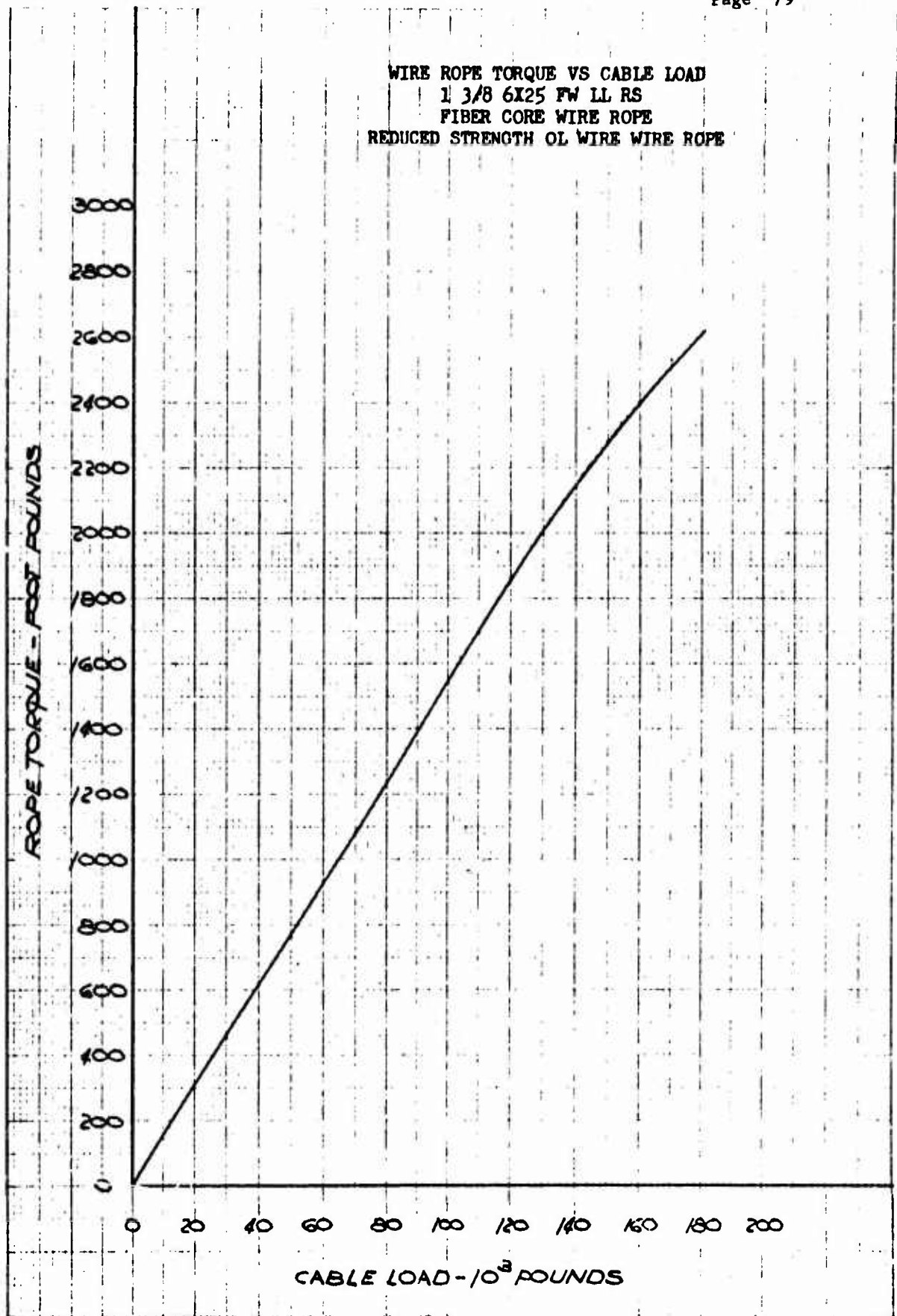


FIGURE 53

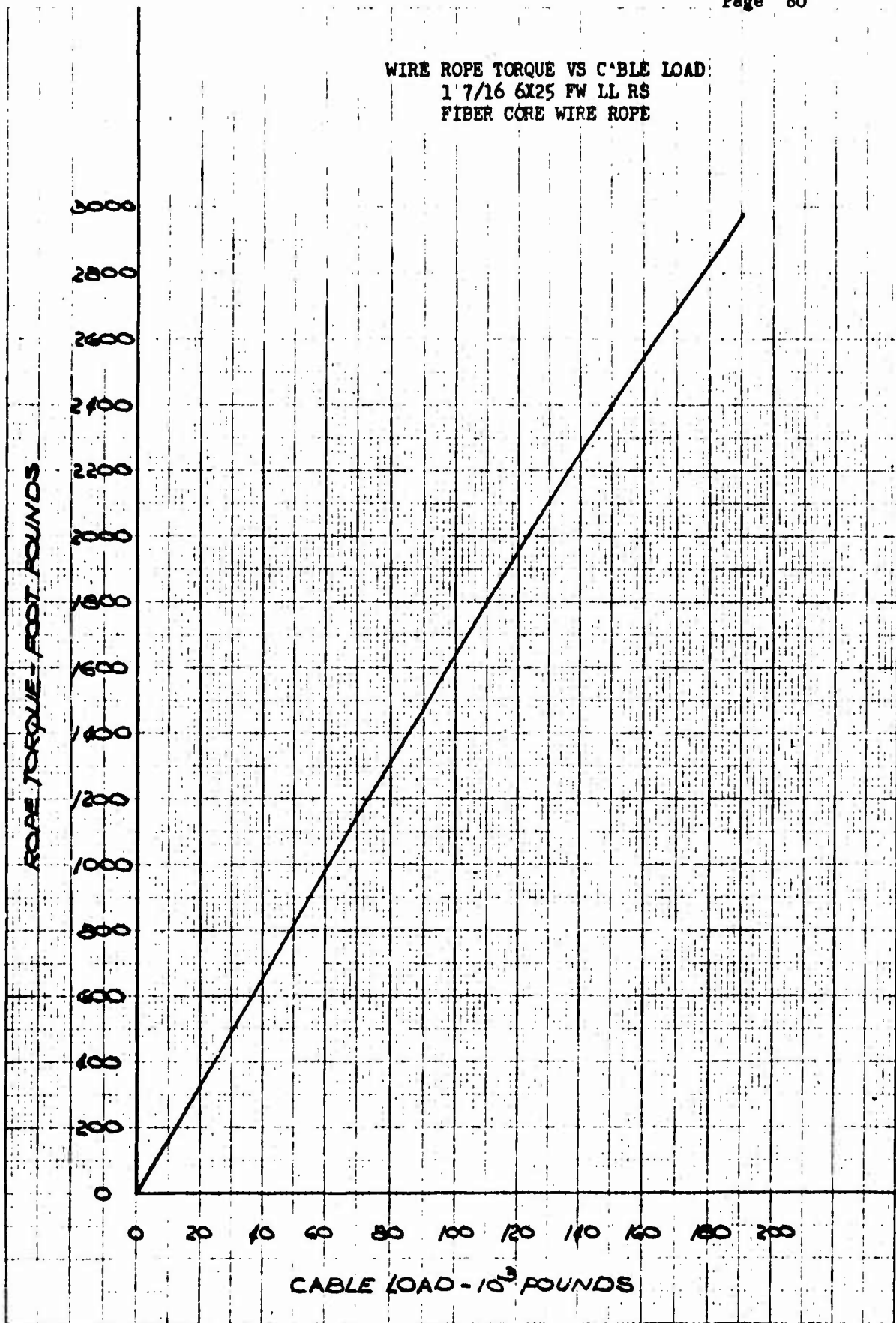


FIGURE 54

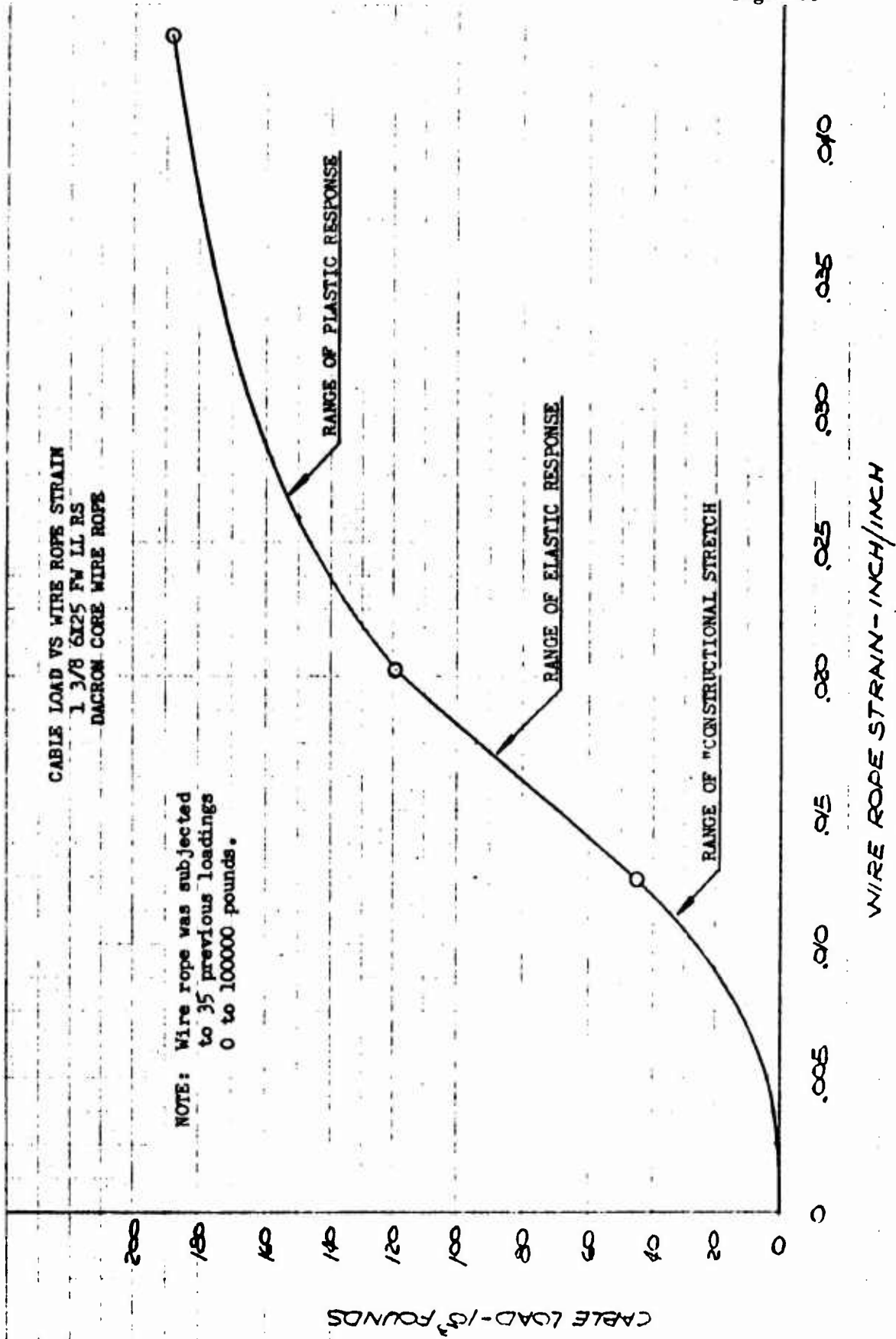


FIGURE 55

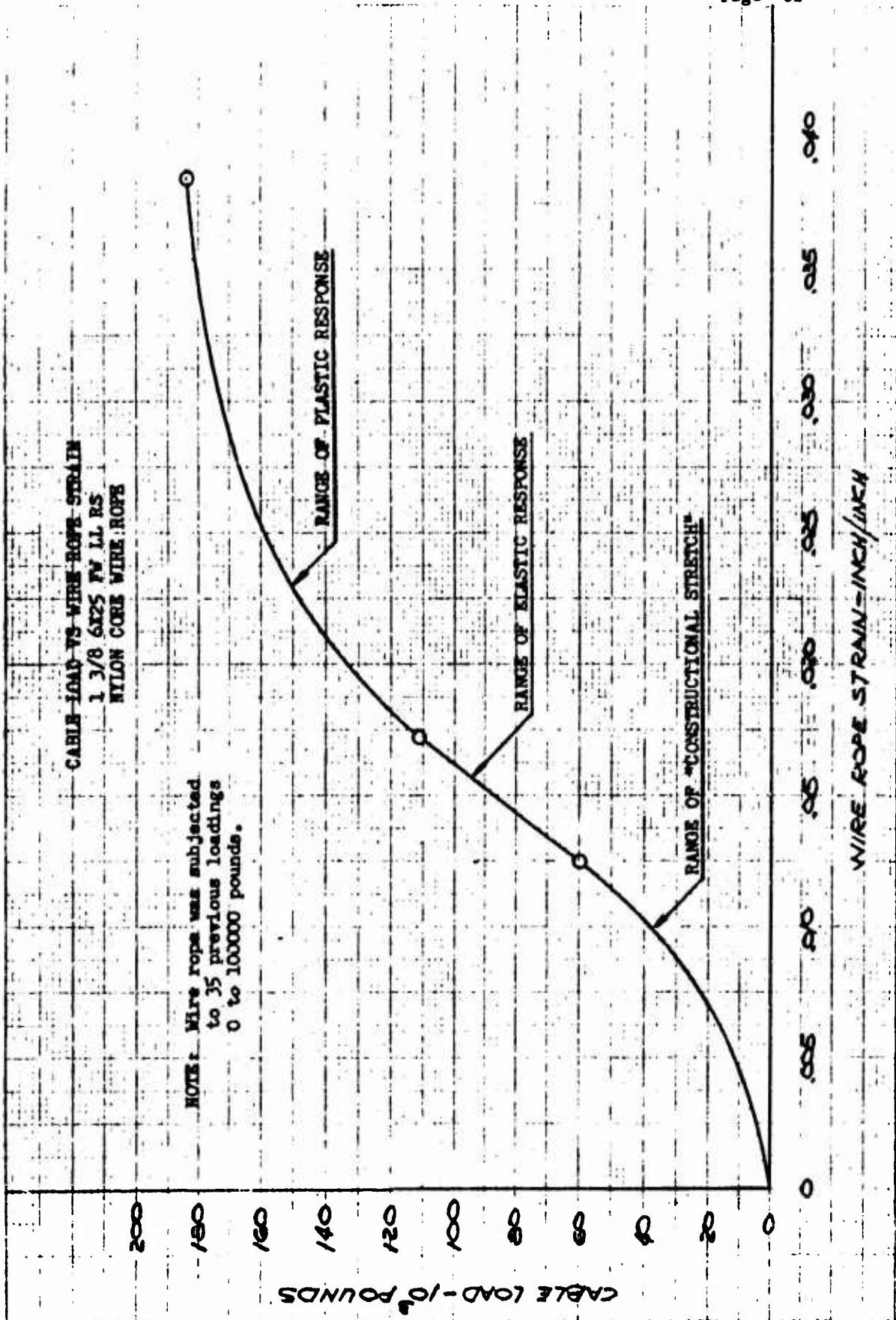


FIGURE 56

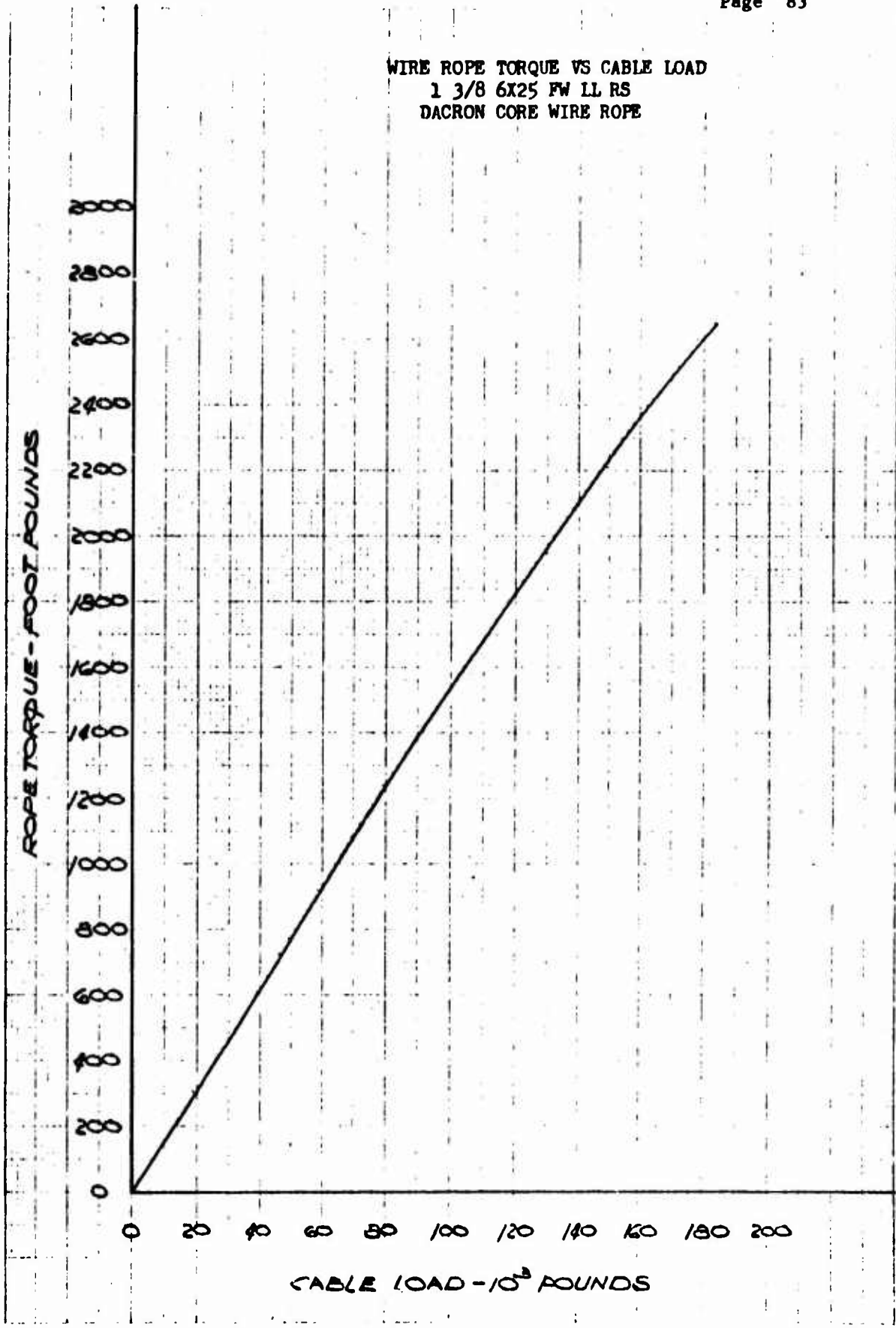


FIGURE 57

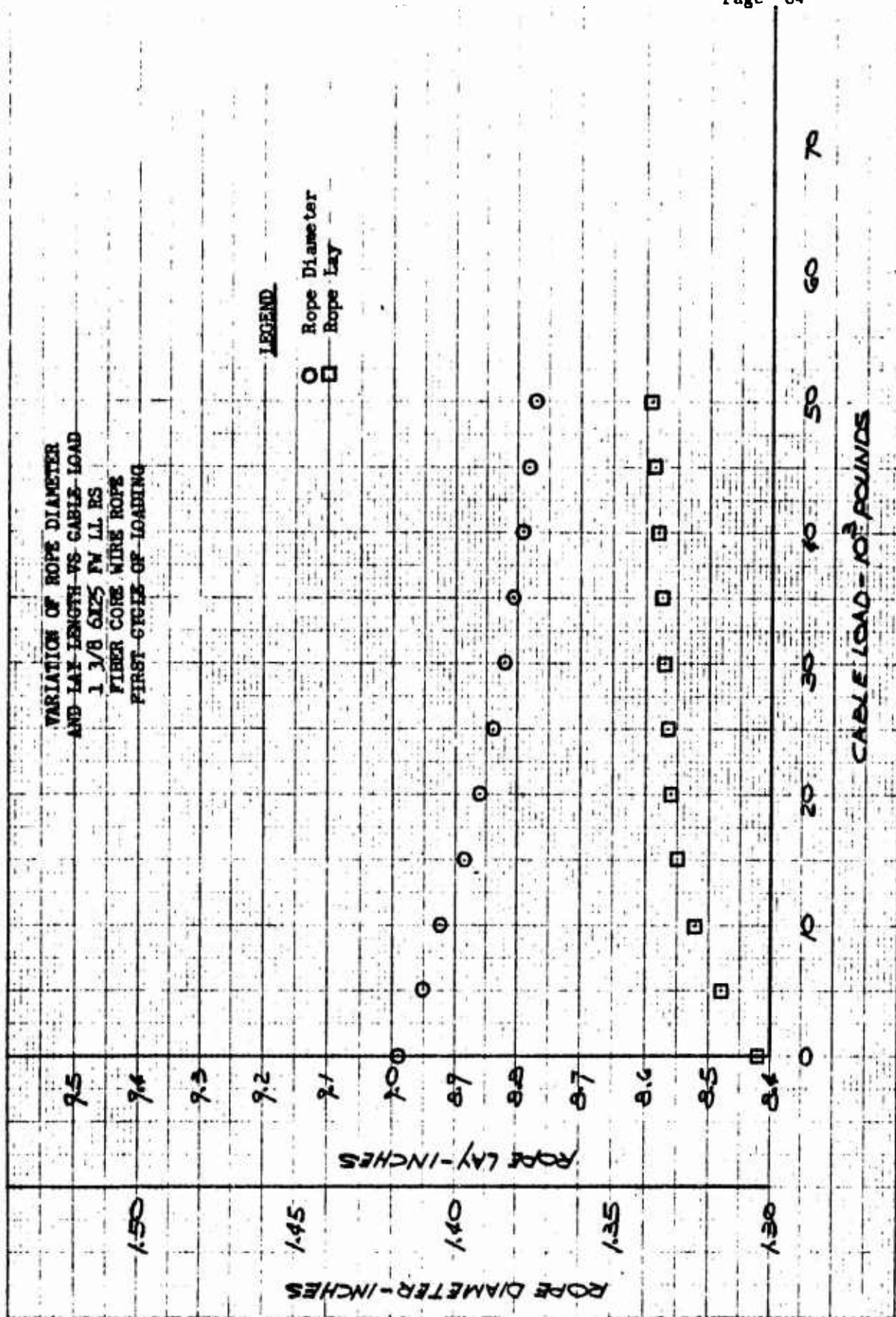


FIGURE 58

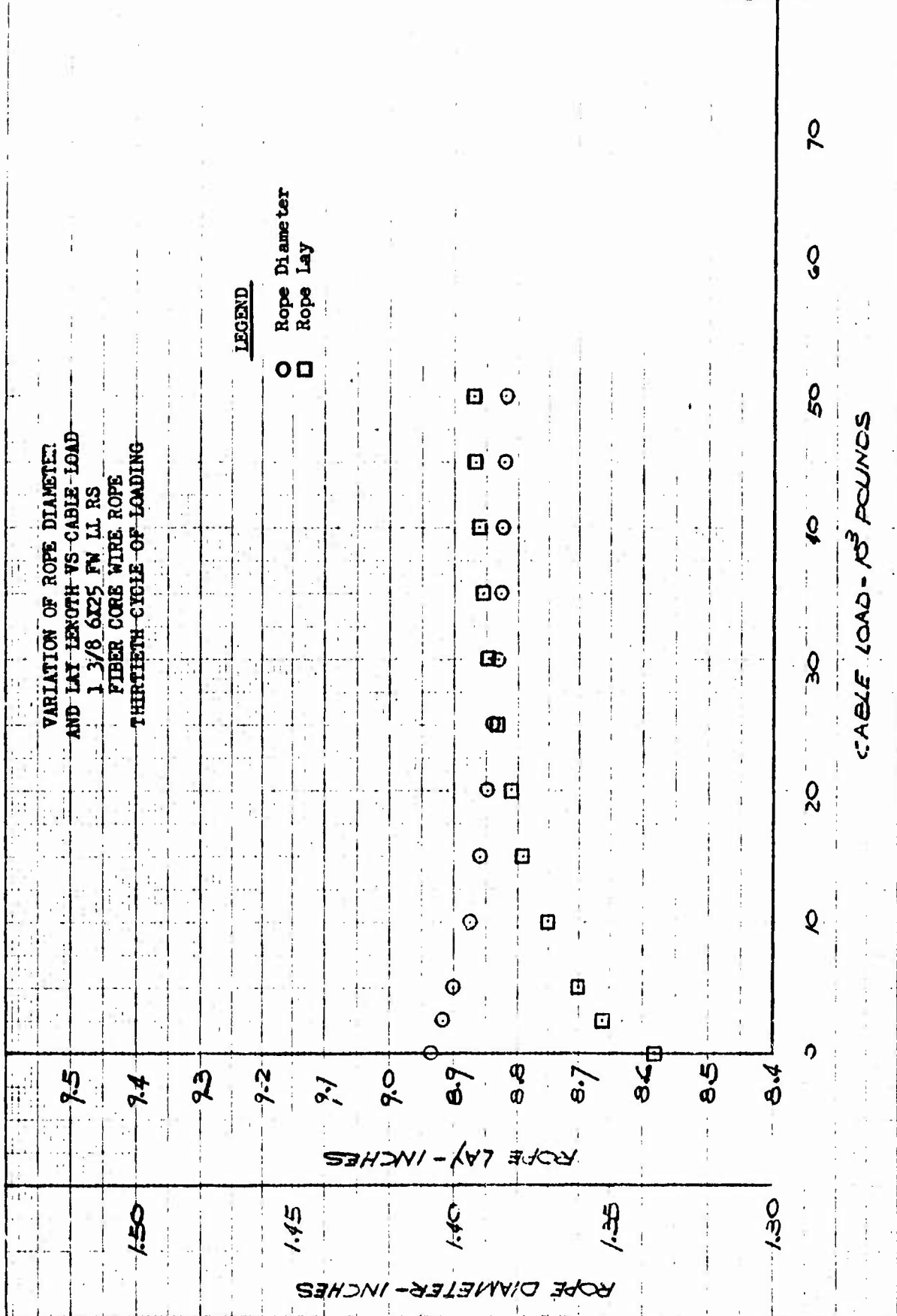


FIGURE 59

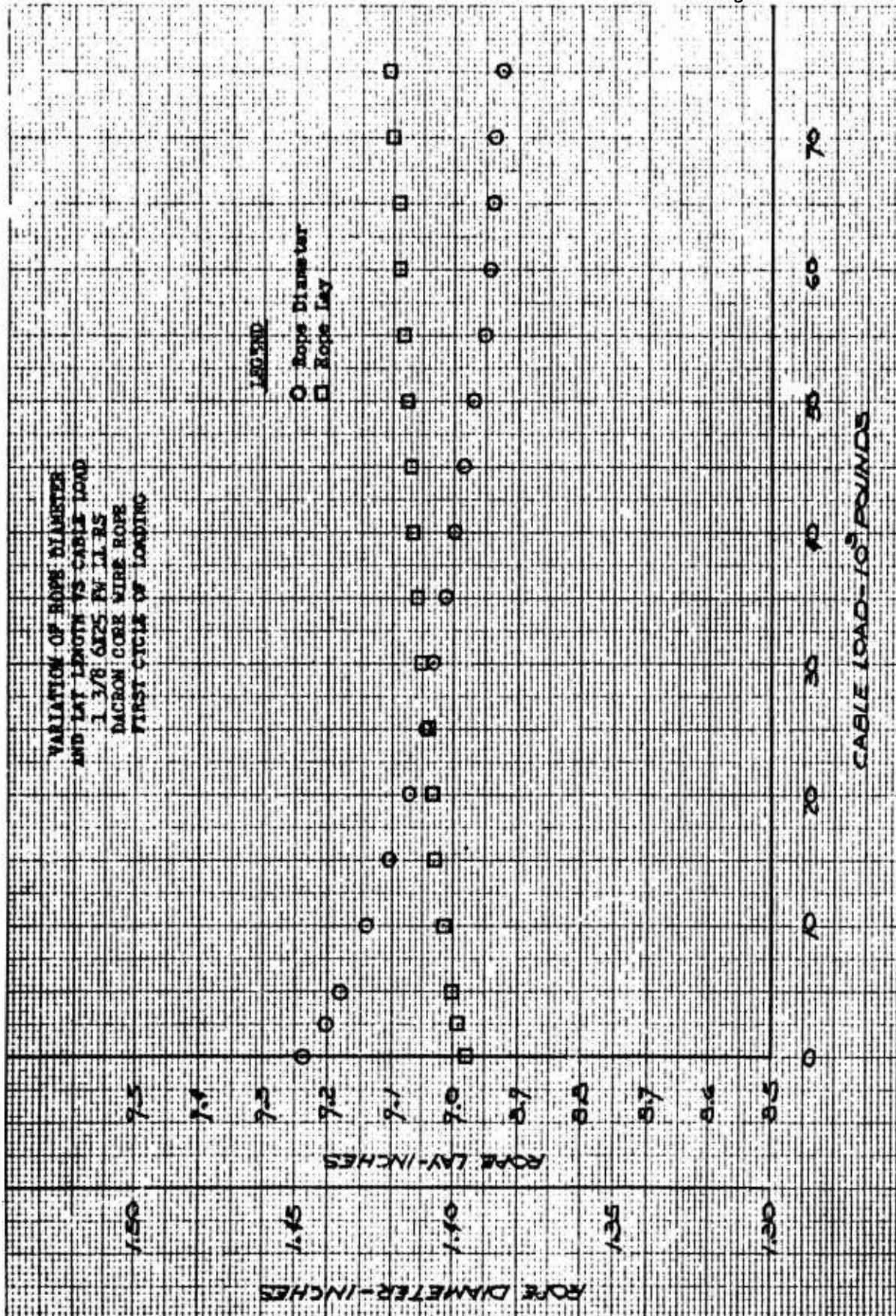


FIGURE 60

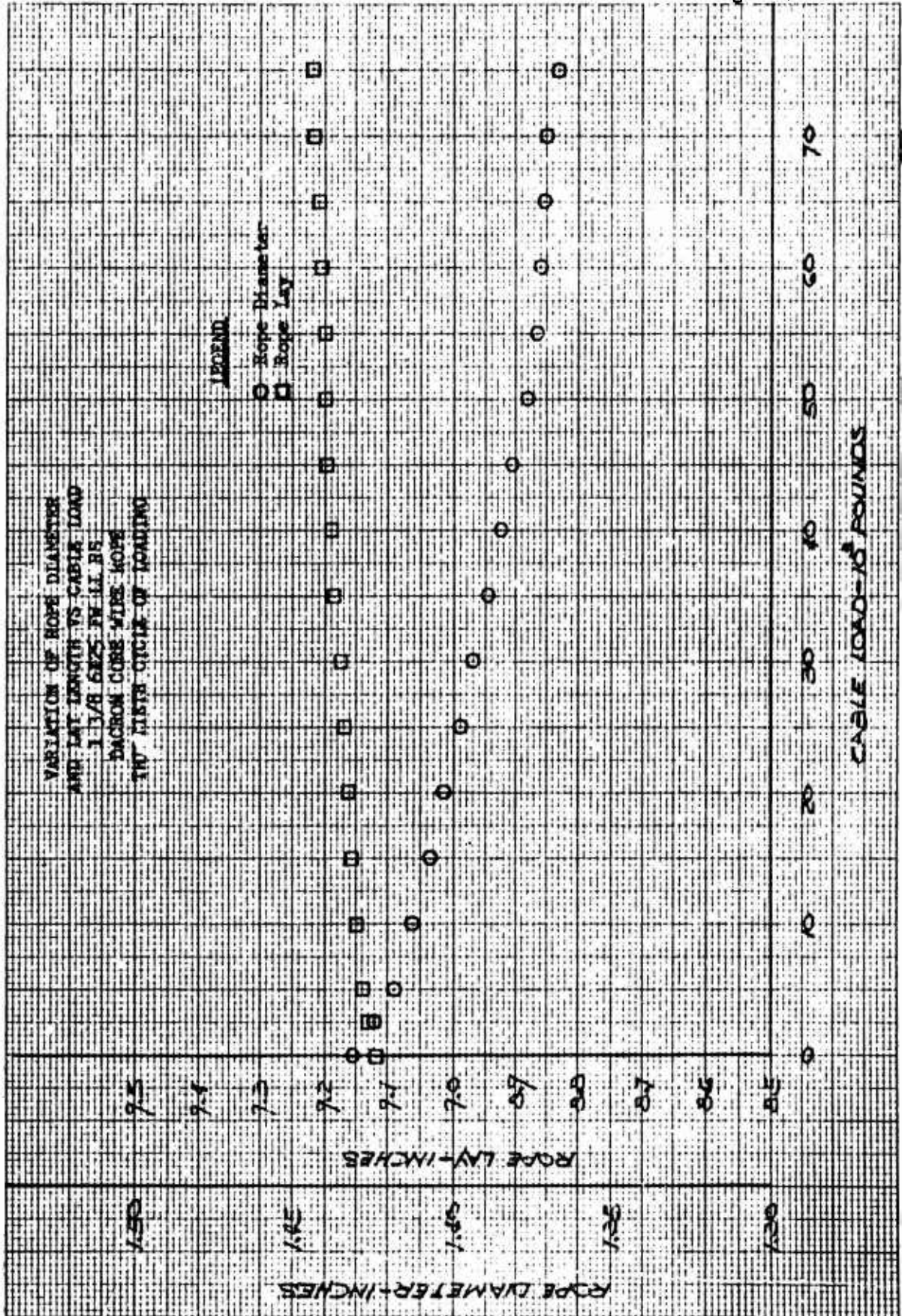


FIGURE 61

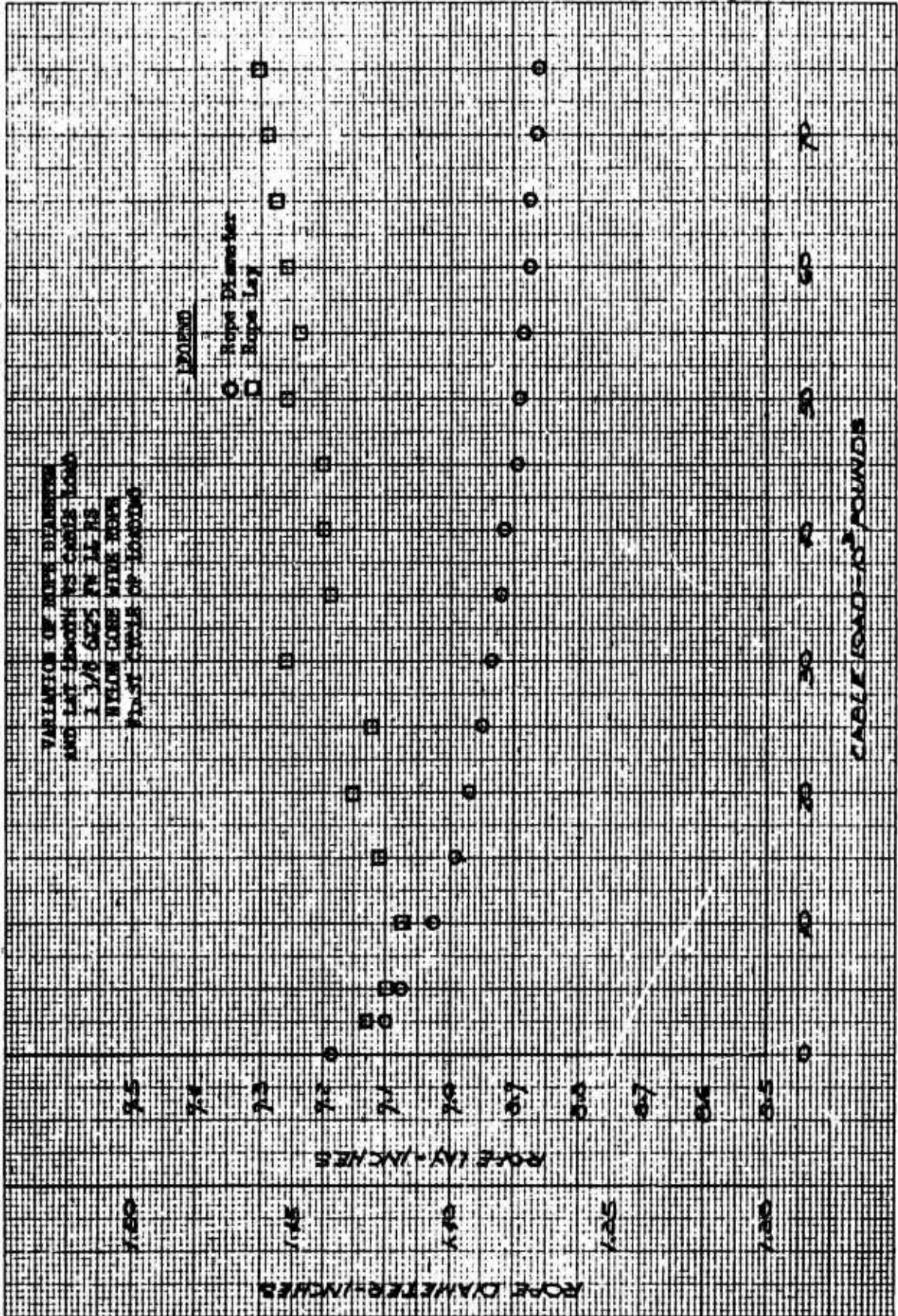


FIGURE 62

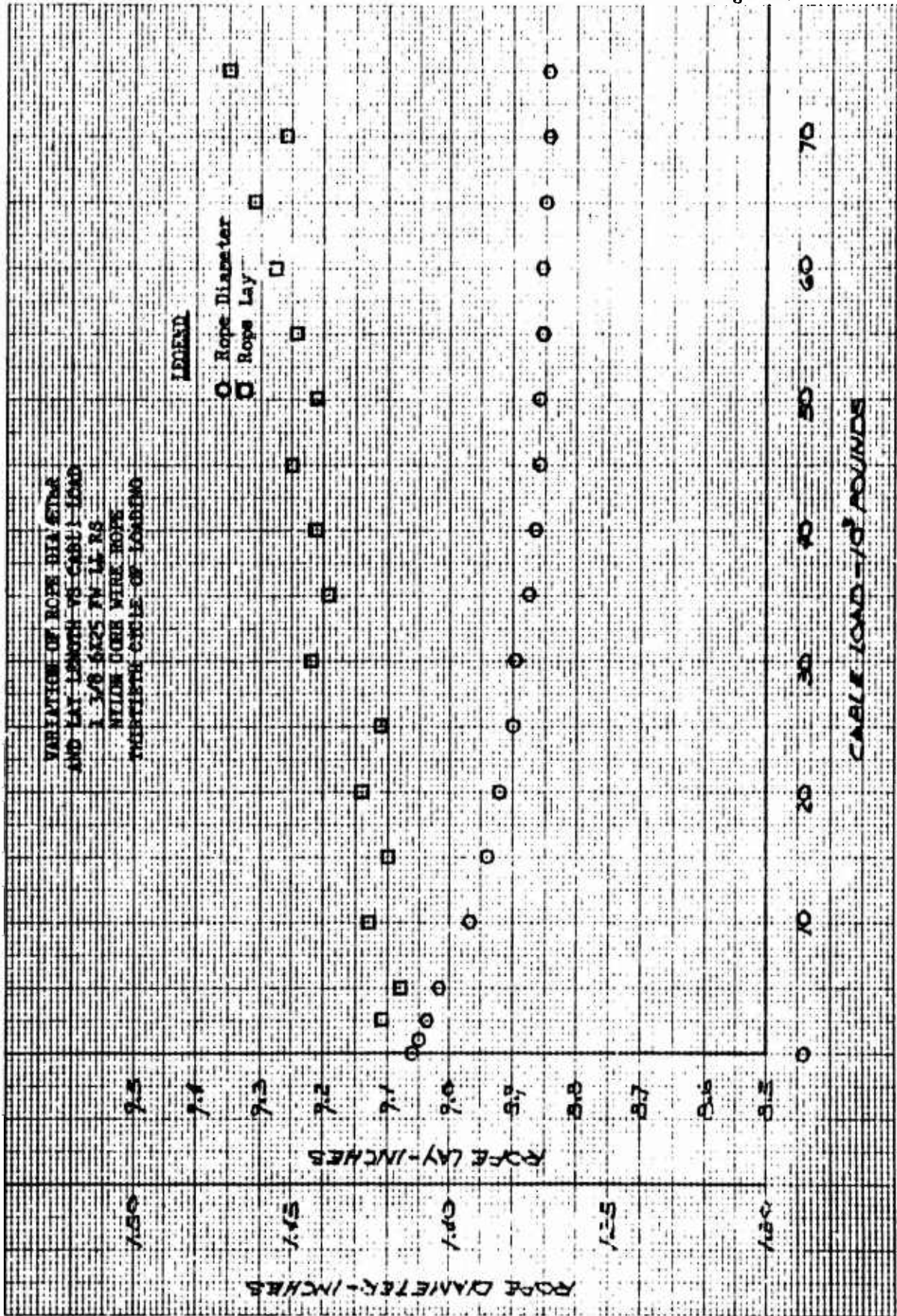


FIGURE 63

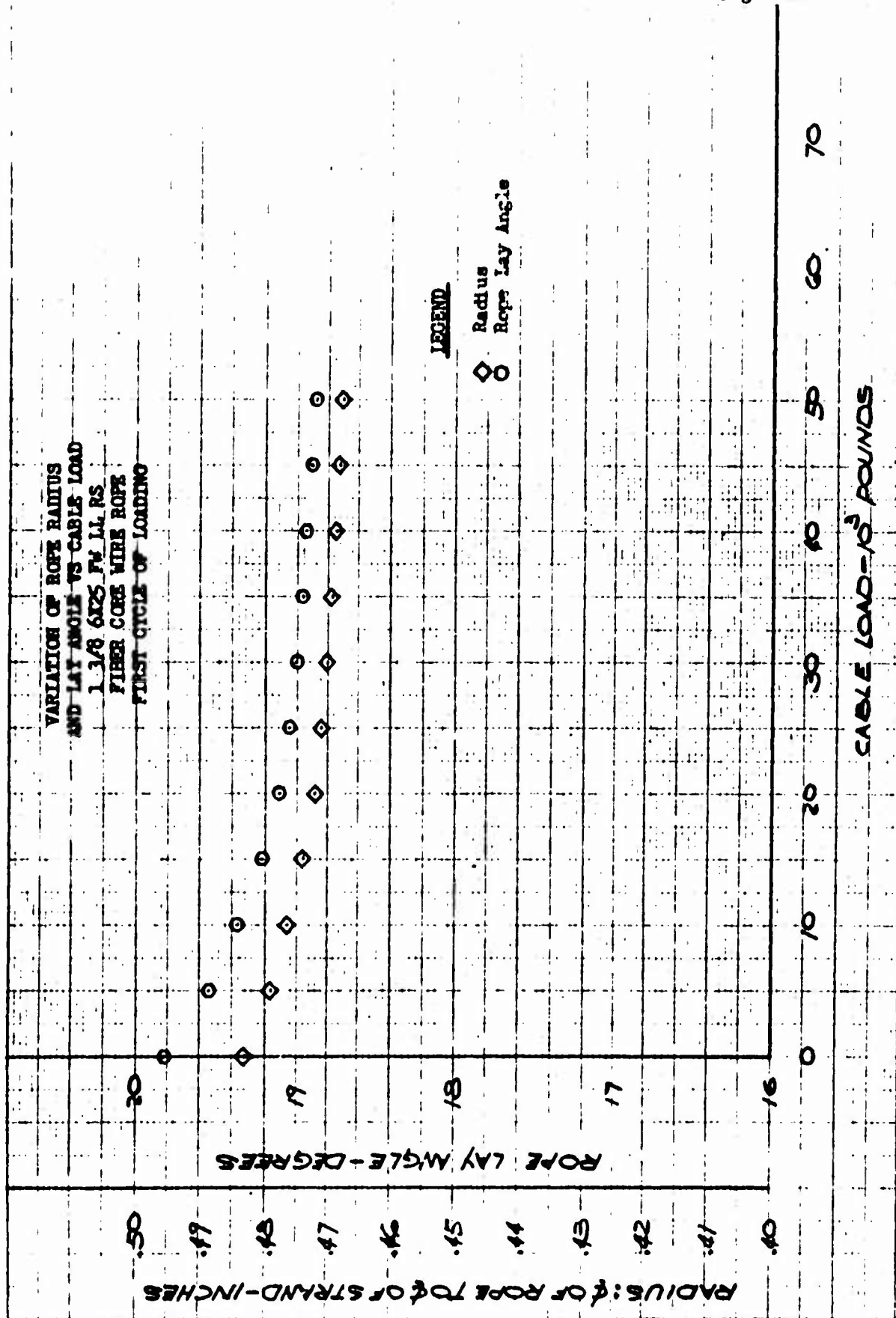


FIGURE 64

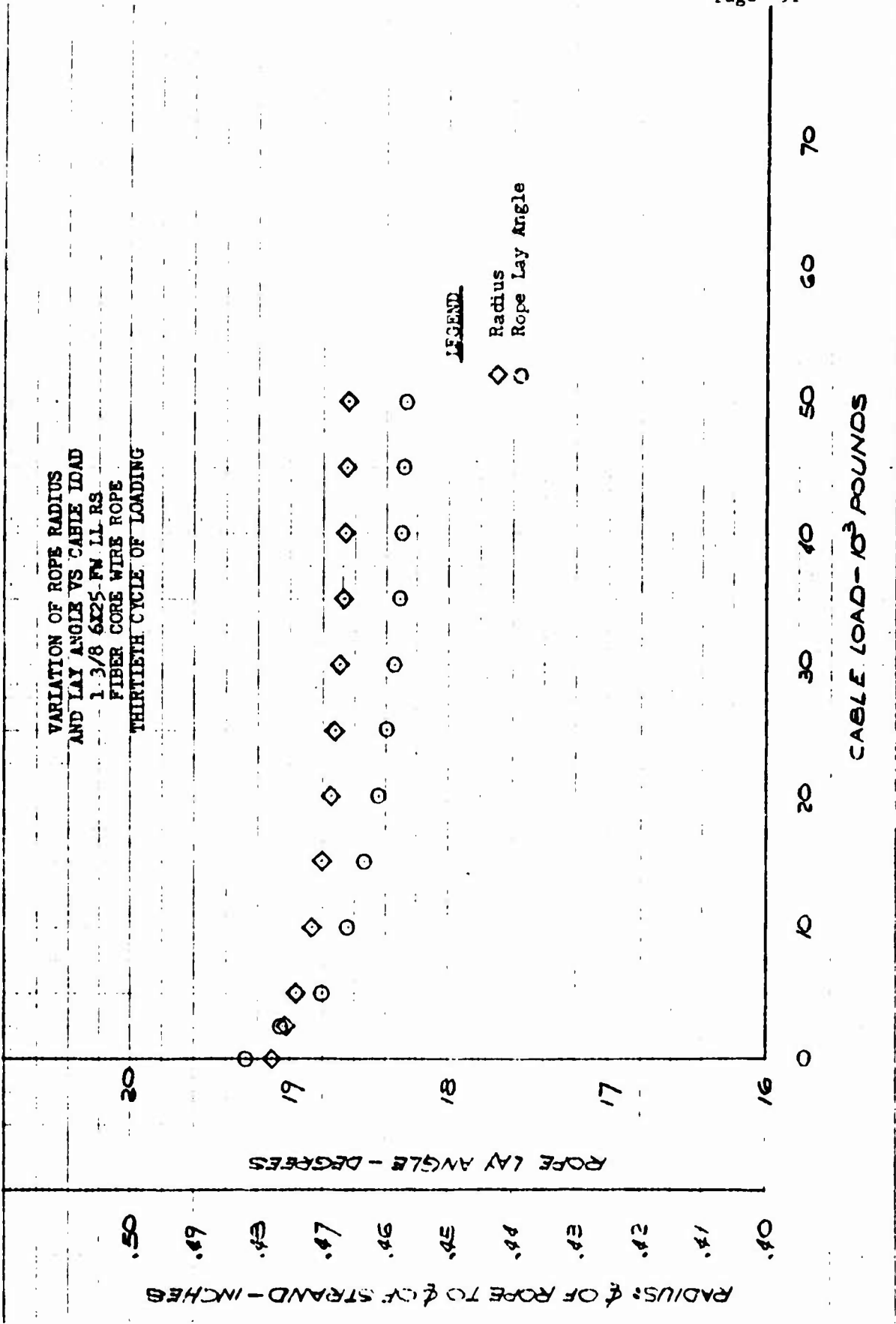


FIGURE 65

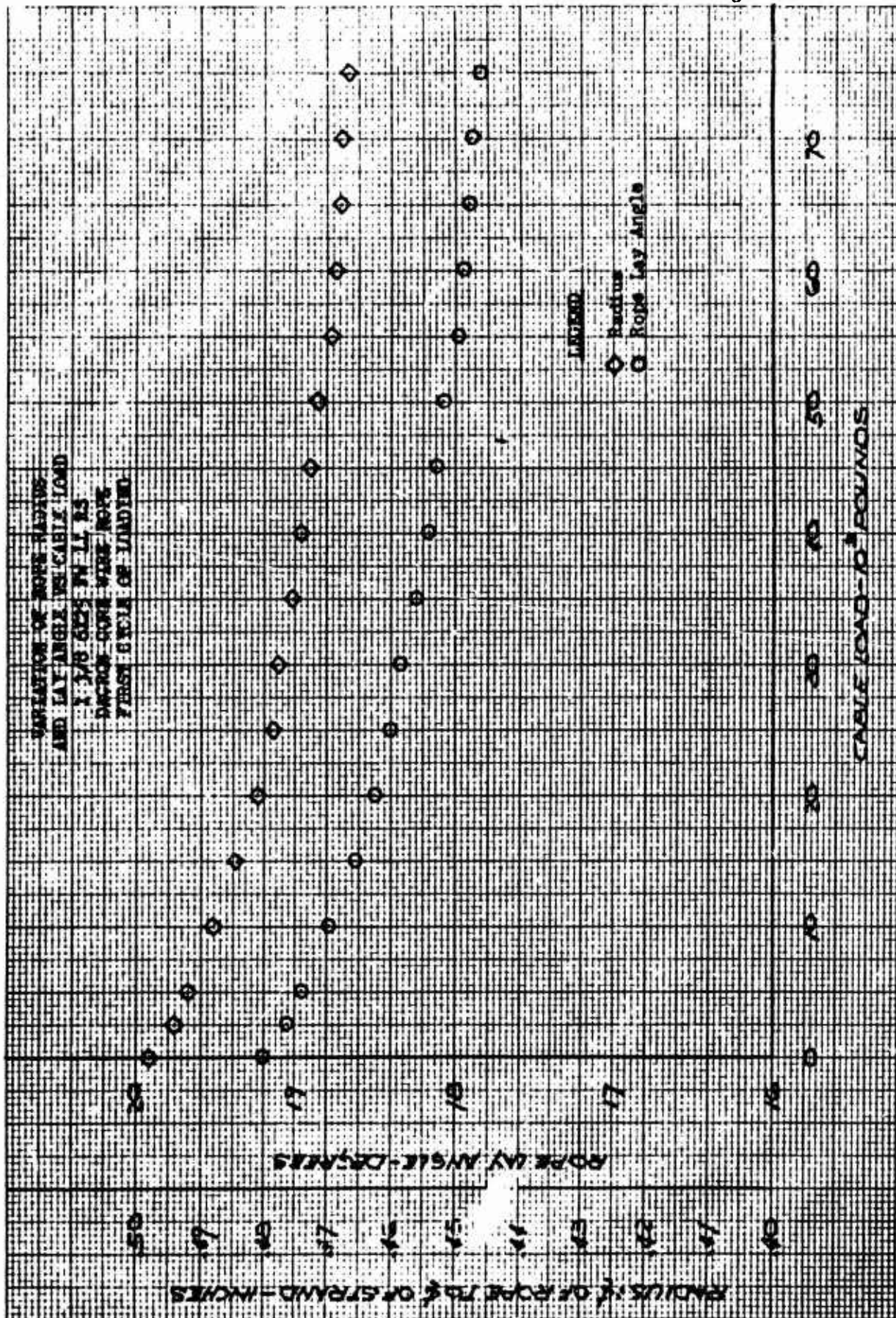


FIGURE 66

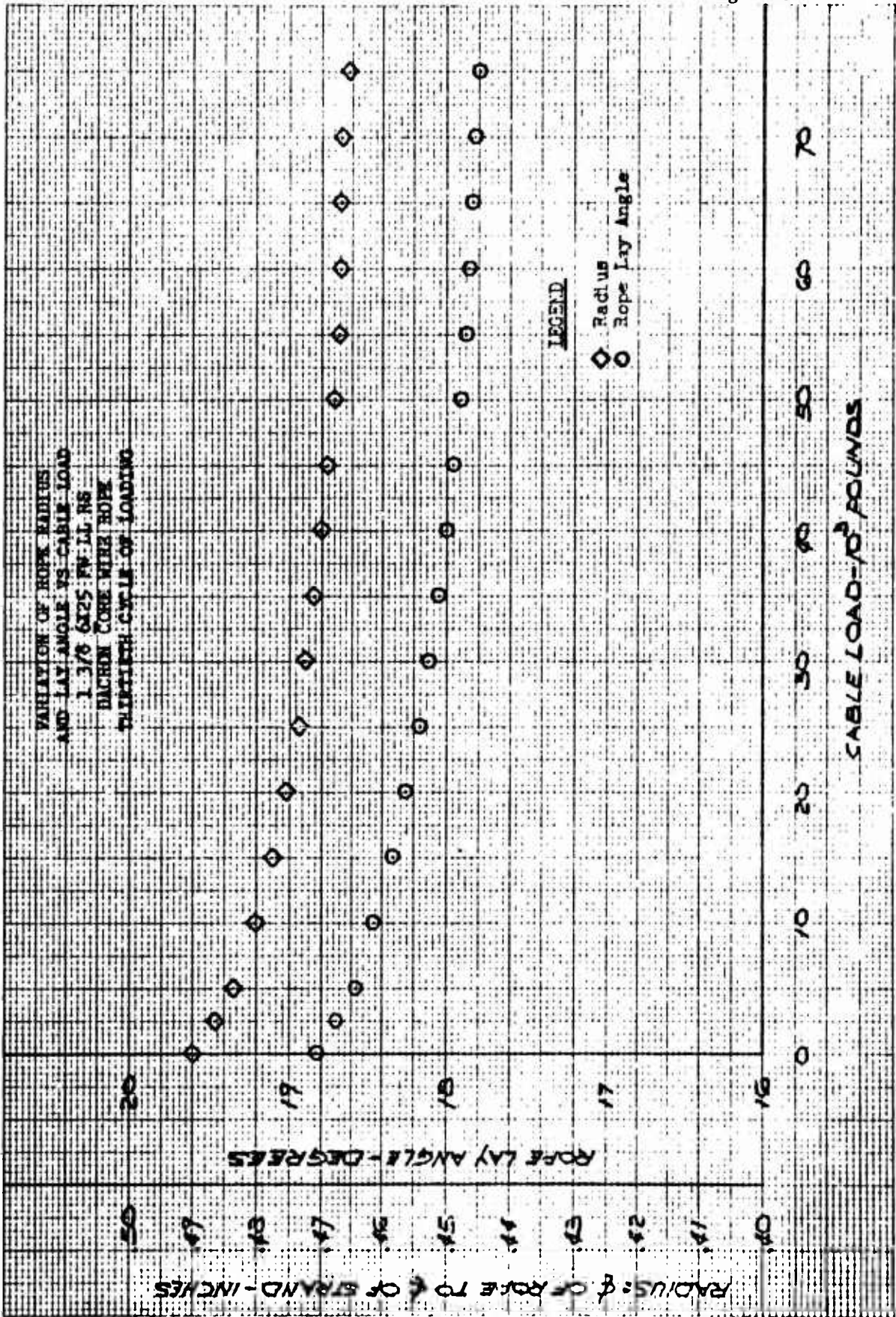


FIGURE 67

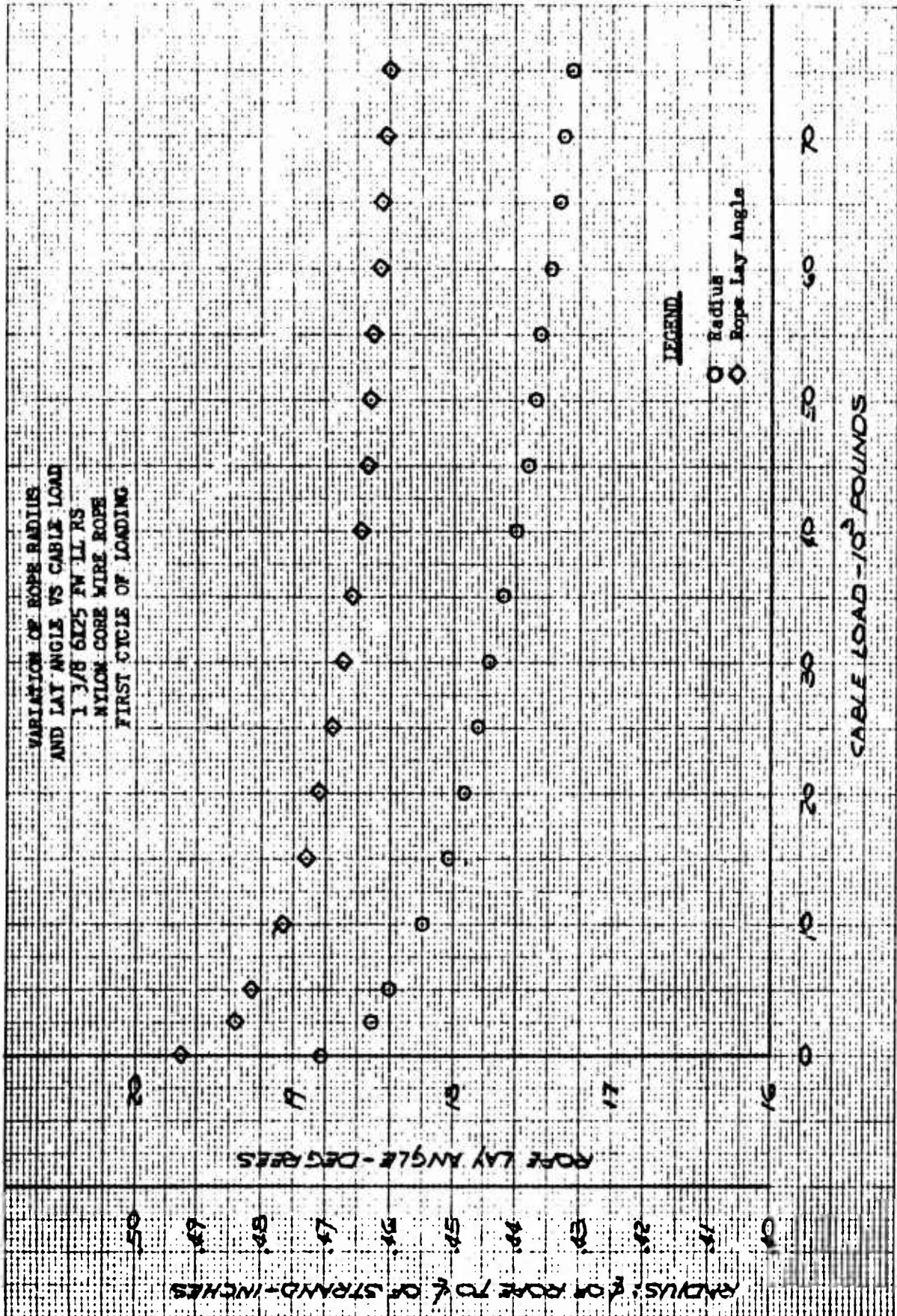


FIGURE 68

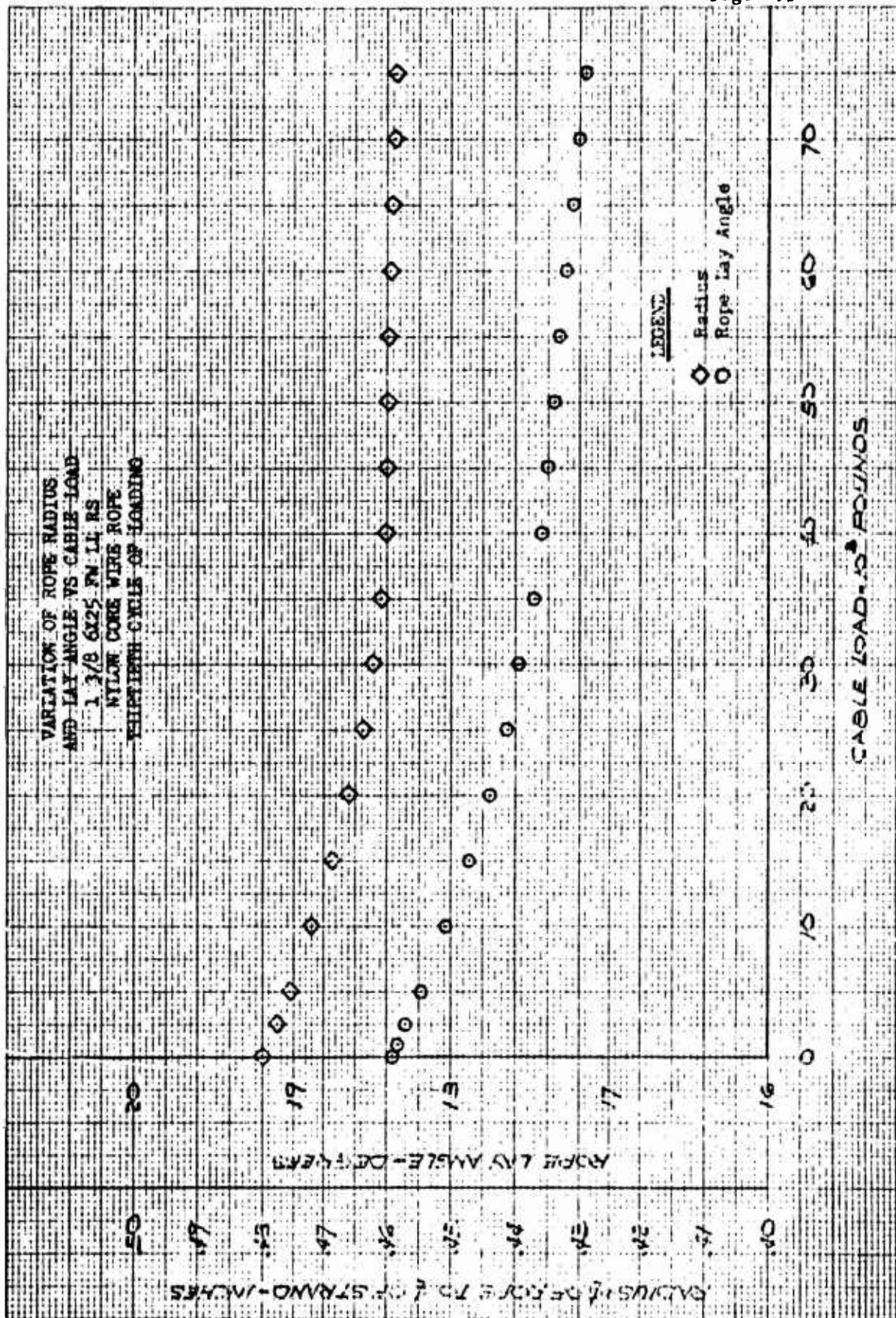


FIGURE 69

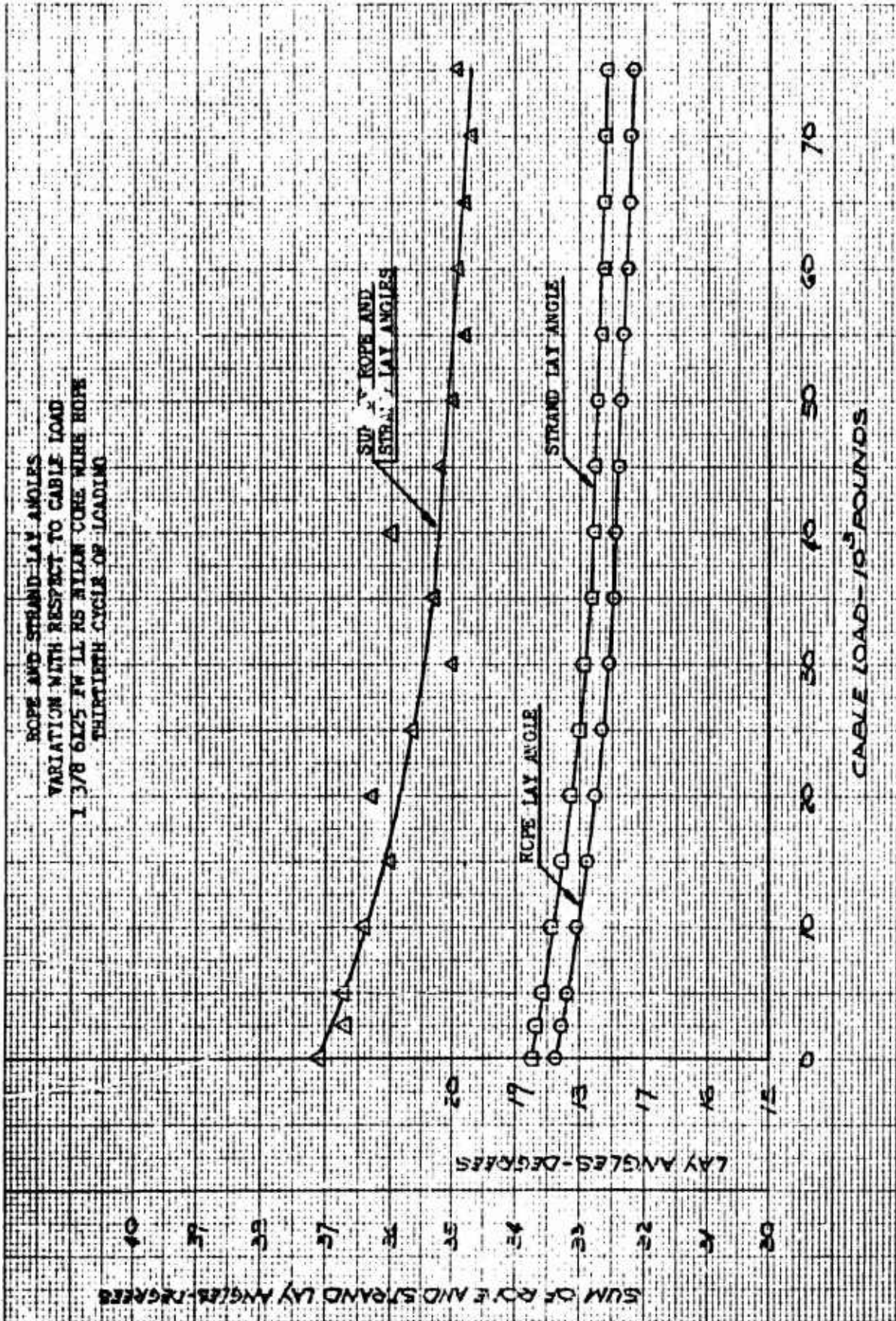


FIGURE 70

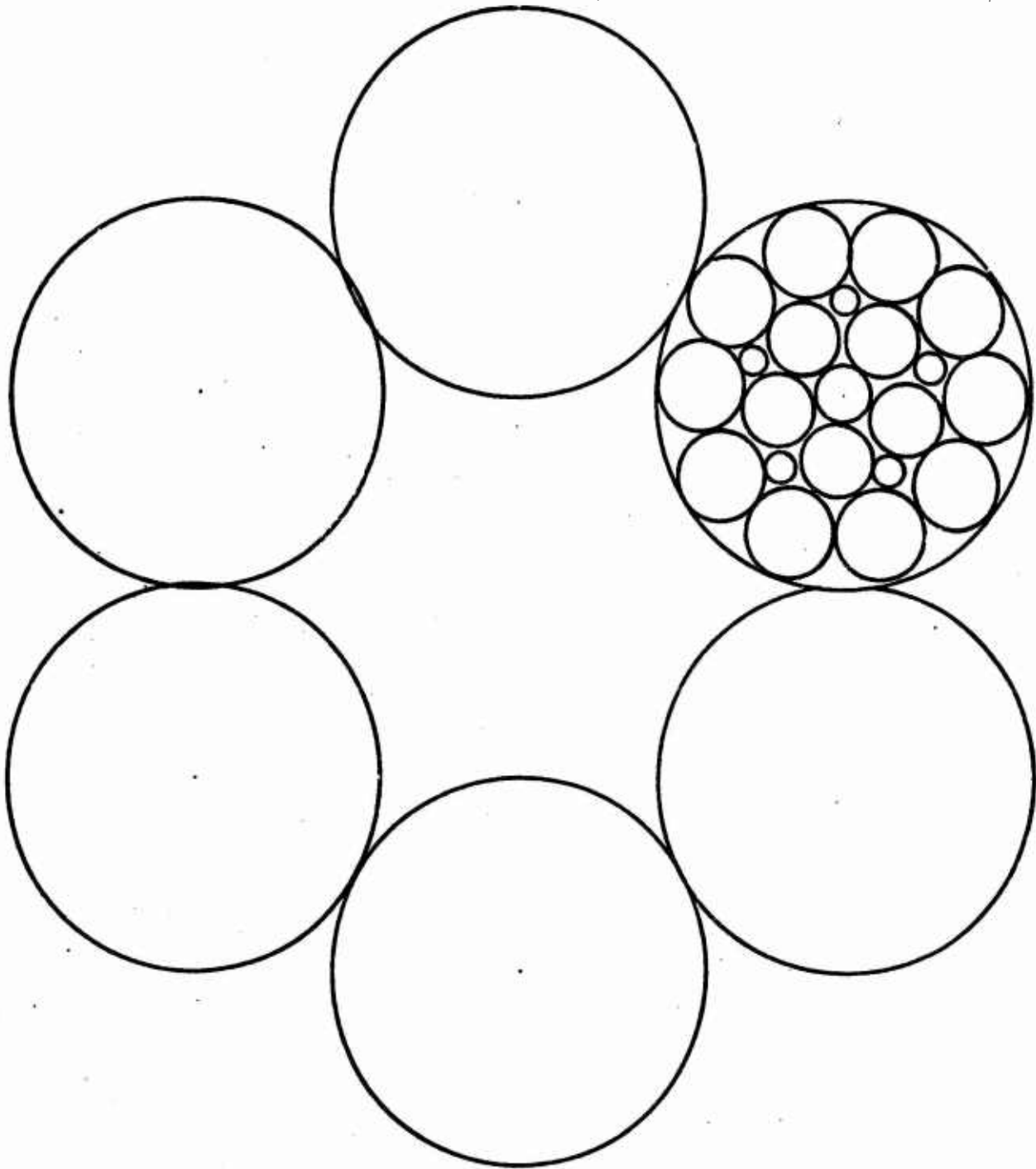


Figure 71
Rope-Strand Cross-section
6 X 21 FW LL RS Wire Rope

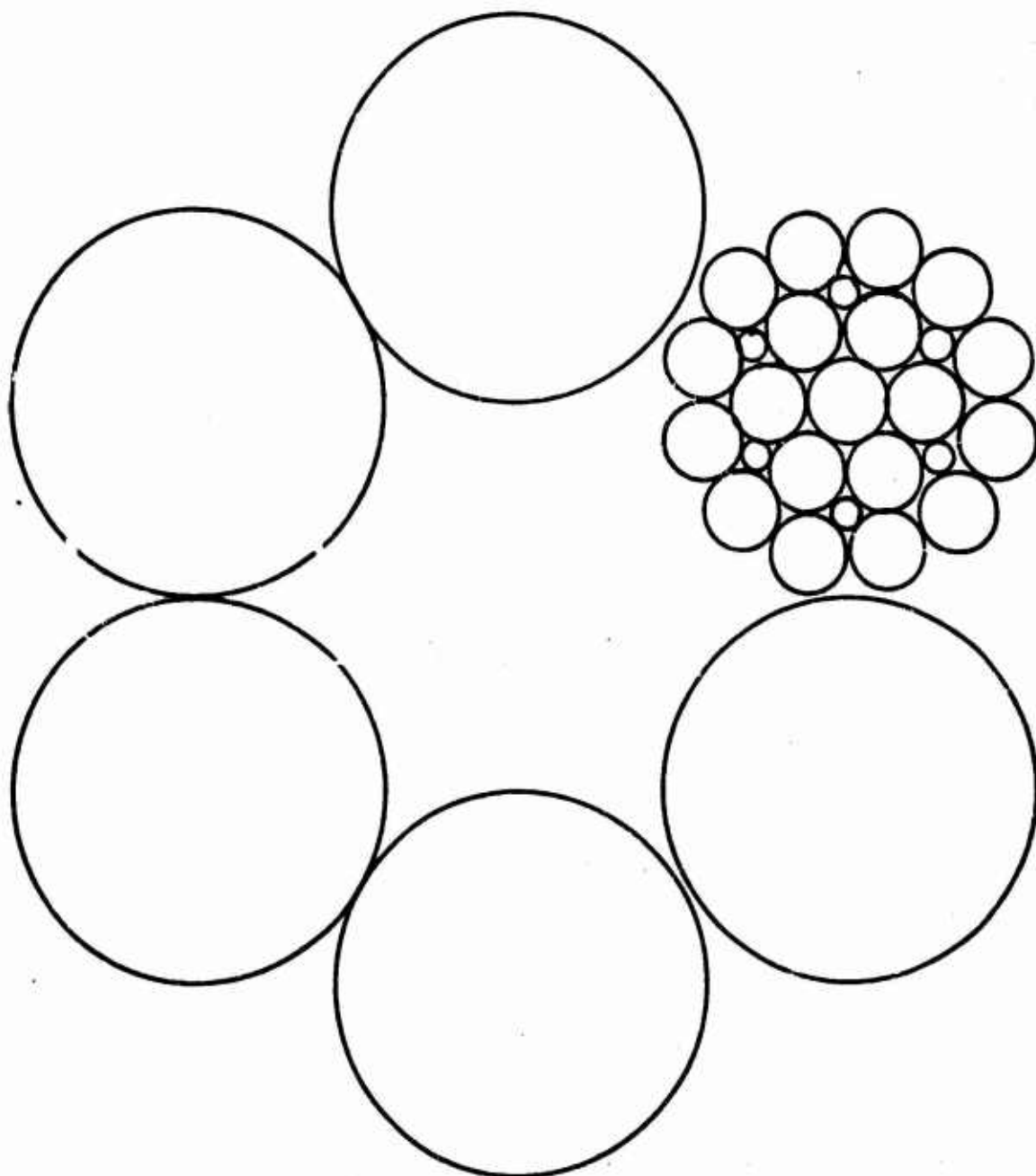


Figure 72
Rope-Strand Cross-section
6 X 25 FW LL RS Wire Rope

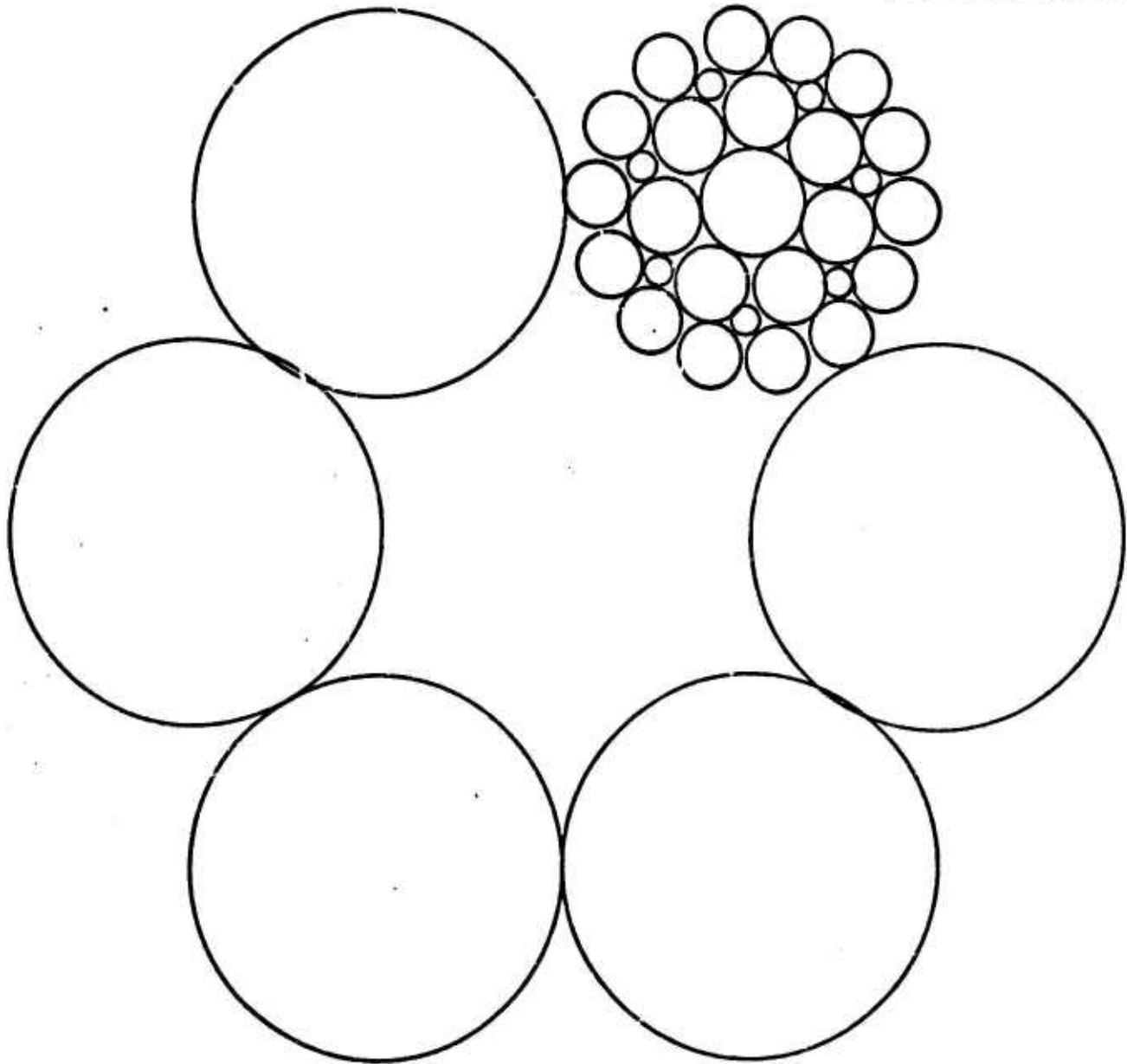


Figure 73
Rope-Strand Cross-section
6 X 29 FW LL RS Wire Rope

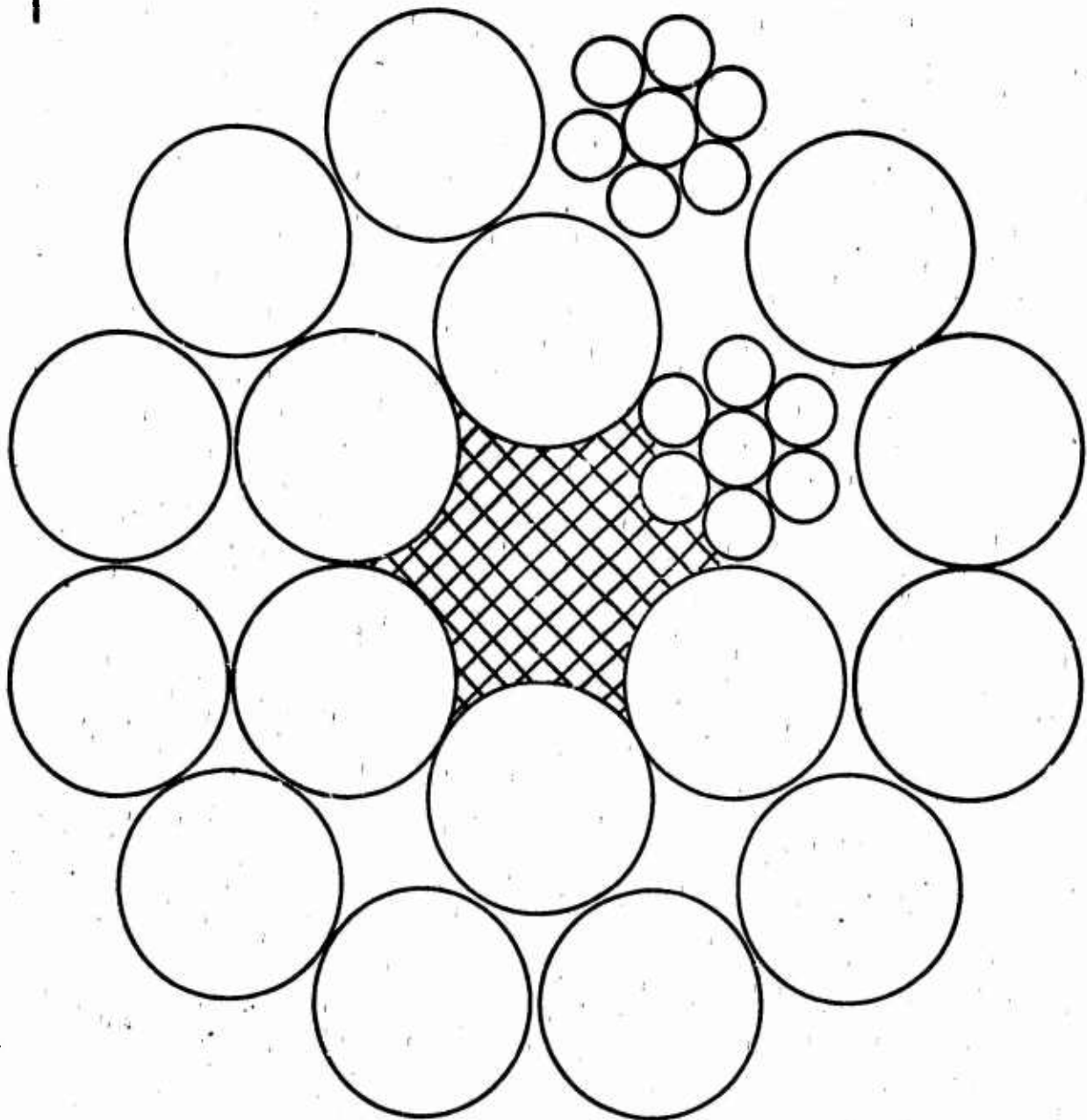


Figure 74
Rope-Strand Cross-section
18 X 7 Non-Rotating Wire Rope

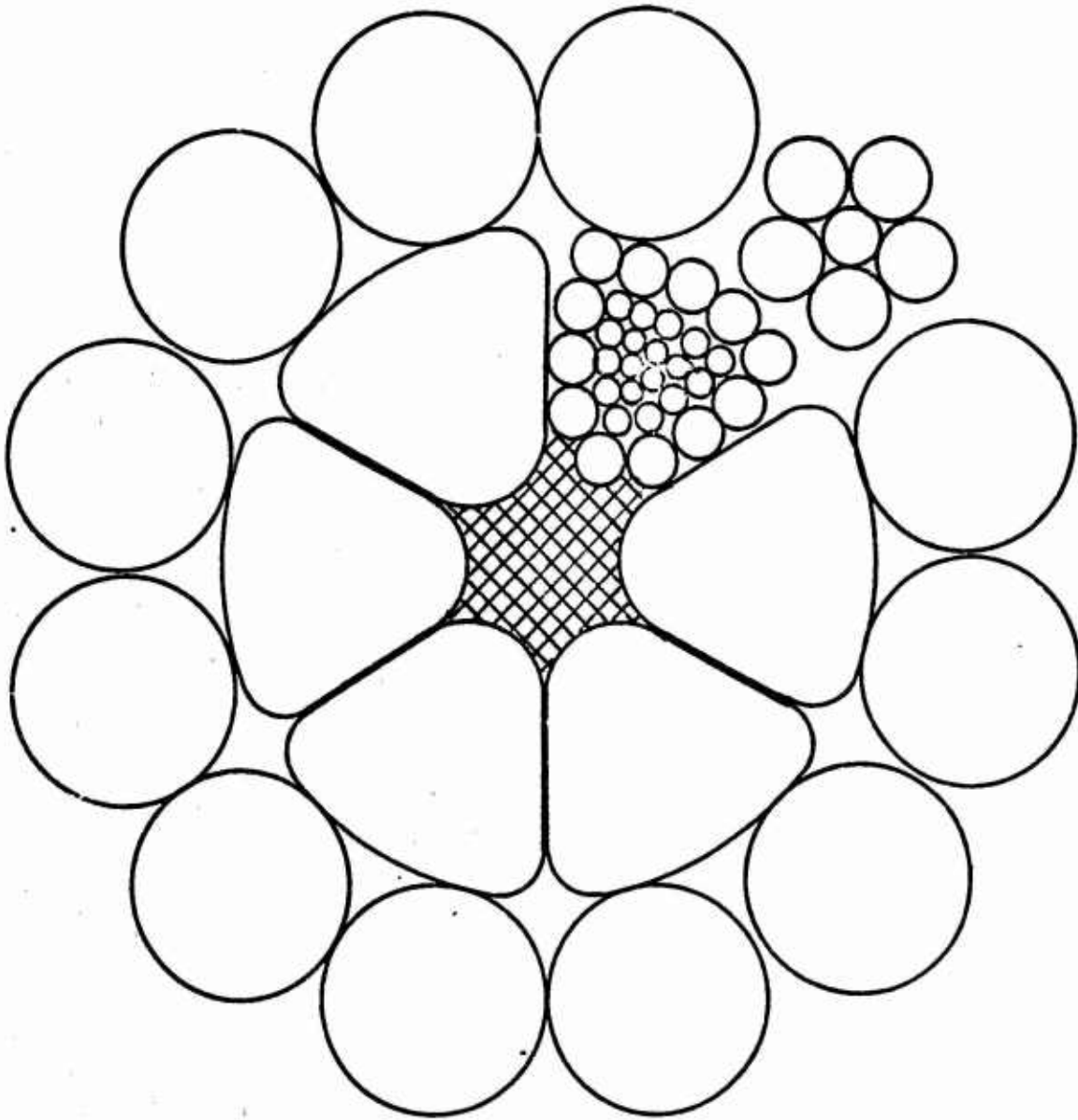


Figure 75
Rope-Strand Cross-section
12 X 6/6 X 30 Non-Rotating Wire Rope

APPENDIX A
WIRE ROPE GEOMETRY

The analysis of wire rope requires the definition of three contravariant basis: (1) an $(\bar{x}, \bar{y}, \bar{z})$ basis with the \bar{x} and \bar{y} vectors in the plane of the rope and \bar{z} vector acting along the centerline of the rope; (2) an $(\bar{e}_{SN}, \bar{e}_{SB}, \bar{e}_{ST})$ basis with the principal normal \bar{e}_{SN} and the binormal vectors \bar{e}_{SB} lying in the plane of the strand and the tangent vector \bar{e}_{ST} acting in the center of the strand and defining the positive direction of the strand; and (3) an $(\bar{e}_{wN}, \bar{e}_{wB}, \bar{e}_{wT})$ basis with the \bar{e}_{wN} and \bar{e}_{wB} lying in the plane of the wire and the tangent vector \bar{e}_{wT} acting in the center of the wire as shown. Each vector triad constitutes an orthogonal dextral set.

The parametric equations of the strand trajectory are given by

$$\begin{aligned}x_1 &= R \cos \delta \\x_2 &= R \sin \delta \\x_3 &= R \cot \beta \delta\end{aligned}$$

where β is the rope lay angle. The position vector \overline{OP} from the origin to the center of the strand is

$$\overline{OP} = \bar{x} R \cos \delta + \bar{y} R \sin \delta + \bar{z} R \cot \beta \delta$$

and the unit vector triad in the strand is determined from

$$\begin{aligned}\bar{e}_{ST} &= \frac{\frac{d\overline{OP}}{d\delta}}{\left| \frac{d\overline{OP}}{d\delta} \right|}, & \bar{e}_{SN} &= \frac{\frac{d\bar{e}_{ST}}{d\delta}}{\left| \frac{d\bar{e}_{ST}}{d\delta} \right|} \\ \bar{e}_{SB} &= \bar{e}_{ST} \times \bar{e}_{SN}\end{aligned}$$

giving

$$\begin{bmatrix} \bar{e}_{SN} \\ \bar{e}_{SB} \\ \bar{e}_{ST} \end{bmatrix} = \begin{bmatrix} -\cos \delta & -\sin \delta & 0 \\ \cos \beta \sin \delta & -\cos \beta \cos \delta & \sin \beta \\ -\sin \beta \sin \delta & \sin \beta \cos \delta & \cos \beta \end{bmatrix} \begin{bmatrix} \bar{x} \\ \bar{y} \\ \bar{z} \end{bmatrix}$$

or in abbreviated form

$$\vec{e}_s = [A] \vec{e}_R$$

The wires constitute a second helix wrapped around the strand tangent vector in the plane of the strand. Its position vector, relative to an origin lying in the plane of the strand at its center, is

$$\vec{r}_p = \vec{e}_{SN} r \cos \phi + \vec{e}_{SB} r \sin \phi + \vec{e}_{ST} r \cot \alpha \phi$$

The unit vectors of the wire coordinate system are obtained from

$$\vec{e}_{WT} = \frac{\frac{d\vec{r}_p}{d\phi}}{\left| \frac{d\vec{r}_p}{d\phi} \right|}, \quad \vec{e}_{WN} = \frac{\frac{d\vec{e}_W}{d\phi}}{\left| \frac{d\vec{e}_W}{d\phi} \right|}$$

$$\vec{e}_{WB} = \vec{e}_{WT} \times \vec{e}_{WN}$$

yielding

$$\begin{bmatrix} 1 \\ 0 \\ 0 \\ 0 \end{bmatrix}_{WN} = \begin{bmatrix} -\cos \phi & \cos \alpha \sin \phi & 0 \\ \cos \alpha \sin \phi & -\cos \alpha \cos \phi & \sin \alpha \\ -\sin \alpha \sin \phi & \sin \alpha \cos \phi & \cos \alpha \end{bmatrix} \begin{bmatrix} 1 \\ 0 \\ 0 \\ 0 \end{bmatrix}_{ST}$$

or

$$\vec{e}_W = [B] \vec{e}_S$$

The transformation of coordinates from the wire basis to the rope basis is given by

$$\vec{e}_W = [B][A] \vec{e}_R = [C] \vec{e}_R$$

where the matrix $[C]$ has components C_{ij} as follows:

$$C_{11} = \cos \phi \cos \delta - \cos \beta \sin \phi \sin \delta$$

$$C_{12} = \cos \phi \sin \delta + \cos \beta \sin \phi \cos \delta$$

$$C_{13} = -\sin \beta \sin \phi$$

$$C_{21} = -\cos \alpha \sin \phi \cos \delta - \cos \alpha \cos \beta \cos \phi \sin \delta - \sin \alpha \sin \beta \sin \delta$$

$$C_{22} = -\cos \alpha \sin \phi \sin \delta + \cos \alpha \cos \beta \cos \phi \cos \delta + \sin \alpha \sin \beta \cos \delta$$

$$C_{23} = -\cos \alpha \sin \beta \cos \phi + \sin \alpha \cos \beta$$

$$C_{31} = \sin \alpha \sin \phi \cos \delta + \sin \alpha \cos \beta \cos \phi \sin \delta - \cos \alpha \sin \beta \sin \delta$$

$$C_{32} = \sin \alpha \sin \phi \sin \delta - \sin \alpha \cos \beta \cos \phi \cos \delta + \cos \alpha \sin \beta \cos \delta$$

$$C_{33} = \sin \alpha \sin \beta \cos \phi + \cos \alpha \cos \beta$$

The cosine of the angle ψ between the centerline of the rope and the tangent vector to an outer layer wire is, by definition,

$$\cos \psi = \frac{\overline{e_{w1}} \cdot \overline{R}}{|\overline{e_{w1}}| |\overline{R}|}$$

which reduces to

$$\cos \psi = C_{33}$$

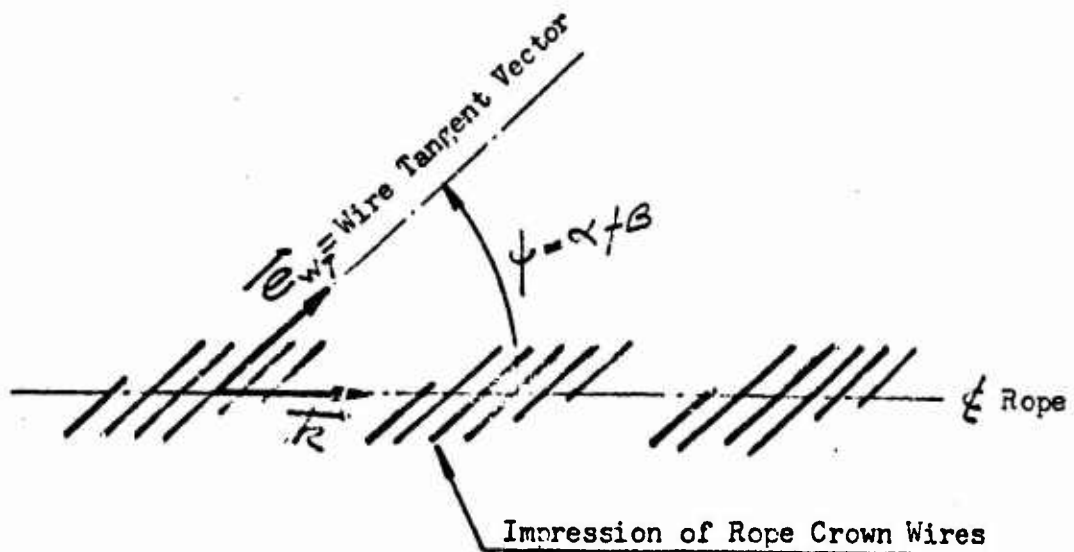
$$\cos \psi = \sin \alpha \sin \beta \cos \phi + \cos \alpha \cos \beta$$

For an outer layer wire on the crown of the rope, $\phi = 180^\circ$ (as the angle is measured from the strand direction vector \vec{e}_{sN} which defines the direction of the strand radius of curvature). Thus we have

$$\cos \phi = \cos \alpha \cos \beta - \sin \alpha \sin \beta$$

$$\cos \phi = \cos(\alpha + \beta)$$

$$\phi = \alpha + \beta$$



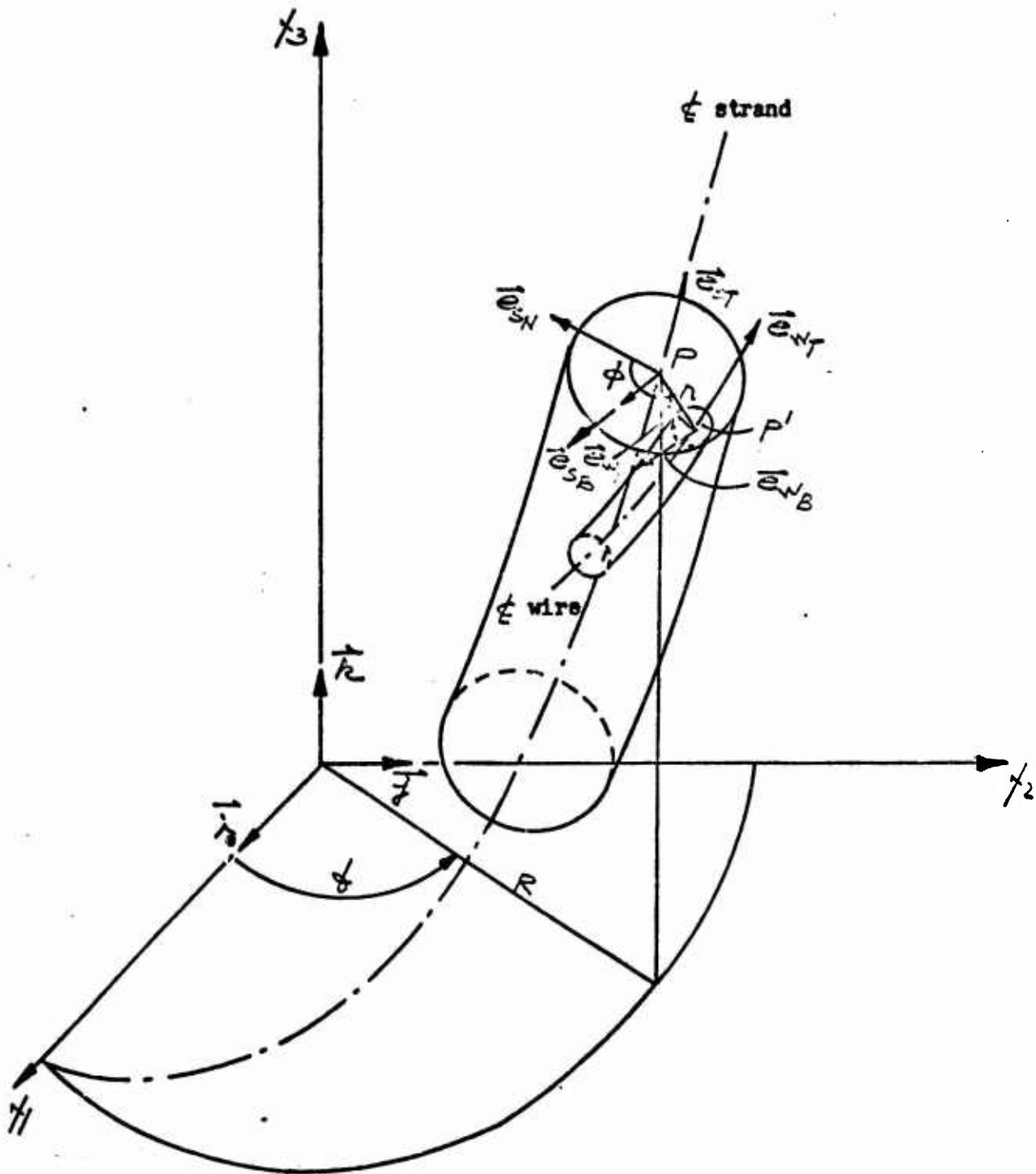


FIGURE A1
WIRE ROPE COORDINATE
GEOMETRY